3-29-2017 12:00 AM

Investigation of Chitosan-based Hydrogels as a Cell Delivery Platform for Adipose-derived Stem/Stromal Cell Transplantation to Promote Angiogenesis in Ischemic Tissues

Jobanpreet Singh Dhillon
The University of Western Ontario

Supervisor
Dr. Lauren Flynn
The University of Western Ontario Joint Supervisor
Dr. David Hess
The University of Western Ontario

Graduate Program in Anatomy and Cell Biology
A thesis submitted in partial fulfillment of the requirements for the degree in Master of Science

Abstract

Stem cell transplantation is under investigation to stimulate angiogenesis in patients with peripheral artery disease. To develop a cell-delivery platform that enhances cell retention and function post-transplantation, the response of human adipose-derived stem/stromal cells (ASCs) encapsulated within *N*-methacrylate glycol chitosan (MGC) hydrogels with or without integrin-binding RGD or IKVAV motifs was explored. ASC viability was enhanced in the MGC and MGC-RGD hydrogels relative to the MGC-IKVAV group under hypoxic (2% O_2) culture conditions, with cell spreading and higher metabolic activity noted in MGC-RGD at 14 days. Analysis of angiogenic gene expression revealed similar patterns between all hydrogel groups, with higher levels of the pro-angiogenic factors *HGF*, *VEGFA*, *ANGPTL4* and *ANGPT2* in 3-D versus 2-D cultures. Characterization of the *in vivo* response following subcutaneous implantation in NOD/SCID mice showed enhanced ASC retention in MGC-RGD, with increased peri-implant $CD31^+$ cell recruitment in the ASC-seeded MGC and MGC-RGD hydrogels relative to unseeded controls.

Keywords

Peripheral artery disease, cell-based therapy, adipose-derived stem/stromal cells, injectable biomaterials, scaffold-based cell-delivery system, *N*-methacrylate glycol chitosan hydrogel, integrin-binding peptides, RGD, IKVAV, therapeutic angiogenesis.

Acknowledgments

First and foremost, I would like to express my sincere gratitude towards my supervisors, Dr. Lauren Flynn and Dr. David Hess, for their endless support, encouragement and patience throughout my time as their graduate student. Their commitment towards their students is undeniable—their knowledge, experience and mentorship has been pivotal in overcoming the challenges I faced over my graduate career. Their passion towards science and innovative research has been truly inspiring to witness. Needless to say, it has been a privilege to be a part of their research team and continuously learn from them.

I would also like to acknowledge Dr. Brian Amsden and Stuart Young (Queen's University) for their assistance throughout my thesis project. I truly appreciate the time Stuart has devoted in preparing the biomaterials for my project, as well as the support and guidance they have both offered during experimental challenges.

Thank-you to my advisory committee members, Dr. Geoffrey Pickering and Dr. Shawn Whitehead, for their commitment to this project and for providing valuable insight to guide me in the right direction. To the team of surgeons at London Health Sciences Centre, thank-you for your clinical collaboration and assistance in adipose tissue acquisition which has made the current work possible.

To all the wonderful members of the Flynn and Hess labs, thank-you for the unforgettable memories and support, both in and out of the lab. I will forever cherish the friendships I have made and the laughs I have shared with the lovely group of individuals in both labs. Special thanks goes to Cody Brown, Stephen Sherman, Gillian Bell, Claire Yu and Arthi Shridhar, who have assisted me in different ways during my thesis.

Lastly, I would like to thank my parents, Boota and Harpreet Dhillon, as well as my younger brother Simran Dhillon for their continuous love, care and encouragement throughout my studies and my life. You have always been there to share the ups and downs of my academic journey, and I would not be where I am today without your efforts, guidance and blessings.

Table of Contents

List of Tables

List of Figures

List of Abbreviations

2-D	2-dimensional
3-D	3-dimensional
ABI	Ankle brachial index
Acr	Acrylate
Akt	Protein kinase B
ALDH	Aldehyde dehydrogenase
Ang-1, -2	Angiopoietin-1, -2
ANGPT1	Angiopoetin-1 (gene)
ANGPT2	Angiopoietin-2 (gene)
ANGPTL4	Angiopoietin-like 4 (gene)
APS	Ammonium persulfate
Arnt	Aryl hydrocarbon receptor translocator
ASCs	Adipose-derived stem/stromal cells
Bcl-2	B-cell lymphoma-2
BM	Bone marrow
BSA	Bovine serum albumin
CD	Cluster of differentiation
CLI	Critical limb ischemia
COL18A1	Collagen XVIII α1 (gene)
Ct	Cycle threshold
CTGF	Connective tissue growth factor (gene)
$CuSO_4$	Copper (II) sulfate
Del-1	Developmental endothelial locus-1
DI	Deionized
DMEM:F12	Dulbecco's Modified Eagle Medium:Ham's F-12 nutrient mixture
DMSO	Dimethyl sulfoxide
DOS	Degree of substitution
EC	Endothelial cell
ECM	Extracellular matrix

EDTA	Ethylenediaminetetraacetic acid
EdU	5-ethynyl-2'-deoxyuridine
eNOS	Endothelial nitric oxide synthase
EPC	Endothelial precursor cell
ERK	Extracellular signal-regulated kinase
ESC	Embryonic stem cell
EthD-1	Ethidium homodimer-1
FAK	Focal adhesion kinase
FAL	Femoral artery ligation
FBS	Fetal bovine serum
FGF-1, -2	Fibroblast growth factor-1, -2
FGF1	Fibroblast growth factor 1 (gene)
GAG	Glycosaminoglycan
GC	Glycol chitosan
GFP	Green fluorescent protein
G-CSF	Granulocyte colony stimulating factor
GM-CSF	Granulocyte/macrophage colony stimulating factor
GMA	Glycidyl methacrylate
GUSB	Beta-glucoronidase
^{1}H NMR	Proton nuclear magnetic resonance
HA	Hyaluronic acid
HEPES	4-(2-hydroxyethyl)-1-piperazineethanesulfonic acid
HGF	Hepatocyte growth factor
HGF	Hepatocyte growth factor (gene)
HIF-1α, -1β	Hypoxia-inducible factor-1α, -1β
HLA	Human leukocyte antigen
HRE	Hypoxia response element
HUVEC	Human umbilical vein endothelial cell
IC	Intermittent claudication
ICAM-1	Endothelial intercellular adhesion molecule-1
IFATS	International Federation for Adipose Therapeutics and Science

IgG	Immunoglobulin G
IKVAV	Isoleucine-lysine-valine-alanine-valine
IL-8	Interleukin-8
IL-10	Interleukin-10
INF-α, -β, -γ	Interferon-α, -β, -γ
ISCT	International Society for Cellular Therapy
ITGB3	Integrin β3 (gene)
$KHCO_3$	Potassium bicarbonate
KRB	Kreb's ringer buffer
LDPI	Laser Doppler Perfusion Imaging
MAPK	Mitogen-activated protein kinase
MCP-1	Monocyte chemoattractant protein-1
MeHA	Methacrylated hyaluronic acid
MGC	*N*-methacrylate glycol chitosan
MI	Myocardial infarction
MMP	Matrix metalloproteinase
MMP14	Matrix metalloproteinase 14 (gene)
MNC	Mononuclear cell
MOM	Mouse-on-mouse
MSC	Mesenchymal stem/stromal cell
MSPVII	Mucopolysaccharidosis type VII
MTT	3-(4,5-dimethylthiazol-2-yl)-2,5-diphenyltetrazolium bromide
NH_4Cl	Ammonium chloride
NO	Nitric oxide
ODDD	Oxidation-dependent degradation domain
PAD	Peripheral artery disease
Passage 1	P1
Passage 2	P2
Passage 3	P3
PB	Peripheral blood
PBS	Phosphate buffered saline

PDGF	Platelet-derived growth factor
PECAM	Platelet-derived endothelial cell adhesion molecule
PEG	Poly(ethylene glycol)
Pen-strep	Penicillin-streptomycin
PHD	Prolyl hydroxylase
PI3K	Phosphoinositide 3-kinase
RGD	Arginine-glycine-aspartic acid
ROS	Reactive oxygen species
RPLP0	Ribosomal protein stalk subunit P0 (gene)
RT-PCR	Reverse transcriptase-polymerase chain reaction
SDF-1	Stromal cell-derived factor-1
SMC	Smooth muscle cell
SVF	Stromal vascular fraction
$TcPO_2$	Transcutaneous oxygen pressure
TCPS	Tissue culture polystyrene
TEMED	*N,N,N'N'*-tetramethylethylenediamine
TGF-α, -β	Transforming growth factor-α, -β
THBS1	Thrombospondin-1 (gene)
TIMPs	Tissue inhibitor of metalloproteinases
TSP-1, -2	Thrombospondin-1, -2
VCAM-1	Vascular cell adhesion molecule-1
VE	Vascular endothelial
VEGF	Vascular endothelial growth factor
VEGFA	Vascular endothelial growth factor A (gene)
w/v	weight/volume

Chapter 1

1 INTRODUCTION

1.1 Clinical Significance

1.1.1 Peripheral Artery Disease (PAD)

Affecting an estimated 800,000 Canadians and over 9 million Americans, peripheral artery disease (PAD) is prevalent in North America.[1] PAD is the manifestation of systemic atherosclerosis resulting in the obstruction of arteries that supply blood to organs other than the heart, with the lower extremities being the most commonly affected site.[1,2] Atherosclerosis is a progressive disease characterized by excessive accumulation of lipid deposits, fibrous tissue, and inflammatory cells in the lumen of arteries and arterioles.[3] The build-up of atherosclerotic plaques in the peripheral arteries reduces oxygenated and nutrient-rich blood flow to vascular beds in the extremities, causing patients to develop disabling complications such as pain with walking (intermittent claudication; IC) and peripheral neuropathy.[4] The significant restriction of blood flow to the periphery can result in critical limb ischemia (CLI)—the most severe form of PAD, which can lead to resting limb pain, non-healing ulcerations that are prone to infection, and tissue necrosis.[2,5]

PAD has been termed a 'silent' cardiovascular disease because many patients do not seek treatment until the condition progresses to advanced stages, along with other cardiovascular comorbidities.[1] While the incidence of PAD increases significantly with age, its prominent risk factors include smoking, diabetes mellitus, hypercholesterolemia, chronic kidney disease, hypertension, metabolic syndrome and obesity.[1,6] Combined with the aging population, sedentary lifestyle and increasing burden of atherosclerotic risk factors, the incidence of PAD is expected to rise dramatically over the next 10 years.[1]

1.1.2 Pathophysiology of PAD

PAD pathophysiology is a chronic and complex process affecting the macro- and microvasculature of peripheral tissues.[2] The blood supply from the abdominal aorta divides at the iliac artery to enter the legs, and then runs serially through the superficial

femoral artery in the thigh into the popliteal artery at the knee in a single continuous vessel with very few branches.[7] In the majority of patients with symptomatic PAD, there is significant occlusion of the iliac, femoral and/or infrapopliteal arteries.[8,9] A chronic state of ischemia is established due to reduced perfusion pressure in the distal vasculature.[10,11] Compensatory mechanisms cause the peripheral arterioles to maximally vasodilate due to the chronic exposure to vasorelaxing factors, subsequently resulting in a lack of tone in the blood vessels (vasomotor paralysis).[11] These structural and functional alterations result in the inability to regulate blood hydrostatic pressure, leading to endothelial cell (EC) damage and edema in the distal portion of the limb, further impairing the compromised microvasculature.[5,11] While a healthy endothelium aids in the modulation of vascular tone and permeability, EC damage resulting from chronic ischemia increases free radical production, impairs nitric oxide (NO) regulation, causes inappropriate platelet activation and leukocyte adhesion, and contributes to the formation of microthrombi.[5,11] Overall, blood flow abnormalities impair oxygen and nutrient exchange at the capillary level, leading to increased inflammation, apoptosis, and tissue necrosis.[5]

1.1.3 Current Treatments for PAD

The current treatments for PAD include lifestyle modifications and pharmacotherapy to improve cardiovascular risk factors, with advanced cases requiring invasive surgical or endovascular interventions such as balloon angioplasty, stenting, or surgical bypass to restore peripheral blood flow.[4] While endovascular treatments or bypass grafting can improve arterial resistance, blood perfusion is often not fully restored in the affected limbs and post-operative edema is common due to the impaired distal microvasculature.[12,13] Therefore, many patients with CLI are not candidates for surgical revascularization or endovascular angioplasty due to diffuse atherosclerosis, and limb amputation is required in ~25% of patients within the first year of diagnosis.[14] Amputation has a detrimental impact on the quality of life, and is associated with high morbidity and mortality rates.[14] Perioperative mortality for below- and above-the-knee amputations is between 5-20%, with a two-year mortality rate of up to 30% post-amputation.[10,15] Furthermore, many survivors require a secondary amputation and less

than 50% of the patients recover full mobility.[16] CLI also places a considerable economic burden on the healthcare system attributed to prolonged hospitalization, complex wound care, and invasive surgical procedures.[17] Taken together, there is a critical need to develop improved therapies to treat CLI.

1.2 *In Vivo* Response to Tissue Ischemia

Under pathological conditions such as obstructive arterial disease, oxygenated blood and nutrient exchange is unable to meet the metabolic demands of the surrounding tissues.[2] As a result, the body initiates several compensatory mechanisms in an attempt to restore circulation to the ischemic tissues by inducing structural and functional changes in the existing vasculature, or by stimulating new blood vessel formation.[2]

1.2.1 Angiogenesis

Angiogenesis is a multi-step process involving the growth of new blood vessels from pre-existing vessels through a series of stages including EC proliferation and migration, abluminal sprouting, and bridging of existing vessels.[16] The process of angiogenesis is tightly regulated by key pro- and anti-angiogenic molecules that function to advance or regress blood vessels through the stroma (Table 1.1).[18] In a model first proposed by Judah Folkman,[19] the angiogenic switch is considered "off" when the effects of the pro-angiogenic factors are balanced with those of the anti-angiogenic factors.[18] However, local hypoxia, inflammation and impaired perfusion can act as triggering events, shifting the balance towards a more pro-angiogenic state.[20]

Table 1.1. Key molecules that regulate pro- and anti-angiogenic response.[18]

Pro-angiogenic molecules	Anti-angiogenic molecules
Vascular endothelial growth factor (VEGF) family	Angiostatin (plasminogen fragment)
Fibroblast growth factor (FGF) family	Endostatin (collagen XVIII fragment)
Angiopoietin-1 (Ang-1)	Angiopoietin-2 (Ang-2)
Hepatocyte growth factor (HGF)	Thrombospondin-1, -2 (TSP-1, -2)
Platelet-derived growth factor (PDGF)	Interferon-α, -β, -γ (INF-α, -β, -γ)
Matrix metalloproteinases (MMPs)	Tissue inhibitor of metalloproteinases (TIMPs)

During ischemic injury, EC transcriptional responses are mediated by hypoxia-inducible factors (HIFs) that regulate the expression of pro-angiogenic, metabolic and cell cycle genes.[20] Under high oxygen tension, prolyl hydroxylase (PHD) enzymes mark hypoxia inducible factor-1α (HIF-1α) for degradation through hydroxylation of 2 proline residues in its oxidation-dependent degradation domain (ODDD).[20] However, under hypoxic (<5% O_2) conditions, the activity of PHD enzymes is attenuated due to limited O_2 and cofactor 2-oxoglutarate required for the enzymatic functions.[20,21] As a result, HIF-1α is stabilized and dimerizes with hypoxia inducible factor-1β (HIF-1β)/aryl hydrocarbon receptor translocator (Arnt).[20] The entire complex translocates to the nucleus where it binds to hypoxia response element (HRE) and upregulates the transcription of over 60 known genes that influence EC proliferation, migration, and vascular growth.[20]

Following the transcriptional changes mediated by HIF-1α, stromal cells within the injured tissues also secrete pro-angiogenic factors such as VEGF and FGF that activate cognate receptors on nearby ECs.[22] Initially, ECs are destabilized by the disruption of cell-cell contacts through VEGF-mediated dissociation of vascular endothelial (VE)-cadherin and Ang-2/Tie-2 interactions with neighbouring mural cells.[23] In addition, VEGF activates ECs to form tip cells, which then guide the developing capillary sprout through the extracellular matrix (ECM).[24] While the tip cell does not divide, the endothelial stalk cells that follow the migrational front undergo rapid proliferation stimulated by VEGF, FGF, HGF and transforming growth factor-α (TGF-α) to form a lumen.[23,24] The tip cell guides the migration of the developing sprout along a gradient of soluble and matrix-bound VEGF.[25] MMPs secreted by proliferating ECs mediate the remodeling of the ECM to facilitate the new vessel growth.[26] Cell-cell linkages between nascent ECs are facilitated by the upregulation of adhesion molecules, including platelet-derived endothelial cell adhesion molecule (PECAM or CD31).[16,23] Stabilization of the growing vessel occurs through inhibition of EC proliferation by transforming growth factor-β (TGF-β), and upregulation of VE-cadherin strengthens the junctions between ECs.[27] Lastly, PDGF facilitates the recruitment and proliferation of tissue-resident pericytes and vascular smooth muscle cells (SMCs) in order to support the new vessel through envelopment and matrix deposition, while Ang-1/Tie-2 mediates vascular

permeability.[16,28] The newly formed capillaries, ~5-20 μm in diameter, fuse with existing vascular beds and blood flow commences.[16]

1.2.2 Vasculogenesis

Vasculogenesis is the *de novo* formation of blood vessels from EC precursor cells, or angioblasts.[29] Until recently vasculogenesis was thought to occur only during embryonic development.[29] However, in 1999, Asahara and Insner reported the existence of circulating human bone marrow (BM)-derived endothelial precursor cells (EPCs) that contribute to post-natal vessel formation.[30] Post-natal vasculogenesis involves the homing of circulating EPCs to sites of ischemic injury, and the formation of new vessel networks through inosculation within advancing or regressing vessel networks.[31,32] Growth factors and chemokines generated as a result of local cellular hypoxia, including VEGF, stromal cell-derived factor-1 (SDF-1), granulocyte/macrophage colony stimulating factor (GM-CSF) and interleukin-8 (IL-8), recruit circulating EPCs to the site of ischemic injury to facilitate microvascular repair.[33] While the role of circulating or vessel-derived EPCs is not completely understood, early studies suggested that these cells differentiate into mature ECs and contribute to capillary formation.[33,34] However, more recent evidence suggests that EPCs also promote the proliferation, migration and survival of existing ECs and pericytes via paracrine mechanisms.[35,36]

1.2.3 Arteriogenesis

Under normal physiological conditions, pre-existing collateral arteries run parallel to the large conduit artery.[26] Arteriogenesis is the process through which an obstruction of the conduit artery causes the remodeling and maturation of collateral vessels to increase perfusion in the distal tissues.[37] Initially, elevation of the pressure gradient due to the vascular obstruction increases the rate of blood flow in the collateral vessels, which augments the fluid shear stress on the vessel walls.[38] This mechano-stimulus alters the state of the endothelium, causing the activation of endothelial nitric oxide synthase (eNOS) and subsequent vasodilation of the collateral arterioles.[38] Mechanical deformation of the ECs also enhances mechanoreceptor-dependent transcription of several adhesion molecules and chemokines, including monocyte chemoattractant

protein-1 (MCP-1), SDF-1 and GM-CSF.[26,38] Attracted by these molecules, circulating monocytes migrate to the affected area, adhere to the endothelium, and migrate into the sub-endothelial space, where they differentiate into macrophages.[26,32] In particular, a transformation towards the M2 macrophage phenotype has been shown to support collateral vessel formation through the production of supportive growth factors and cytokines, including VEGF, FGF, and HGF, as well as enzymes such as MMPs.[39,40] The secreted molecules work in concert to cause rapid proliferation of the ECs and vascular SMCs required for collateral artery enlargement.[26] Ultimately, arteriogenesis can result in the rapid enlargement of the collateral artery diameter up to 20× its original size in an effort to reduce vascular resistance and restore downstream perfusion.[38]

1.3 Strategies for Revascularization of Ischemic Limb

Alternative treatments are extremely limited for patients with diffuse PAD or CLI that do not qualify for surgical revascularization or endovascular procedures. *In vivo* compensatory responses to ischemic injury are compromised in patients with PAD, especially those involved with microvascular remodeling and maturation of collateral vessels.[32] Moreover, the number of circulating EPCs are attenuated in these patients, likely due to the adverse effects of associated cardiovascular risk factors and co-morbidities, such as hyperglycemia and hyperlipidemia.[41] Therefore, intrinsic repair mechanisms become insufficient to overcome the burden of disease, demanding the need for new strategies to augment revascularization.

As a result, the last 2 decades have seen extensive pre-clinical and clinical research into the development of new therapeutic interventions to promote vascular regeneration in patients with PAD. These approaches have primarily focused on the delivery of pro-angiogenic growth factors through gene therapy approaches or controlled release strategies, and cell-based therapies to enhance blood flow to the ischemic regions. Although there has been some success in pre-clinical and clinical trials, several hurdles remain that limit efficacy and delay widespread use of these alternative therapies.

1.3.1 Gene Therapy Approaches for PAD

The identification of pro-angiogenic growth factors in the 1980s, such as VEGF and FGF, led to their investigation in pre-clinical models of PAD to enhance angiogenesis and support functional improvement in ischemic limbs.[26] Due to the short half-life (minutes) and pleiotropic effects of growth factors, a large number of pre-clinical and clinical trials have focused on utilizing gene therapy to provide a method for the sustained release of pro-regenerative factors.[26] Gene transfer using plasmids or viral vectors, such as adenovirus or lentivirus, have served as a method for the localized or systemic delivery of specific pro-angiogenic factors to induce vascular regeneration in ischemic tissues.[26]

In terms of pre-clinical testing, while other *in vivo* models are emerging, inducing murine hindlimb ischemia through the ligation of the superficial femoral artery is the most frequently used model of CLI to date.[42] Using these models, gene therapy approaches have been utilized to stimulate angiogenesis and reperfusion by inducing the expression of various pro-angiogenic cytokines, including VEGF, FGF-2 and PDGF, and even the transcription factor HIF-1α.[43–49] For example, intra-arterial delivery of adenovirus-mediated gene transfer of VEGF in an ischemic hindlimb rat model improved perfusion and promoted the recovery of tissue oxygenation in the ischemic limb as compared to PBS controls over 4 weeks.[44] Similarly, another study used a rabbit hindlimb ischemia model to demonstrate that repeated intramuscular injections of VEGF-encoding plasmids at day 7 and 21 post-surgery increased capillary density, arteriolar density and reduced muscle lesions as compared to the empty-plasmid control group over 50 days.[45] Dual gene FGF-2/PDGF-BB plasmid administered intramuscularly into the ischemic hindlimb in rats also enhanced vessel density and limb perfusion as compared to the control plasmid group at 4 weeks.[46] In addition, mediators of angiogenic function, such as eNOS, have also been studied in pre-clinical trials using gene therapy.[49] For example, Brevetti *et al*. reported that adenovirus-mediated transfer of eNOS cDNA via intra-arterial administration in a rat hindlimb ischemia model increased the size and number of collateral arteries, enhanced muscle oxygen tension and augmented limb perfusion as compared to PBS or adenoviral vector controls at 14 days.[49]

While gene therapy has shown promise in pre-clinical models, clinical trials have generated mixed results. In two phase I trials, VEGF-encoding plasmids were injected intramuscularly into the limbs of CLI patients with severe ulcers and ischemic rest pain.[50,51] Patients showed improvements in ankle brachial index (ABI; a ratio of blood pressures in the foot), improved distal flow, enhanced wound healing and attenuated rest pain at 4-8 weeks after treatment. However, several patients developed peripheral edema in both trials, corresponding temporarily to the rise in VEGF serum levels. In a phase I/IIa trial, HGF-encoding plasmid was administered intramuscularly in the calf or distal thigh of patients with PAD, and the treatment was repeated 4 weeks after the initial injection.[52] A 2-month follow-up revealed that the patients had improved ABI, ulcer healing and pain relief without any side-effects. In a phase II clinical trial, the RAVE (Regional Angiogenesis with Vascular Endothelial Growth Factor) study assessed the effects of adenovirus encoding VEGF injected intramuscularly at a low- or high-dose in patients with IC.[53] No differences in peak walking time, onset of claudication and quality-of-life assessment were observed between the placebo and the low- or high-dosage treatment groups at 12 weeks. Similar trends were observed when a plasmid-expressing developmental endothelial locus-1 (Del-1) or an adenoviral construct encoding HIF-1α were administered intramuscularly in patients with IC, as the treatment and placebo groups showed similar improvements in peak walking time at 3 or 6 months.[32,54,55] Furthermore, intramuscular delivery of plasmid-based FGF-1 in CLI patients has also failed to significantly improve transcutaneous oxygen pressure ($TcPO_2$) or healing of chronic ulcers as compared to the placebo group at 25 weeks.[56] In general, large-scale clinical trials involving gene therapy have demonstrated limited improvements for patients with moderate to severe PAD.

A postulated reasons for the poor translation of gene therapy in clinical trials may be the low DNA transmission efficiency at the targeted ischemic sites after treatment.[26] In addition, vectors such as adenovirus and lentivirus employed in gene therapy may elicit a local and/or systemic inflammatory response.[26] Another potential danger of gene-based therapy involves vector-mediated insertional mutagenesis, as observed in the Fischer

Trial where one patient developed lymphoproliferative disorder ~2.5 years after the retroviral-based treatment.[57]

1.3.2 Cell-based Therapy Approaches for PAD

With the growing understanding of the roles of progenitor and stem/stromal cells co-ordinating concurrent post-ischemic angiogenesis, vasculogenesis and arteriogenesis processes, cell-based therapies have drawn attention as potential treatment options for patients with PAD.[58–60] A variety of cell types have been studied in pre-clinical and clinical trials, including unselected mononuclear cells and marker-specific hematopoietic cells selected from bone marrow or peripheral blood. While early evidence suggested that these cells facilitated vascular regeneration by incorporating directly into the nascent blood vessels, recent studies have shown that the majority of transplanted cells are found adjacent to the newly-formed vasculature and provide paracrine signals to support vascular growth.[61–63] As an illustration, Ziegelhoeffer *et al*. demonstrated via cell tracing of green fluorescent protein (GFP^+)-labeled BM-derived mononuclear cells that intravenously delivered cells in a murine model of hindlimb ischemia failed to colocalize with the ECs or SMCs of the nascent vessels.[64] Instead, GFP^+ cells were localized in the perivascular space of collateral vessels, with a 3-fold higher expression as compared to the vessels in the non-ligated control limb. Multiple studies have supported the notion that transplanted hematopoietic progenitors or more mature cells of the monocyte/macrophage lineage primarily act as trophic mediators during angiogenesis, through the secretion of a broad array of growth factors and chemokines in a temporally and spatially controlled manner.[63,65] Therefore, cell-based strategies may provide a suitable means for continuous delivery of pro-angiogenic factors over an extended period at the target site to facilitate vascular regeneration.

1.3.2.1 Strategies Using Unselected Mononuclear Cells

Mononuclear cells (MNCs), harvested from bone marrow (BM-MNCs) or peripheral blood (PB-MNCs), are comprised of a highly heterogeneous mix of both primitive progenitors and mature hematopoietic cells (90%), and a smaller component of non-hematopoietic cells including rare EPCs and stromal cells.[66,67] In pre-clinical testing,

intramuscular injection of autologous BM-MNCs enhanced collateral vessel and capillary density, and improved perfusion in a rabbit hindlimb ischemia model at 4 weeks as compared to the BM-fibroblast transplanted groups or saline-injected controls.[68] The first randomized, controlled trial for the treatment of ischemic limbs using the MNC population was the TACT (Therapeutic Angiogenesis using Cell Transplantation) study, in which patients with severe limb ischemia received intramuscular injections of autologous BM-MNCs in the affected limb.[69] The study reported improved rest pain, $TcPO_2$, ABI and pain-free walking as compared to the saline-injected control group at 6 months. A 2-year follow-up to the study added that patients injected with BM-MNC had improved walking time/distance and ulcer healing.[70] Considering that cell collection from the blood offers faster recovery and eliminates the need for anesthesia as compared to multiple bone marrow aspirations, PB-MNCs have been investigated as a cell source for pro-regenerative therapy to treat ischemic limbs.[32] For example, Ozturk *et al*. administered autologous PB-MNCs intramuscularly in the affected limbs of diabetic patients with CLI.[71] At 12-weeks, patients demonstrated reduced pain and showed improvements in $TcPO_2$, ABI, walking distance and ulcer healing as compared to the baseline and placebo group.

1.3.2.2 Strategies Using Selected Mononuclear Cells

The discovery of circulating EPCs by Asahara *et al.*[30] showed that a subpopulation of MNCs, which can be isolated based on surface markers such as the progenitor marker CD34, represented a mixture of pro-angiogenic hematopoietic and endothelial cell lineages that were capable of homing to sites of ischemia to facilitate vascular repair.[32,67] In a pre-clinical study, *ex vivo* expanded human EPCs administered through an intracardiac injection in a murine hindlimb ischemia model enhanced capillary density and blood flow in the ischemic limb over 4 weeks as compared to mice injected with EPC-conditioned media.[72] Clinical feasibility of granulocyte colony stimulating factor (G-CSF)-mobilized CD34+ cells for ischemic limb treatment was evaluated in a phase I/IIa trial, where cells were harvested by leukapheresis, purified for CD34-expression, and injected intramuscularly (3 doses: 10^5, 5×10^5, 10^6 cells/kg) into the more severely ischemic leg of patients with bilateral PAD.[73] Although no dose-dependent relationship

was established after 12 weeks, the treated leg exhibited significant improvements in ulcer size, pain and walking distance as compared to baseline levels, and exhibited increased $TcPO_2$ as compared to the untreated leg. Long-term clinical benefits of autologous G-CSF-mobilized CD34+ cells were also reported by Losordo *et al*. in the ACT-34 CLI (Autologous Cell Therapy-34 Critical Limb Ischemia) phase I/II study, where intramuscular administration of the cells within the ischemic lower limb of patients with moderate to severe CLI reduced the incidence of amputation in the cell-treated groups as compared to the control group at 12 months.[74]

High aldehyde dehydrogenase (ALDH) activity has also been used as a marker to isolate pro-angiogenic cell populations within the heterogeneous mix of MNCs. ALDH is an oxidizing enzyme with high expression in primitive hematopoietic progenitors, and BM-MNCs can be selected for high ALDH expression in the population that is $CD34^+$, $CD133^+$, $CD13^+$ and $CD117^+$.[75,76] Pre-clinically, human BM-MNCs selected for high ALDH expression and administered in a murine hindlimb ischemia model through tail vein injection enhanced perfusion recovery and increased blood vessel density as compared to PBS-injected and unpurified MNC-treated groups over 21 days.[77] A phase I controlled clinical trial compared the efficacy of unselected BM-MNCs and BM-MNCs selected for high ALDH activity by injecting autologous cells in the gastrocnemius muscle of the affected limb in patients with CLI.[78] Although both groups demonstrated significant ABI improvements from baseline at 12 weeks, neither group showed significant improvement in ischemic ulcers or $TcPO_2$.

1.3.2.3 Current Limitations of Cell-based Therapeutic Approaches

Although direct intramuscular administration of pro-regenerative cells at ischemic sites has shown some potential in stimulating new blood vessel growth, the application of cell-based interventions in the clinical setting faces several limitations. First, the feasibility of cell-based therapies is dependent on the abundance and accessibility of the cell source. Depending on the cell types used, therapy is predicted to require at least 10^7 to 10^9 cells per patient.[79] In terms of the cell type used, mononuclear cells are a highly heterogeneous cell population, with only a small fraction possessing pro-angiogenic capacity.[80] For example, the low frequency (1-2%) of pro-angiogenic $CD34^+$ hematopoietic progenitor

cells in the mononuclear cell population isolated from bone marrow or umbilical cord may require clinicians to obtain large sample volumes that may not be practical in all cases.[69,79,81] Significant *in vitro* expansion of pro-regenerative cells needed for cell-based therapy may also contribute towards diminished cell function.[82] In addition, autologous cells from patients with chronic diabetes and associated comorbidities have been shown to have impaired function and reduced survival, thus limiting their pro-angiogenic effects.[83,84]

Another major roadblock for cell-therapy is the poor localization, retention and survival of transplanted cells in the targeted tissues.[85,86] While current approaches stimulate angiogenesis by injecting cell suspensions either intra-arterially or directly into the ischemic tissue, the viability and desired function of transplanted cells at the targeted sites remains limited. As an illustration, Collins *et al*. reported that human BM-MSCs injected into the ischemic rat heart showed only 9% and 1% cell retention within the targeted tissue at 24 hours and 5 days post-transplantation, respectively.[87] Poor retention may be explained by cell washout after direct injection, cell migration into the circulation and peripheral tissues, or cell death due to local hypoxic and inflammatory conditions.[85]

While the clinical trials with cell-based therapy have been safe, well tolerated, and showed some beneficial effects, with the exception of the ACT-34 CLI trial, limb salvage rates were generally not reduced to clinically significant levels and the field still awaits a successful phase II – III study for CLI.[32] As such, there is a critical need to select potent pro-angiogenic cell populations and design cell delivery modalities that improve cell survival, retention and paracrine function post-transplantation to better stimulate vascular regeneration and functional recovery in ischemic tissues.

1.4 Mesenchymal Stem/Stromal Cells for Cell-based Angiogenic Therapies

Mesenchymal stem/stromal cells (MSCs) are fibroblast-like plastic adherent cells that can be derived from a variety of tissues, including bone marrow, adipose tissue and skeletal muscle, and hold the potential to circumvent some of the practical limitations associated with cell-based therapies for PAD.[88] MSCs are efficiently expanded in culture and retain

the capacity to differentiate into multiple different cell types associated with the mesodermal lineage, including adipocytes, osteocytes, chondrocytes and myocytes.[89] While the regulation of paracrine activity in MSCs is not completely understood, studies have shown that these cells migrate to sites of ischemic injury from their perivascular niche, and secrete bioactive factors that can stimulate angiogenesis, limit apoptosis, modulate inflammation, and enhance endogenous cell recruitment to the site of injury.[90,91] In addition, MSCs have been shown to be resilient to apoptosis under serum-starvation or hypoxic conditions, making them a promising source for cell-based therapies targeted for ischemic tissues.[92] MSCs can be used for autologous or allogeneic therapeutic applications due to their ability to evade immune-surveillance resulting from the low expression of the major histocompatibility complex II antigen.[93,94] In addition to their pro-angiogenic paracrine capacity, MSCs demonstrate immuno-modulating effects at ischemic sites via the suppression of inflammatory cytokine production and by attenuating T-cell activation, proliferation, and migration.[94]

Due to their pro-regenerative properties, MSCs have also been pursued as a potential candidate for cell-based therapies.[95] In a pre-clinical trial, autologous BM-MSCs injected intramuscularly in a femoral artery ligation (FAL)-induced rabbit hindlimb ischemia model significantly increased limb perfusion and capillary/muscle fiber density in the treated limbs as compared to saline-injected control limbs at 28 days.[96] Similarly, human placental-derived MSCs cultured under hypoxic conditions (2% O_2) significantly improved microvessel density, blood perfusion and physiological status (limb salvage and foot necrosis) in the treated limb as compared to PBS controls over 28 days following intramuscular injection in a murine hindlimb ischemia model.[97]

In a randomized controlled clinical trial, either BM-MNCs or BM-MSCs were injected intramuscularly into the lower limbs of diabetic patients with CLI.[98] While both groups significantly improved pain-free walking time at 6 months as compared to saline injected controls, the BM-MSC treated group showed significantly greater collateral blood vessel scores and faster ulcer healing time (8 vs. 12 weeks) relative to the BM-MNC group, suggesting the potential benefits of MSCs over unselected BM-MNCs. More recently, human BM-MSCs isolated from healthy donors were expanded *in vitro* and injected into

the gastrocnemius muscle of the ischemic lower limb of patients with CLI.[99] At 24 weeks, patients demonstrated significantly higher ABI and reduced pain as compared to baseline levels and the placebo group. Given these positive outcomes, MSCs provide a clinically-applicable pro-regenerative cell population for future cell-based therapy.

1.4.1 Adipose-derived Stem/Stromal Cells (ASCs)

Adipose-derived stem/stromal cells (ASCs) have gained interest as an attractive MSC cell-type for regenerative therapies due to their relative abundance, accessibility, and secretory functions.[93,100] ASCs are derived from adipose tissue and have promising characteristics for applications in therapeutic angiogenesis.[93] ASCs actively secrete multiple pro-angiogenic factors and cytokines, including VEGF, FGF-2, HGF, PDGF and TGF-β, that are involved in the process of vascular regeneration.[101] ASCs can also be readily expanded in culture, and have been shown to establish a regenerative milieu *in vivo* through paracrine mechanisms.[93,102–104]

In addition to their pro-angiogenic stimulatory potential, ASCs offer practical advantages for their clinical applicability in cell-based therapies. Although MSCs can be sourced from the patient's own bone marrow, the retrieval process is invasive, painful and may not be ideal for individuals with adverse vascular conditions such as CLI. In contrast, adipose tissue can be harvested via minimally-invasive liposuction techniques under local anesthesia, with minor morbidity.[93] In addition, compared to the MSC frequency of 1:50,000–1:1,000,000 in bone marrow, ASC frequency in human adipose tissue ranges between 1:30–1:100 per total nucleated cells, and therefore requires less tissue to generate significant numbers of ASCs for cell-based therapies.[85,100,105,106] Furthermore, a limited volume of bone marrow can be safely harvested from each donor, which could necessitate significant *in vitro* expansion of BM-MSCs for cell-based therapies. Adipose tissue however, offers a source of MSCs in high abundance with large proliferative potential, thereby enhancing the feasibility of safely harvesting the required volumes of adipose tissue and minimizing culture times for *ex vivo* expansion.[79,88]

In pre-clinical testing, intramuscular injection of human ASCs into the ischemic limb of nude mice with FAL-induced hindlimb ischemia significantly enhanced vascular density

and blood flow in the treated limb as compared to the saline-injected control limb at 14 days.[107] Similarly, ASCs isolated from murine inguinal fat pads and transplanted intramuscularly into the ischemic hindlimb of mice enhanced capillary density within the thigh adductor muscles and improved blood flow as compared to saline-injected controls at 4 weeks.[108] The first phase I clinical trial utilizing autologous MSCs isolated from abdominal fat of CLI patients, ACellDream (Adipose Cell Derived Endothelial Regenerative Endothelial Angiogenic Medicine), demonstrated that intramuscular administration of the cells in the ischemic limb improved rest pain, $TcPO_2$ and wound-healing response at 24 weeks.[109] Intramuscular administration of autologous adipose-derived MSCs around the edges of chronic ulcers in PAD patients significantly reduced the depth and diameter of the wounds over 90 days, while also reducing the wound-associated pain.[110] Therefore, ASCs have demonstrated pro-regenerative potential in cell-based therapies.

1.4.2 Immunophenotype of ASCs

The primary stromal vascular fraction (SVF) isolated after adipose tissue digestion consists of a heterogeneous cell population, including ASCs, vascular endothelial and smooth muscle cells, pre-adipocytes, fibroblasts, erythroblasts, pericytes and hematopoietic cells.[111] This heterogeneity is reduced by using expansion conditions that select for plastic-adherent stromal cells. ASC characterization has been defined under the guidelines of the International Society for Cellular Therapy (ISCT) and the International Federation for Adipose Therapeutics and Science (IFATS).[112] To adhere to the ASC characterization criteria, ASCs must: (1) maintain plastic adherence in cell culture, (2) express a standardized immunophenotypic profile, and (3) maintain tri-lineage differentiation capacity along the adipogenic, osteogenic, and chondrogenic lineages.

According to the ISCT and IFATS, ASCs must show >80% expression of defined stromal cell markers (CD90, CD44, CD29, CD73 and CD105) and <2% expression of hematopoietic (CD45) and endothelial (CD31) cell specific markers.[112] ASCs have been shown to express a fairly robust immunophenotypic profile as summarized in Table 1.2.[93,112–114] As demonstrated by Mitchell *et al*., successive passaging of ASCs may alter expression of certain cell surface markers.[100] For example, while the surface marker

expression of CD34 and CD146 were ~60% and 21% in the initial SVF, the expression of each marker declined to ~2% by passage 3 for human ASCs.[100]

Table 1.2. Immunophenotypic profile of ASCs.[93,112–114]

Marker type	Category	Antigen
Positive (>80%)	Adhesion molecules	CD29 (integrin β1) CD105 (endoglin) CD50 (intercellular adhesion molecule 1) CD54 (intercellular adhesion molecule 3) CD166 (activated lymphocyte cell adhesion molecule)
	Receptor molecules	CD44 (hyaluronic acid receptor) CD71 (transferrin receptor)
	Surface enzymes	CD73 (ecto 5'nucleotidase) CD13 (aminopeptidase) CD10 (neutral endopeptidase)
	Surface glycoproteins	CD90 (Thy-1) CD147 (neurothelin) CD146 (melanoma cell adhesion molecule)* CD34 (progenitor associated marker)*
Negative (<2%)	Adhesion molecules	CD31 (platelet endothelial cell adhesion molecule) CD106 (vascular cell adhesion molecule)
	Receptor molecules	CD45 (leukocyte common antigen) CD3 (T-cell co-receptor)
	Surface glycoprotein	CD133 (hematopoietic and endothelial progenitor marker)

**Variable levels of expression.*[100]

1.4.3 Influence of Hypoxia on ASCs

As PAD progresses, the lack of oxygenated blood flow to the distal limb creates a hypoxic microenvironment, resulting in cell apoptosis and subsequent necrosis of the affected tissues.[115] A $TcPO_2$ of <20 mm Hg (<2% O_2) in the lower extremity is correlated with impaired healing, requiring patients to undergo revascularization procedures or amputation to treat the severe conditions.[115] Therefore, the efficacy of cell-based therapy

for PAD relies on the transplanted cells being able to survive and function in microenvironments with low oxygen tension.

Under hypoxic conditions, ASCs have been shown to upregulate expression of several pro-angiogenic genes, including VEGF, FGF-2, HGF, Ang-1, PDGF and SDF-1, and cytokines such as interleukin-10 (IL10) and interleukin-8 (IL-8).[116–118] The elevated expression of these pro-angiogenic molecules is achieved through the activity of HIF-1α under low oxygen tension (<5% O_2).[119–121] One study showed that the conditioned medium obtained from human ASCs cultured under hypoxic conditions (1% O_2) can improve endothelial cell growth and reduce apoptosis.[122] In addition, hypoxic pre-conditioning of human ASCs enhances their ability to bind to vascular cell adhesion molecule-1 (VCAM-1) and endothelial intercellular adhesion molecule-1 (ICAM-1), suggesting the potential for augmented attachment to endothelial cells in ischemic regions.[123] Hypoxic conditions (1% O_2) have also been shown to enhance human ASC proliferation *in vitro* by >1.5-fold as compared to ASCs cultured under 20% O_2 over 7 days.[124] Collectively, ASCs are generally resilient to hypoxic conditions in terms of survival and function, thus providing support for their use in cell-based therapies to promote angiogenesis at ischemic sites.

1.5 Biomaterials for Scaffold-based Cell Delivery

As discussed earlier, poor retention and survival of transplanted cells are major limitations identified in previous studies of cell-based therapies for PAD.[85,125,126] As a result, scaffold-based cell delivery strategy has emerged to circumvent cell loss by providing anchorage for the transplanted cells while promoting cell viability and function at ischemic sites.[127] Scaffolds can be developed to have similar porosity and nanostructure as the native ECM to support *in vivo* engraftment, and can also be modified with cell-signaling moieties to facilitate cell-cell and cell-ECM interactions.[127] Therefore, in-depth analysis of biomaterial design is required to develop promising scaffolds for cell-based therapy.

1.5.1 Scaffold Design Requirements

Designing a cell-delivery scaffold for enhancing transplanted ASC survival within the context of PAD requires careful consideration of material requirements. Ideally, the scaffold should retain viable cells at the target site over the course of tissue regeneration. In addition, the scaffold should provide anchorage for encapsulated cells to support cell function by promoting the sustained delivery of pro-regenerative paracrine factors into the ischemic region.[85] To facilitate the intended role of ASCs as trophic mediators, the scaffold must allow for easy diffusion of nutrients and factors between encapsulated ASCs and the surrounding microenvironment.[128] Furthermore, the mechanical properties of the scaffold should align with those of the surrounding tissues at the target site to minimize physical irritation, prevent inflammation and facilitate integration of the scaffold after delivery.[129] For instance, the Young's modulus of the medial gastrocnemius in the limb of resting human subjects is ~16 kPa.[130] Accordingly, a scaffold with similar mechanical properties would promote better integration within the target muscle in patients with PAD. In addition, the scaffold should be pliable, durable, and able to resist repeated mechanical deformation during muscle contractions with minimal risk of fracture.[129] Lastly, the transplanted scaffold should also undergo biodegradation at a slow rate to retain the transplanted cells during the course of the therapy, and break down in a manner that does not interfere with ongoing vascular remodeling processes.[16]

In general, two methods of scaffold delivery have been investigated in the context of pro-angiogenic cell therapies. One option is the surgical implantation of cell-seeded pre-formed scaffolds. Although pre-formed scaffolds allow for greater control over scaffold shape, this approach requires invasive surgical techniques for implantation at target sites.[85] A less invasive approach is to deliver a bolus of cells suspended in an aqueous polymer precursor solution (pre-polymer) as an injectable substrate that subsequently cross-links *in situ* to form a robust hydrogel scaffold, effectively encapsulating the delivered cells.[16,85] Injectable delivery offers several advantages for PAD treatment including minimally-invasive cell delivery using a small gauze needle, shorter procedure time, and minimal damage to the already compromised ischemic region.[85] Due to these

benefits, our collaborative team has focused on investigating the use of cross-linkable polymers as an *in situ*-gelling cell delivery scaffold.

1.5.1.1 Hydrogels

Hydrogels are water-swollen polymer networks that are physically or chemically cross-linked.[16] They can be prepared from biocompatible and biodegradable polymers that provide a supportive microenvironment for cell-delivery applications.[131] Since hydrogels are inherently well hydrated, they allow for easy diffusion of gasses, nutrients, metabolic products and bioactive molecules from within the scaffold to the surrounding tissues.[131] Additionally, the mechanical properties of the hydrogel can be controlled through cross-linking density, electrostatic interactions of the polymer chains, and the degree of swelling to tailor their use towards the *in vivo* environment of the target tissue.[16] Generally, the pre-polymer solution is combined with the cells of interest in an aqueous medium and injected into the target site, where it subsequently cross-links to form a scaffold *in situ*.

Several natural and synthetic polymers have been investigated as cell delivery vehicles. Scaffolds comprised of synthetic polymers, including poly(ethylene glycol), poly(lactic acid), poly(N-isopropylacrylamide) and poly(vinyl alcohol), offer several advantages such as batch-to-batch consistency, amenability to chemical functionalization, and precise control over mechanical and degradation properties.[85] However, they lack the innate bioactivity of natural materials that can better support cell adhesion, viability, migration, and differentiation.[85,132] Furthermore, acidic degradation products of synthetic polymers such as poly(lactic acid) can be cytotoxic and may trigger inflammatory responses.[133,134] Concerns regarding *in vivo* excretion also exist with synthetic scaffolds. For example, poly(N-isopropylacrylamide) may accumulate in the liver and spleen to a significant extent within 48 h of intravenous administration, regardless of its molecular weight.[135] To circumvent the limitations of synthetic materials, several major classes of naturally-derived or semi-synthetic polymers have been studied within the context of ischemic conditions, as described in detail in section 1.5.2.

1.5.1.2 Cross-linking Strategy

An injectable cell-delivery scaffold requires a cross-linking mechanism that allows for cell loading in the aqueous phase, but then forms a cell-encapsulated matrix following injection. An efficient mechanism should initiate gelation in a triggered or controlled fashion in order to prevent premature or delayed cross-linking, and the cross-linking should not initiate an immunogenic response.[85] Most importantly, the cross-linking mechanism should be cytocompatible to encapsulated cells, as well as the surrounding host tissues.[85]

Although several physical and chemical methods have been investigated to facilitate cross-linking of hydrogel polymer networks, there are a limited number of clinically-applicable cross-linking strategies appropriate for cell encapsulation. For instance, glutaraldehyde cross-linking of hydroxylated polymers requires methanol, low pH and high temperatures.[136,137] These conditions, along with the inherent reactivity of glutaraldehyde to amines, amides and thiol groups in proteins, would render this approach cytotoxic for the encapsulated cells and could further damage the ischemic tissues.[138]

Hydrophilic polymers including hyaluronic acid (HA), chitosan, and chondroitin sulfate can be modified to undergo chemical cross-linking via radically-initiated methacrylate or acrylate polymerization.[129,139] The methacrylate and acrylate groups contain highly reactive double bonds that propagate cross-linking through free-radical polymerization.[140,141] This cross-linking approach can offer flexibility in terms of the pH, osmolarity, and temperature conditions, and may present an attractive strategy for *in situ* gelation of polymer scaffolds. For instance, low-intensity UV cross-linking of methacrylated glycol chitosan in the presence of the photo-initiator Irgacure 2959 has been shown to generate hydrogels with high cross-linking efficiency.[140] Although UV cross-linking of methacrylated polymers is effective *in vitro*, direct access of a UV light at the site of delivery increases invasiveness of implantation and limits clinical applicability. Alternatively, a chemical initiator to catalyze free-radical polymerization using ammonium persulfate (APS) and the accelerator *N,N,N'N'*-

tetramethylethylenediamine (TEMED) offers an attractive cross-linking approach. This system of redox initiators generates free radical species, which subsequently facilitate methacrylate cross-linking at 37ºC.[142,143] The efficacy of this thermally-sensitive cross-linking approach has been previously shown *in vitro* and *in vivo*.[129,144] For example, one study used 25 mM APS/TEMED to encapsulate rat BM-MSCs in diacrylate-modified oligo[poly(ethelene glycol) fumarate] hydrogels at 37ºC.[144] Over a 28-day culture period, the encapsulated cells were able to maintain viability and differentiate in the presence of osteogenic supplements. Therefore, APS/TEMED-facilitated free-radical polymerization of methacrylate- or acrylate-functionalized scaffolds offers a promising cross-linking strategy for *in situ* gelation and cell encapsulation.

1.5.1.3 Cell-adhesive Peptide Ligand Functionalization

With increasing understanding of the important roles of cell-ECM interactions in mediating cell function, there is great interest in the development of novel biomaterials that mimic the native tissue microenvironment. While cross-linking allows for the manipulation of the mechanical properties of the scaffolds, biomaterials can be functionalized with bioactive moieties to further direct cell function. Some studies have explored the incorporation of full-length ECM proteins such as collagen, fibronectin, vitronectin and laminin. Alternatively, polymers can be modified with small bioactive peptide ligands derived from these common ECM proteins, such as the integrin-binding RGD, IKVAV or YIGSR sequences.[145,146]

These ECM-derived peptide ligands bind to integrins—a diverse class of α/β heterodimeric transmembrane cell-adhesion receptors (Figure 1.1).[147] While each α/β-heterodimer has its own ligand binding specificity, many integrins bind more than one peptide ligand.[148,149] Integrin-mediated binding of cells with ECM-derived peptide ligands has been shown to mediate a variety of cell responses including attachment, growth and motility.[150–152] Although the specific mechanisms are still being elucidated, integrin engagement facilitates transduction pathways through phosphorylation of intracellular proteins and second messenger signaling to promote cell adhesion, survival, proliferation and migration (Figure 1.1).[153,154] Individual cells can also vary their adhesive and migratory properties by selective expression of integrins with varying α/β

subunit composition.[149] Importantly, cells detached from their ECM have been shown to undergo apoptosis in an integrin-mediated pattern known as anoikis.[155] As an illustration, fibronectin or vitronectin binding via integrins $\alpha_5\beta_1$ and $\alpha_v\beta_3$ in hamster ovary cells decreased the activity of apoptosis-inducing caspase-3 protein, and enhanced the expression of B-cell lymphoma-2 (Bcl-2), a regulatory protein that inhibits apoptosis.[156] In general, the functionalization of scaffolds with integrin-binding cell-adhesive peptides is of interest in the field to promote long-term cell survival, retention and support pro-regenerative cell functions.

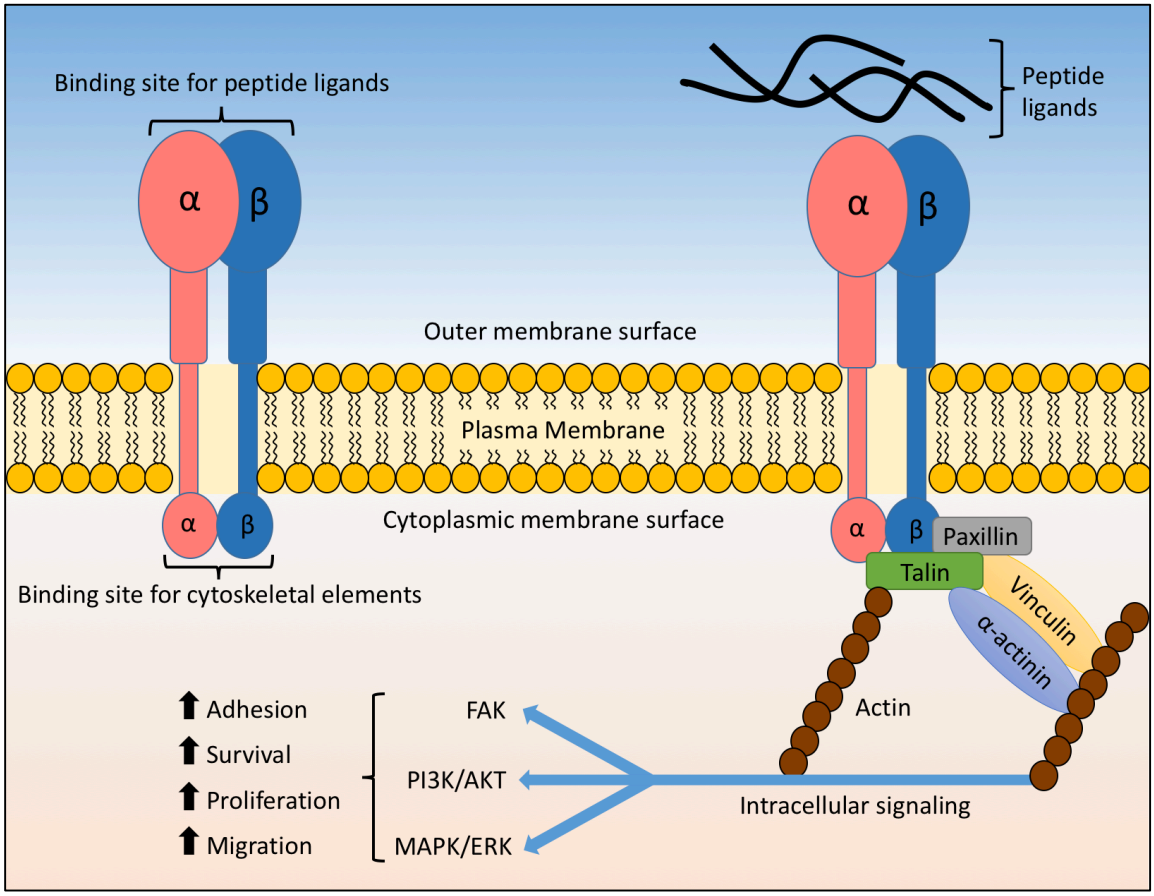

Figure 1.1. Schematic representation of integrin structure. Integrins are heterodimeric receptors consisting of non-covalently bound α and β subunits. Both α and β subunits have an extracellular domain that binds to peptide ligands (e.g. RGD, IKVAV, etc.), and a short cytoplasmic tail that interacts with cytoskeletal elements. Integrin engagement facilitates downstream intracellular signaling, influencing various transduction pathways and mediating multiple cell functions. Image adapted from Millard *et al*.[157] FAK: focal adhesion kinase; PI3K: phosphoinositide 3-kinase; Akt: protein kinase B; MAPK: mitogen-activated protein kinase; ERK: extracellular signal-regulated kinase.

1.5.1.3.1 Arginine-Glycine-Aspartic Acid (RGD) Motif

The tri-peptide arginine-glycine-aspartic acid motif, or RGD, is an integrin-binding sequence derived from fibronectin and collagen.[158] RGD is a well characterized adhesion motif that was originally shown to facilitate binding through the $\alpha_1\beta_1$ complex.[158] Currently, as many as 12 out of the 20 known integrins have been shown to recognize the RGD sequence, including $\alpha_v\beta_3$ and $\alpha_5\beta_1$.[158] Since RGD is found in many cell adhesion proteins, it has been used to promote cell attachment to various biomaterials and can be recognized by many cell types, including MSCs.[159–161] For example, rat BM-MSCs seeded within RGD-modified oligo[poly(ethylene glycol) fumarate] hydrogels have demonstrated improved cell adhesion and spreading.[162] More recently, mouse BM-MSCs encapsulated within HA hydrogels demonstrated enhanced cell attachment, spreading and β_1 integrin expression in a dose-dependent manner when presented with RGD motifs.[163] In a comparative study, RGD-modified poly(ethylene glycol) (PEG) hydrogels demonstrated improved viability of seeded human BM-MSCs as compared to unmodified controls over 7 days, while this effect was less pronounced in IKVAV-modified hydrogels.[164]

1.5.1.3.2 Isoleucine-Lysine-Valine-Alanine-Valine (IKVAV) Motif

Laminin is a basement membrane glycoprotein with diverse biological roles.[165] The isoleucine-lysine-valine-alanine-valine motif, or IKVAV, derived from the laminin-α1 chain has been suggested as the sequence that facilitates cell adhesion, spreading and outgrowth.[165] Interestingly, rat pre-adipocytes demonstrated enhanced $\alpha_1\beta_1$-mediated adherence on laminin-1 treated ECM substrates as compared to fibronectin and collagen treated groups.[166] Immobilization of IKVAV motifs on collagen type I hydrogels has also been shown to stimulate migration, adhesion, and capillary network formation in vascular endothelial cells.[167] Further, human neural stem cells encapsulated within silk fibroin-based hydrogels covalently modified with IKVAV peptides enhanced cell viability and differentiation capacity relative to non-peptide modified controls.[168] In addition, supplementation of IKVAV peptide in cell culture media has been shown to induce proliferation of human BM-MSCs in a dose-dependent manner, mediated through the activation of the extracellular signal-regulated kinase 1/2 (ERK1/2) and protein

kinase B (Akt) signaling pathways, and through augmented cell cycle progression into S phase.[169] Taken together, the pro-survival effects of the integrin-binding RGD and IKVAV peptide ligands have been well documented, providing a rationale for incorporating these motifs within cell-delivery scaffolds.

1.5.2 Polymers for Hydrogel Scaffold

1.5.2.1 Chitosan

Chitosan is the deacetylated form of the linear polysaccharide chitin—a component of crustacean exoskeletons—and consists of random (1-4)-linked β-D-glucosamine and N-acetyl-D-glucosamine monomers (Figure 1.2A).[85] Chitosan is an attractive material for cell-delivery applications due to its cytocompatible, biodegradable, hemostatic, antimicrobial and wound healing properties.[170–172] Chitosan has also been suggested to induce neovascularization in ischemic tissues due to its innate pro-angiogenic nature.[173,174] The electrostatic interactions of chitosan with glycosaminoglycans (GAGs), proteoglycans and other negatively charged species in the body have the potential benefit of sequestering pro-regenerative growth factors and facilitating scaffold integration with the native tissues.[175] Chitosan can undergo degradation *in vivo* through the action of lysozymes via hydrolysis, generating biocompatible oligosaccharides and glucosamines.[170,176] In addition, components of chitosan have been shown to improve cell viability by protecting the cells from reactive oxygen species (ROS), such as H_2O_2, generated in the ischemic tissues.[174] In addition, chitosan-based hydrogels have been previously explored to promote cell retention *in vivo*. For example, a temperature-sensitive chitosan hydrogel was used to encapsulate and deliver rat ASCs in a rat MI model.[174] The findings indicated that a higher retention of transplanted cells was noted with hydrogel-based cell delivery as compared to PBS controls over 28 days.

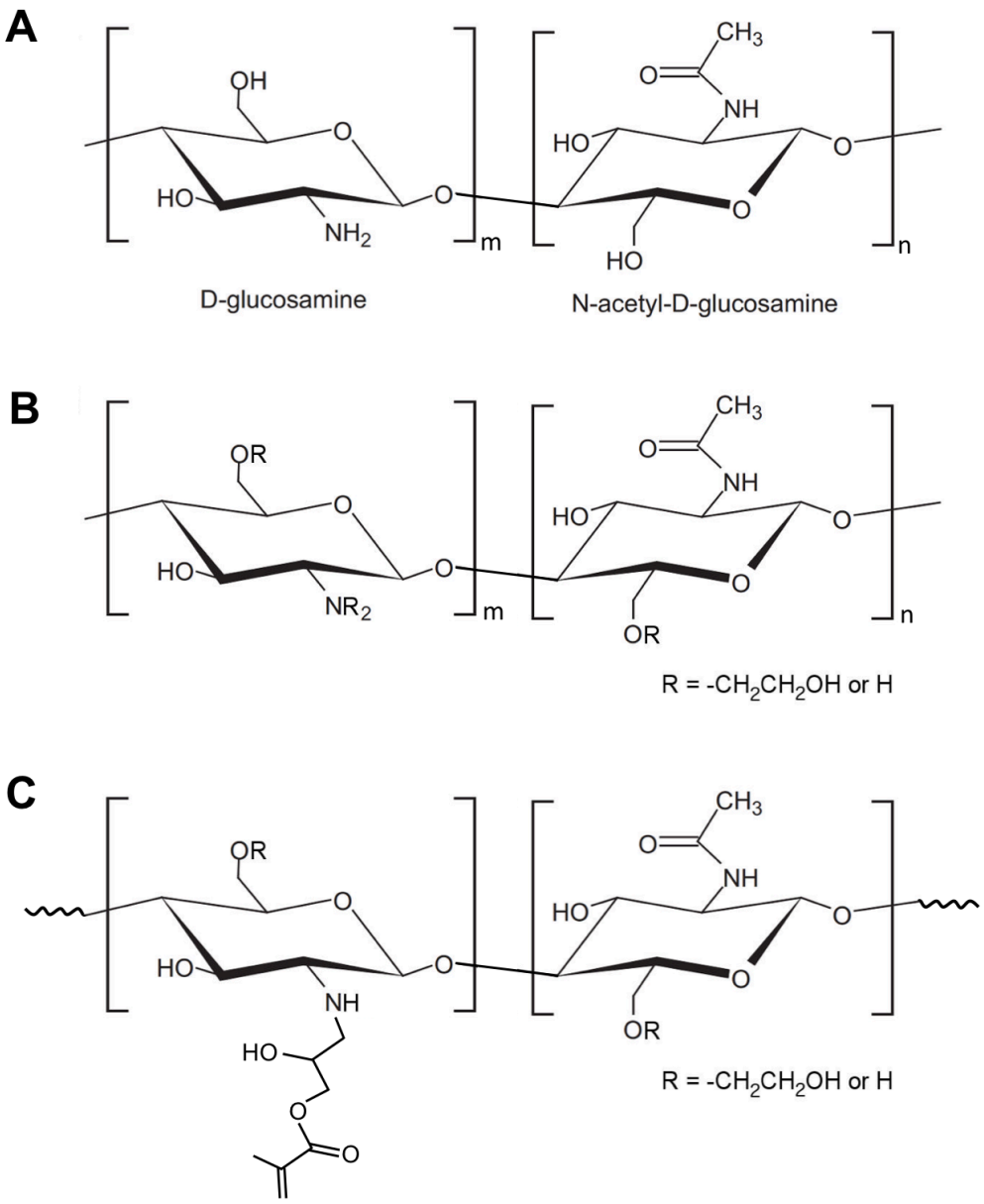

Figure 1.2. Chemical structure of chitosan and its derivatives. (A) Chitosan, composed of (1-4)-linked β-D-glucosamine and N-acetyl-D-glucosamine monomers, (B) glycol chitosan, and (C) *N*-methacrylate glycol chitosan. Images adapted form Russo *et al*.[85]

Although chitosan demonstrates limited solubility in aqueous environments at physiological pH, its glycosylated form known as glycol chitosan (GC) (Figure 1.2B) is soluble between pH 2-12.[177] Furthermore, GC can be functionalized with methacrylate groups via a ring opening reaction with glycidyl methacrylate (GMA) to form *N*-methacrylate glycol chitosan (MGC) (Figure 1.2C).[140] To initiate cell encapsulation, the MGC pre-polymer and cell suspension can be mixed with APS and TEMED at room

temperature. Although the formation of radical species begins immediately, the slow rate of this reaction at room temperature allows for easy handling of the material. Upon injection or incubation at 37ºC, the elevated temperature increases the rate of the initiator decomposition and free-radical formation. The increased molecular kinetics at higher temperatures also enhances the mobility of the polymer chains, resulting in cross-linking of the methacrylate groups and rapid gelation of the MGC to facilitate cell encapsulation.[129,144,178] Therefore, the pro-regenerative and cytocompatible nature of chitosan, combined with the practical advantages offered by the MGC polymer, lend support for its use as a bioscaffold in cell-based delivery, as investigated in this thesis.

1.5.2.2 Alginate

Derived from brown seaweed and algae, alginate is a natural anionic polysaccharide composed of (1-4)-linked β-D-mannuronic acid (M unit) and α-L-guluronic acid (G unit).[85] Addition of divalent cations such as Ca^{2+} and Ba^{2+} causes the G unit blocks on adjacent chains to bind and form an ionic cross-linked network.[85] Silva *et al.* demonstrated that the combination of VEGF and human umbilical cord blood-derived EPCs pre-seeded on implantable peptide-modified alginate scaffolds was able to improve vessel density, restore perfusion and salvage ischemic limbs in a murine model of hindlimb ischemia.[179] In addition, alginate has been studied as an injectable cell delivery vehicle in pre-clinical models of MI, where the increased post-MI concentration of calcium ions facilitates the physical cross-linking process.[180,181] As such, the gelation and degradation of alginate hydrogels is dependent on the local cation concentration in ischemic tissues and ion efflux into the surrounding tissues, respectively. This leads to an uncontrolled cross-linking approach, with degradation products being eliminated by the kidneys if below the excretion limit of 48 kg/mol.[182] Furthermore, the hydrophilic nature of alginate necessitates grafting of cell-adhesive peptide ligands to promote encapsulated cell viability, as the unmodified scaffold limits protein adsorption and cellular attachment.[183]

1.5.2.3 Collagen

Being a key component in the ECM, type I collagen derived from bovine or porcine tissues has been studied as a natural scaffold.[85] It is also commercially-available and can be prepared as an injectable hydrogel by acid-solubilization.[184] Collagen can undergo entropy-driven self-assembly through fibriollogenesis to form a physically cross-linked hydrogel capable of encapsulating cells upon *in vivo* injection at neutral pH and 37ºC.[184,185] Although collagen-based hydrogels support cell encapsulation and attachment, the solubilization process causes the hydrogel to lack elements of structural integrity and organization, including stiffness and elasticity.[186] Furthermore, the cross-linking process is sensitive to *in situ* variations of pH and salt concentration, resulting in poor control over gelation and degradation of the scaffold.[186] Delivery of radio-labeled MSCs via collagen hydrogels in a pre-clinical rat model of MI demonstrated that the hydrogel transiently improved MSC retention as compared to saline-delivered cells at 4 weeks.[187] However, the scaffold attenuated long-term survival of encapsulated MSCs by impairing oxygen and nutrient exchange.

1.5.2.4 Fibrin

Fibrin is a fibrous, non-globular protein that is involved in the coagulation cascades, and thus contains intrinsic sites for cell binding.[85] Fibrin hydrogels are formed when fibrinogen is cleaved by thrombin, resulting in the rapid aggregation of the insoluble fibrin peptides that creates a fibril network capable of encapsulating cells.[188] Due to the cross-linking nature of fibrin, the physical properties of the hydrogels, including gelation kinetics, stiffness and elastic moduli, can be tailored by altering the concentrations of thrombin and fibrinogen.[189] Enzymatic degradation of fibrin produces non-immmunogenic amino acid products that may also contribute towards angiogenesis.[190] Fibrin has been previously used as a delivery vehicle for MSCs or growth factors in pre-clinical models of ischemia, and has been shown to promote functional repair in rat MI models over PBS controls.[191] However, fibrin hydrogels have demonstrated poor mechanical properties *in situ*.[192,193] Furthermore, commercially-available fibrin glues have failed to show improvement in long-term cell retention and function after injection.[194]

1.5.2.5 Hyaluronic Acid

Hyaluronic acid, or HA, is a linear glycosaminoglycan composed of repeating disaccharide units of (1-4)-linked β-D-glucuronic acid and (1-3)-linked β-*N*-acetyl-D-glucosamine.[85] As a widely distributed component of the ECM in mammalian tissues, HA is involved in cellular proliferation and differentiation, and has been shown to have pro-angiogenic effects.[195] In a pre-clinical model of murine hindlimb ischemia, delivery of human umbilical vein endothelial cells (HUVECs) in combination with injectable HA resulted in prolonged cell retention, survival and cellular engraftment into the endothelium.[196] HA can also be modified to produce a cross-linkable methacrylated HA (MeHA) that can undergo free-radical mediated polymerization to form a hydrogel.[129] Cell-free delivery of MeHA hydrogels has demonstrated potential in promoting the remodeling of ischemic tissues in a pre-clinical ovine MI model.[139] However, the long-term potential of HA as a cell-delivery scaffold is hindered by its rapid enzymatic degradation *in vivo*, with unmodified HA degrading into glucuronic acid and N-acetylglucosamine at a rate of 5 g/day.[197]

1.5.2.6 Matrigel™

Generated by murine tumor cells, Matrigel™ is a commercially-available material composed of laminin, entactin, collagen IV and other ECM components.[85] Previous pre-clinical research with a rat MI model demonstrated that the delivery of human embryonic stem cells (ESC)-derived cardiomyocytes in a Matrigel™ scaffold at ischemic sites resulted in poor cell viability and retention.[198] When the study was repeated with a combination of cells and pro-survival growth factors delivered via the Matrigel™ scaffold, the comprehensive approach led to augmented cell survival and cell retention at the targeted ischemic site at 4 weeks.[198] Despite these promising results, the xenogenic and tumorogenic origins of Matrigel™ prohibits its widespread translation in clinical applications.[199]

1.6 Summary

The rising incidence and limited treatment options for PAD motivate the need for new minimally-invasive treatment approaches to help stimulate new blood vessel formation

and tissue regeneration.[1] Using an integrative approach combining cell-based therapy with scaffold-based delivery may improve angiogenesis inducing therapies for PAD and CLI. ASCs isolated from human adipose tissue offer a promising source for cell-based therapy due to their accessibility, high proliferative capacity, and paracrine function that stimulates pro-angiogenic responses and modulates inflammation.[93,102–104] To address the poor survival and retention of transplanted cells, ASCs will be delivered in a thermally-sensitive MGC pre-polymer that cross-links into a hydrogel through free radical polymerization using an APS/TEMED initiator system.[142,143] To promote ASC adhesion and retention within the hydrogel, MGC will be functionalized with integrin-binding peptide ligands, including RGD found in fibronectin and collagen, or IKVAV derived from the laminin-α1 chain.[145,165] The overarching goals of this thesis were to: (i) assess the viability and pro-angiogenic capacity of human ASCs encapsulated in the MGC hydrogels through *in vitro* and *in vivo* studies, and (ii) examine the effects of modifying the MGC with cell-adhesive RGD or IKVAV motifs on encapsulated cell function. Overall, this project aims to provide fundamental insight into the angiogenic function of human ASCs within 3-D engineered cellular microenvironments, and represents a critical next step in the rational design of a cell delivery vehicle for therapeutic angiogenesis.

1.6.1 Hypotheses

The underlying hypotheses for this project were that *in situ* cross-linking MGC hydrogels would provide a cell-supportive platform to facilitate human ASC encapsulation and retention with high cell viability, and that modification of the MGC with peptides incorporating the integrin-binding RGD or IKVAV sequences would modulate the angiogenic potential of the delivered ASCs.

1.6.2 Specific Aims

The specific aims of this Master's project were:

1) To assess the viability of human ASCs encapsulated within (i) MGC, (ii) MGC-RGD, and (iii) MGC-IKVAV hydrogels cultured under simulated hypoxic conditions (2% O_2) for up to 14 days.

2) To assess the expression of angiogenesis-associated genes in human ASCs encapsulated within (i) MGC, (ii) MGC-RGD, or (iii) MGC-IKVAV hydrogels and cultured for 7 days under simulated hypoxic conditions (2% O_2) relative to 2-D tissue culture polystyrene (TCPS) controls.
3) To assess *in vivo* human ASC retention and markers of angiogenesis in the (i) MGC, (ii) MGC-RGD, or (iii) MGC-IKVAV hydrogels at 14 days following subcutaneous implantation in immunocompromised NOD/SCID mice.

Chapter 2

2 MATERIALS AND METHODS

Unless otherwise specified, all chemical reagents used in this project were purchased from Sigma-Aldrich Canada Ltd. (Oakville, ON).

2.1 *N*-Methacrylate Glycol Chitosan (MGC) Hydrogel

2.1.1 MGC Synthesis and Peptide Functionalization

The *N*-methacrylate glycol chitosan (MGC) was prepared by Stuart Young (PhD Candidate) in Dr. Brian Amsden's Lab at Queen's University following published protocols.[140,141,200]

Preparation of MGC: Glycol chitosan (GC, 85% degree of deacetylation; Wako Chemicals Inc., Virginia, USA) was dissolved in deionized water at 1% (w/v) and filtered to remove insoluble impurities. The solution was dialyzed using 50 kDa molecular weight cutoff membrane against distilled water, and then lyophilized to obtain purified GC. The purified GC was dissolved at 2% w/v in a 0.2 M sodium phosphate buffer at pH 9, and reacted with either a 0.15 or 0.22 molar ratio of glycidyl methacrylate (GMA) to free amine of GC. The reaction was neutralized with 1.0 M hydrochloric acid, and the solution was dialyzed using a 12-14 kDa molecular weight cutoff membrane against distilled water. The resulting MGC solution was lyophilized, yielding a white crystalline powder.[140] The degree of *N*-methacrylate substitution (DOS) was defined as the number of grafted methacrylate groups per 100 residues.

Functionalization of MGC with an RGD-containing peptide: The GGGG**RGD**S peptide (RGD, 94% purity; CanPeptide Inc., Pointe-Claire, QC) peptide was dissolved at 2% (w/v) in 0.15 M sodium phosphate buffer at pH 5.5. Next, 2.3 molar equivalents of *N*-acryloxysuccinimide were dissolved in dimethylformamide and added dropwise, accounting for 10% of the final reaction volume. The reaction was stirred at 4°C, then diluted by half with distilled water and dialyzed using a 500 Da molecular weight cutoff membrane against distilled water. The purified solution was lyophilized to obtain *N*-

terminal acrylated GGGG**RGD**S (Acr-RGD). MGC with a 5% degree of methacrylation was dissolved at 0.5% (w/v) in a 0.2 M sodium phosphate buffer at pH 8.5. The Acr-RGD was added at a rate of 0.0625 mole per mole of MGC residue, and the solution was stirred at 37°C. The solution was then dialyzed using a 6-8 kDa molecular weight cutoff membrane against 0.2 M sodium chloride, and then against distilled water. The purified solution was lyophilized to obtain MGC functionalized with the GGGG**RGD**S peptide (MGC-RGD).[141]

Functionalization of MGC with an IKVAV-containing peptide: MGC with a 7% degree of methacrylation was dissolved at 0.5% (w/v) in a 0.2 M sodium phosphate buffer at pH 8.5. The CSRARKQAAS**IKVAV**SADR peptide (IKVAV, 93% purity; CanPeptide Inc., Pointe-Claire, QC) was added at a rate of 0.05 mole per mole of MGC residue. A 2-fold molar equivalent of *N*-hexylamine was added, and the reaction was stirred at 37°C. The solution was dialyzed as described for MGC-RGD, and lyophilized to obtain MGC functionalized with the IKVAV-containing peptide (MGC-IKVAV).

The degrees of methacrylation and peptide functionalization were determined by proton nuclear magnetic resonance (^{1}H NMR) spectroscopy, with targets of 5% for methacrylation and 2.5% for peptide functionalization. The peptide-modified pre-polymers were blended with unmodified MGC in a 40:60 ratio (MGC-peptide to MGC) to obtain a final peptide concentration of 1.18 mM for both the MGC-RGD and MGC-IKVAV groups.

2.1.2 Hydrogel Physical Characterization

2.1.2.1 Hydrogel Preparation

Lyophilized MGC, MGC-RGD or MGC-IKVAV was transferred into a sterile tissue culture plate and sterilized by exposure to low-intensity UV light for 30 min. The MGC, MGC-RGD and MGC-IKVAV hydrogels were prepared by dissolving the pre-polymer in sterile deionized water (for sol content assessment) or PBS (for mechanical characterization) at 2.5%, 2.71% and 3.13% (w/v) respectively, to account for differences due to the weight of the peptide groups. The pre-polymer was dissolved overnight at 37°C under agitation at 700 RPM.

Stock solutions of ammonium persulfate (APS; BioShop Canada Inc., Burlington, ON) and *N,N,N',N'*-tetramethylethylenediamine (TEMED; BioShop Canada Inc., Burlington, ON) were prepared in water (for sol content assessment) or PBS (for mechanical characterization), both at a concentration of 200 mM. For each hydrogel group, a 1 mL solution comprising of 95% dissolved pre-polymer, 2.5% APS and 2.5% TEMED was prepared and mixed well through gentle stirring. The mixture was transferred into a 1 mL syringe and immediately placed in an incubator at 37°C for 15 min to facilitate cross-linking.

2.1.2.2 Sol Content Measurement

The cross-linking efficiency of the unseeded MGC, MGC-RGD and MGC-IKVAV hydrogels was determined by measuring the sol content of the hydrogels.[140] Immediately following cross-linking, the hydrogels were cut into 500 µL samples (n=2) and snap-frozen in liquid nitrogen. The hydrogels were lyophilized for 12 h and the total dry mass ($m_{dry,total}$) was recorded. Each hydrogel was incubated at 37°C in 2 mL of deionized water for 18 hours, with water exchanges at 6-h intervals. Following extraction of the residual unreacted pre-polymer, the hydrogels were snap-frozen in liquid nitrogen and lyophilized for 12 h. The lyophilized hydrogels were re-weighed to obtain the dry mass of polymer incorporated into the network ($m_{dry,network}$). The sol content was calculated using the following equation:

$$\text{Sol Content (\%)} = \frac{(m_{dry,total} - m_{dry,network})}{(m_{dry,total})} \times 100\%$$

2.1.2.3 Equilibrium Compressive Modulus Measurement

Mechanical testing was conducted by Stuart Young (PhD candidate, Amsden lab; Queen's University) to measure the equilibrium compressive modulus of the MGC, MGC-RGD and MGC-IKVAV hydrogels.[201] Following cross-linking, 50 µL hydrogels (n=6) were swollen to equilibrium in PBS (pH 7.4). The dimensions of the swollen hydrogels were measured using digital calipers immediately before testing. Unconfined stress-relaxation measurements were conducted using a MACH-1™ micromechanical tester (Biomomentum Inc., Laval, QC) with a 1 kg load cell equipped with an upper steel

plate and an advancing steel base. Each hydrogel was placed on the stage in a PBS bath. Compression was applied axially at increments of 4% strain at a rate of 10%·s^{-1} to a total strain of 32%, at which point the nominal stress-strain curve achieved plateau. The resulting force decay was recorded at each step until an equilibrium stress was reached. Nominal stress was calculated from the applied force divided by the initial cross sectional area of the sample. The equilibrium compressive modulus was then obtained from the slope of the linear region of the nominal equilibrium stress-stain curve.

2.2 Adipose-derived Stem/Stromal Cell (ASC) Isolation, Culture, and Characterization

2.2.1 Adipose Tissue Collection

Abdominal and breast adipose tissue samples were collected from female patients undergoing elective plastic and reconstructive procedures at the London Health Sciences Centre in London, Ontario. Informed consent was obtained prior to surgery, and the study was reviewed and approved by the Human Research Ethics Board at Western University (REB #105426). Freshly-harvested adipose tissue samples were placed in 100 mL of sterile, cation-free phosphate buffered saline (PBS; Lonza, Mississauga, ON) supplemented with 20 mg/mL bovine serum albumin (BSA). The samples were transported to the lab on ice and adipose-derived stem/stromal cell (ASC) isolation was performed within 2 h of tissue collection. Patient age, weight, height and explant site were recorded for all donors.

2.2.2 ASC Isolation

Human ASCs were isolated using established protocols as described in Flynn *et al.*[202] The fresh adipose tissue was finely minced using sterile scissors and any fibrous or cauterized tissue was removed from the sample. The minced tissue was added to 25 mL of digest solution consisting of 2 mg/mL collagenase type I (Worthington Biochemical Corp., Lakewood, NJ), 3 mM glucose, 25 mM 4-(2-hydroxyethyl)-1-piperazineethanesulfonic acid (HEPES) and 20 mg/mL BSA in Kreb's Ringer Buffer (KRB) to a maximum volume of 40 mL. The tissue was enzymatically digested for 45 min at 37°C under constant agitation at 100 RPM. Undigested tissue fragments were removed by filtration

through a 250 μm pore-size stainless steel filter and the filtrate was allowed to gravity separate for 5 min. The upper layer of mature adipocytes was carefully aspirated without disturbing the lower layer containing the stromal vascular fraction (SVF), including the ASC population. To neutralize the collagenase, an equal volume of complete cell culture medium comprised of Dulbecco's Modified Eagle Medium:Ham's F12 nutrient mixture (DMEM:Ham's F12), supplemented with 10% fetal bovine serum (FBS; Wisent Bio Products, Montreal, QC) and 1% penicillin-streptomycin (pen-strep; Life Technologies Inc., Burlington, ON) was added to the sample before centrifugation at 1200 × g for 5 min. The supernatant was discarded and the cell pellet was resuspended in 20 mL of erythrocyte lysing buffer (0.154 M NH_4Cl, 10 mM $KHCO_3$ and 0.1 mM EDTA in sterile deionized water) for 10 min under agitation at 100 RPM before re-centrifugation. The supernatant was aspirated and the cell pellet was resuspended in 20 mL of complete cell culture medium. The cell suspension was filtered through a 100 μm pore-size nylon filter, and re-centrifuged. The cell pellet was resuspended in complete medium and the cells were plated onto T-75 tissue culture polystyrene (TCPS) flasks (Corning, New York, USA) at 30,000 cells/cm^2. After a 24 h incubation at 37°C (20% O_2/5% CO_2), the cells were washed with 10 mL of sterile PBS to remove unattached cells and cellular debris, and the complete medium was replaced.

2.2.3 ASC Culture and Cryopreservation

The complete medium was exchanged every 2 days until 80% confluence. Plastic adherent cells were released through incubation at 37°C in 0.25% trypsin/0.1% EDTA (Life Technologies Inc., Burlington, ON) for 5 min. The passage 1 (P1) cells were collected, centrifuged and resuspended in cell freezing medium comprised of 80% FBS, 10% DMEM:Ham's F12 medium and 10% dimethyl sulfoxide (DMSO; Fisher Scientific, Ottawa, ON) at a concentration of 1 × 10^6 cells/mL. The ASCs were subjected to a controlled freezing protocol using a freezing container at -80 °C (Nalgene, 5100-0001) and stored in liquid nitrogen in a cryopreservation unit (Thermo Scientific CY509107) until further use.

2.2.4 ASC Expansion

Cryopreserved P1 ASCs were thawed and plated on T-75 flasks at a density of 1×10^6 cells per flask in complete medium, and cultured at 37°C (20% O_2/5% CO_2). The complete medium was exchanged every 2 days. At 80% confluence, the ASCs were trypsin-released and plated on new T-75 flasks in a 1 to 3 ratio. Passage 3 (P3) cells were used for all cell characterization and encapsulation experiments. All studies included 2-3 technical replicates for all scaffold conditions seeded with ASCs from the same donor (n=2-3), and the experiments were repeated to have 2-4 biological replicates using cells from different donors (N=2-4).

2.2.5 ASC Immunophenotype Characterization

ASC immunophenotype was assessed by flow cytometry (n=3, N=3) using a Guava® easyCyte 8HT benchtop flow cytometer (EMD Millipore Corp., USA) following published protocols.[203] Single marker staining was performed with monoclonal flourophore-conjugated anti-human antibodies (eBioscience, San Diego, CA) as follows: CD90 (Cat. # 11-0909-41), CD44 (Cat. # 25-0441-81), CD29 (Cat. # 12-0299-71), CD73 (Cat. # 11-0739-41), CD105 (Cat. # 12-1057-41), CD31 (Cat. # 12-0319-42), CD45 (Cat. # 11-0459-41), CD146 (Cat. # 11-1469-41) and CD34 (Cat. # 17-0349-41). Controls of unstained cells were also included in all analyses.

Passage 2 (P2) ASCs were trypsin-released, centrifuged and resuspended in complete medium. A total viable cell count was performed on the ASCs using the Guava® ViaCount Assay (Millipore Corp.). Cells were resuspended at a density of 2.4×10^5 cells/mL in PBS supplemented with 10% FBS. For each marker, 1 mL of cell suspension was transferred into an eppendorf tube, and centrifuged at 1200 × g for 5 min at 4°C in a pre-cooled micro-centrifuge. The supernatant was aspirated and the ASCs were resuspended in 600 µL of ice-cold PBS supplemented with 3% BSA (PBS + 3% BSA). All subsequent steps were performed under minimal lighting. 5 µL of the stock antibody solution was added to the cell suspension. The samples were vortexed briefly and incubated for 30 min at 4°C. The cells were washed 3 times by centrifuging at 400 × g for 5 min at 4°C, aspirating the supernatant, and resuspending the ASCs in 600 µL of ice-

cold PBS + 3% BSA. After the final wash, the cells were fixed in 0.5% paraformaldehyde (Fisher Scientific, Ottawa, ON) for 15 min at 4°C. The cells were washed again with ice-cold PBS + 3% BSA for a total 3 rinses, and then stored in a dark environment at 4°C until flow cytometry was performed.

2.3 ASC Encapsulation within the Hydrogels

The MGC, MGC-RGD or MGC-IKVAV pre-polymer solution and APS/TEMED reagents were prepared in sterile PBS, as described in Section 2.1.2.1. P2 ASCs were trypsin-released and resuspended at 5×10^7 cells/mL in complete medium. For each hydrogel group, a 1 mL solution comprising of 75% pre-polymer, 20% cell suspension, 2.5% APS and 2.5% TEMED was prepared and mixed well through gentle stirring. The mixture was transferred into a 1 mL syringe and immediately placed in an incubator at 37°C for 15 min to facilitate cross-linking. Following gelation, the cross-linked hydrogel was extruded from the syringe and cut into 50 μL cylinders, each containing ~500,000 encapsulated ASCs. Each hydrogel was transferred into an individual 12-well insert (Greiner Bio-one, North Carolina, USA) and cultured in complete medium.

To simulate the hypoxic microenvironment prevalent in the extremities of CLI patients,[115,204,205] the ASC-encapsulated hydrogels were cultured at 37°C under simulated hypoxic conditions (2% O_2/5% CO_2/93% N_2) in a Whitley H35 Hypoxystation (HypOxygen, Maryland, USA). The complete medium was exchanged every 2 days for the duration of the studies.

2.4 *In Vitro* Characterization of ASC following Encapsulation

2.4.1 ASC Viability

ASC viability following encapsulation and culture in the various hydrogel groups (MGC, MGC-RGD, MGC-IKVAV) was assessed at 24 h, 7 d and 14 d using the LIVE/DEAD® Viability/Cytotoxicity Kit for mammalian cells (Life Technologies Inc., Burlington, ON) involving staining with calcein AM and ethidium homodimer-1 (EthD-1) (n=3, N=3). At each time point, the hydrogels were rinsed with PBS and stained with 2 μM calcein AM

and 4 μM EthD-1 at 37°C for 1 h. Following incubation, triplicate samples of each hydrogel group were imaged using a 5× objective lens on a Zeiss LSM 800 confocal microscope (ZEISS, Canada). The mosaic stitch technique was used to capture the entire cross-sectional area of the hydrogel.[141] A total of 4-5 layers were scanned and imaged for each hydrogel along its depth (z-axis), with each layer separated by 50 μm. The images were then processed to quantify the number of calcein$^+$ live cells and EthD-1$^+$ dead cells using Image J analysis software. The ASC viability was calculated as a percentage of the live to total cells, and the average number of live and dead cells per plane was also determined for each sample.

2.4.2 ASC Metabolic Activity

The 3-(4,5-dimethylthiazol-2-yl)-2,5-diphenyltetrazolium bromide (MTT; Life Technologies Inc., Burlington, ON) assay was used to measure the metabolic activity of ASCs encapsulated in the MGC, MGC-RGD or MGC-IKVAV hydrogels at 24 h, 7 d and 14 d (n=3, N=3).[206] Unseeded hydrogels were also analyzed as a control. A working MTT solution (0.5 mg/mL) was prepared in DMEM:Ham's F12 medium. The hydrogel samples were submerged in 2 mL of MTT solution, and incubated at 37°C for 4 hours. Following incubation, each hydrogel was washed twice with sterile PBS and weighed. The hydrogels were transferred into 1.5 mL eppendorf tubes with 800 μL of DMSO and manually crushed using a plastic eppendorf pestle. The samples were then incubated for 1 h at 37°C under gentle agitation at 100 RPM to extract the water-insoluble formazan product. The supernatant was collected following centrifugation at 15,000 × g for 15 min, and the samples were diluted 1:1 in DMSO. The samples were vortexed briefly and 200 μL of sample was pipetted into a 96-well plate in triplicate. Sample absorbance was measured at 540 nm and corrected for background absorbance at 690 nm using a CLARIOstar® High Performance Monochromator Multimode Microplate Reader (BMG Labtech, Guelph, ON). To account for minor differences in gel size, the data was normalized based on individual gel weight (mg). The average normalized absorbance of the unseeded controls for each of the hydrogel groups was subtracted to account for any non-specific background associated with the hydrogels.

2.4.3 ASC Angiogenic Gene Expression

The human angiogenesis RT^2 Profiler™ PCR array (Qiagen, Toronto, ON) was used to assess the mRNA expression of 84 genes associated with angiogenesis in the ASCs encapsulated within the MGC, MGC-RGD, and MGC-IKVAV hydrogels (N=4). ASCs cultured in 2-D on uncoated TCPS were included as a calibrator to normalize the levels between donors. The RNeasy® kit (Qiagen, Toronto, ON) was used to extract the total RNA from the hydrogels or TCPS controls cultured under simulated hypoxic conditions (2% O_2) for 7 d.[207] For each hydrogel group, triplicate samples of two hydrogels were rinsed with PBS and minced with scissors in 1 mL of TRIzol reagent (n=6 total per hydrogel group). The samples were then disrupted using an ultrasonic homogenizer with 3 sets of 10-second bursts with intervals of cooling on ice, followed by 5 min incubation at room temperature. To prepare the TCPS controls, 500,000 P3 ASCs were seeded in individual wells of a 6-well plate and cultured under simulated hypoxic conditions (2% O_2). At 7 d, the cells were rinsed with PBS and incubated in 1 mL of TRIzol reagent for 5 min. For both the hydrogel samples and TCPS controls, 200 μL of chloroform was added and the samples were incubated at room temperature for 10 min before centrifugation at 10,000 × g for 10 min. The upper aqueous phase was transferred into new 1.5 mL eppendorf tubes, and 250 μL of 70% ethanol was added to each sample. The samples were transferred to RNeasy mini spin columns and processed according to the manufacturer's instructions. The triplicate samples were pooled (n=6 gels total) and post-extraction clean-up was performed by adding 0.1× the volume of 3 M sodium acetate, 2.5× the volume of 100% ethanol, and 0.01× the volume of 5 mg/mL glycerol to the aqueous RNA sample. After overnight incubation at -30°C, the RNA was washed with 30 μL of 80% ethanol 3 times with centrifugation at 12,000 × g for 30 min between each wash. The RNA was resuspended in 30 μL of nuclease-free water, and sample concentration and purity were determined using a NanoDrop 1000 spectrophotometer (Thermo Scientific).

The RT^2 First Strand kit (Qiagen, Toronto, ON) was used to prepare cDNA from the extracted RNA. Each sample was first treated with a DNA elimination step by incubating 400 ng of RNA, 2 μL genomic-DNA elimination buffer and nuclease-free water for 5

min at 42°C. Subsequently, 10 µL of the sample was mixed with 10 µL of reverse-transcription mix containing 5× reverse transcription buffer, primer mix, RT enzyme mix and RNase-free water. The samples were incubated at 42°C for 15 min and then at 95°C for 5 min to stop the reaction.

Following manufacturer's instructions for the PCR reactions, 91 µL of nuclease-free water was added to each 20 uL cDNA sample and mixed well through pipetting. The PCR component mix was prepared for each sample by mixing 102 µL of the diluted cDNA sample with 650 µL of 2× RT^2 SYBR Green Mastermix and 548 µL of RNase-free water, for a total volume of 1300 µL. For each sample, 10 µL of the prepared PCR component mix was dispensed into each well of the 384-well RT^2 Profiler PCR array plate. The plate was tightly sealed with optical adhesive film and centrifuged for 1 min at 1000 × g to remove any bubbles. The plate was run on a CFX384 Touch™ Real-Time PCR detection system (Bio-Rad, Mississauga, ON). The cycle threshold (Ct) values were obtained and processed using the online software provided by Qiagen's data analysis center. The stably expressed housekeeping gene, ribosomal protein lateral stalk subunit P0 (*RPLP0*), was used to normalize the data. Fold change in the mRNA expression of the 84 analyzed genes was used to compare the MGC, MGC-RGD and MGC-IKVAV groups normalized to the TCPS control group. Genes displaying >2-fold upregulation or downregulation in mRNA expression relative to the TCPS controls across all donors were selected and statistically analyzed.

2.5 *In Vivo* Characterization of ASC Retention following Encapsulation and Angiogenic Response to the Hydrogels

2.5.1 Subcutaneous Implantation of Hydrogels in NOD/SCID Mice

A subcutaneous implantation model was used to assess cell retention and the angiogenic potential of human ASCs encapsulated within the MGC, MGC-RGD or MGC-IKVAV hydrogels. The animal studies were reviewed and approved by the Human Research Ethics Board at Western University (REB #2016-015). Adult NOD/SCID mice (8-10 weeks old) used for this study were derived from Jackson laboratories: NOD.CB17-

Prkdcscid/J; stock number: 001303. The NOD/SCID mice provide a favorable microenvironment to support human cell engraftment and function due to reduced innate immunity (NOD mutation), and complete T- and B-cell deficiency (SCID mutation).[208]

Each mouse was implanted with one seeded hydrogel and its corresponding unseeded control. The 50 μL hydrogel samples were subcutaneously implanted on the dorsa of each mouse, below each scapula, with surgical assistance from Stephen Sherman (PhD candidate, Hess Lab) at the Robarts Research Institute. Two mice were used for each hydrogel group and the study was repeated with ASCs from 3 different donors (n=2, N=3).

Prior to surgery, the mice were injected with 42 mg/kg of ketamine hydrochloride and 1 mg/kg of xylazine, and the animals were maintained on 2% isoflurane (Baxter Corp., Mississauga, ON) during the surgical procedure. For each experimental group, one 50 μL hydrogel containing ~500,000 encapsulated human ASCs was implanted in a subcutaneous pocket created in the right dorsal flank, and a second 50 μL unseeded hydrogel was implanted subcutaneously in the left dorsal flank. Mice were given 2 mg/kg of metacam after the surgery.

At 24 h prior to euthanasia, the mice were intraperitoneally injected with 200 μg 5-ethynyl-2'-deoxyuridine (EdU; Thermo Fisher, Waltham, MA) to label dividing cells. After 14 days, the mice were anesthetized with isoflurane and euthanized by cervical dislocation, and the scaffolds were excised within their surrounding tissues. The samples were embedded in OCT medium (Tissue Tek, Sakura Finetek, Torrance, CA) and cryosectioned (10 μm) with assistance from Gillian Bell (Research Assistant, Hess Lab) at Robarts Research Institute.

2.5.2 Detection of Human ASCs and Murine CD31$^+$ Cells

The sections were analyzed by immunofluorescence microscopy for human leukocyte antigen (HLA)-ABC to label human ASCs,[209] murine CD31 to visualize CD31$^+$ cell recruitment and EdU to assess cellular proliferation,[208,209] along with DAPI

counterstaining of nuclei. All incubation steps during staining were performed at room temperature.

HLA-ABC staining: Sections were washed twice with PBS for 10 min and permeabilized with 0.1% TritonX-100 for 20 min. The sections were washed again with PBS for 10 min and incubated with a mouse-on-mouse (MOM) blocking agent (Vector Labs, Burlingame, CA) for 1 h. The sections were incubated with MOM diluent for 5 min, and then with mouse anti-human HLA-ABC antibody (1:100 dilution in MOM diluent; BD Biosciences, Mississauga, ON) for 30 min. Next, the sections were washed twice with PBS for 2 min, and incubated with fluorescein-labeled horse anti-mouse IgG (1:200 dilution in MOM diluent) for 30 min. Finally, the sections were washed twice with PBS for 2 min, rinsed with deionized water, and mounted in VectaShield with DAPI (Vector Labs, Burlingame, CA). Primary antibody negative controls ($HLA\text{-}ABC^-$) were prepared by substituting the mouse anti-human HLA-ABC antibody with MOM diluent.[209]

EdU and CD31 staining: Sections were washed twice with PBS for 10 min and permeabilized with 0.1% Triton X-100 for 20 min. The sections were washed again with PBS for 10 min, and incubated for 30 min with EdU labeling cocktail consisting of 860 μL reaction buffer, 100 μL buffer additive, 40 μL $CuSO_4$ and 2.5 μL Alexa Fluor Azide provided in the Click-iT™ imaging kit (Invitrogen, Burlington, ON). The sections were washed twice with PBS for 2 min and blocked by incubation in rabbit serum (Vector Labs, Burlingame, CA) for 1 h. The sections were then incubated with rat anti-mouse CD31 antibody (1:100 dilution in rabbit serum) for 1 h. Next, the sections were washed twice with PBS for 2 min and incubated with fluorescein-labeled rabbit anti-rat IgG (1:200 dilution in rabbit serum) for 30 min. Finally, the sections were washed twice with PBS, rinsed in deionized water, and mounted in VectaShield with DAPI (Vector Labs, Burlingame, CA). EdU^- controls were prepared by removing the $CuSO_4$ reaction-catalyzing reagent from the EdU labeling cocktail. Primary antibody negative ($CD31^-$) controls were prepared by substituting the primary antibody with rabbit serum.[208,209]

2.5.3 Imagine and Quantification of HLA-ABC$^+$, EdU$^+$ and CD31$^+$ Cells

Analysis of human ASC retention: Images of the immunostained sections were taken with an Axioscope Z2 fluorescence microscope (ZEISS Germany), analyzing 8-10 non-overlapping areas selected randomly within the scaffold per section, from a total of 3 sections per hydrogel implant using AxioVision software (n=2, N=3). Scaffold area was calculated by converting each image to an 8-bit binary copy and using ImageJ software to analyze the total scaffold area in mm^2. The number of HLA-ABC$^+$ DAPI$^+$ cells were counted for each image in a blinded fashion and expressed as the average number of HLA-ABC$^+$ DAPI$^+$ cells/mm^2 of hydrogel scaffold.

Analysis of murine CD31$^+$ cell recruitment and proliferation: Images of the immunostained sections were taken with an Axioscope Z2 fluorescence microscope, analyzing 4-5 areas selected randomly at the scaffold-tissue boundary per section, from a total of 3 sections per hydrogel implant using AxioVision software (n=2, N=2). The number of CD31$^+$ cells co-localized with visible DAPI-stained nuclei were counted for each image in a blinded fashion and expressed as the mean number of CD31$^+$ cells/mm^2. The number of CD31$^+$ EdU$^+$ DAPI-stained cells were also counted for each image in a blinded fashion and reported as the number of proliferating CD31$^+$ cells.

2.6 Statistical Analysis

All data are expressed as mean ± standard deviation, and the number of biological (N) and technical (n) replicates are indicated for all experiments. Unless otherwise stated, statistical analyses were performed using GraphPad Prism 6 by one-way or two-way analysis of variance (ANOVA). Multiple comparisons were performed with Tukey's post-hoc comparison of means. Differences were considered statistically significant at $p<0.05$.

Chapter 3

3 RESULTS

3.1 Hydrogel Characterization

3.1.1 Sol Content Analysis

Sol content provides a measure of the amount of the methacrylated glycol chitosan (MGC) pre-polymer that has not been incorporated into the hydrogel network during cross-linking. A lower sol content value is desirable as it indicates higher cross-linking efficiency. In comparing the 3 hydrogel groups, the sol content value for the MGC-IKVAV group was 15.0 ± 0.9%, which was significantly higher than the values of 7.4 ± 0.1% for the non-peptide modified MGC group and 8.9 ± 0.9% for the MGC-RGD group (Figure 3.1A), thus indicating that modification of the MGC with the IKVAV peptide influenced the cross-linking process.

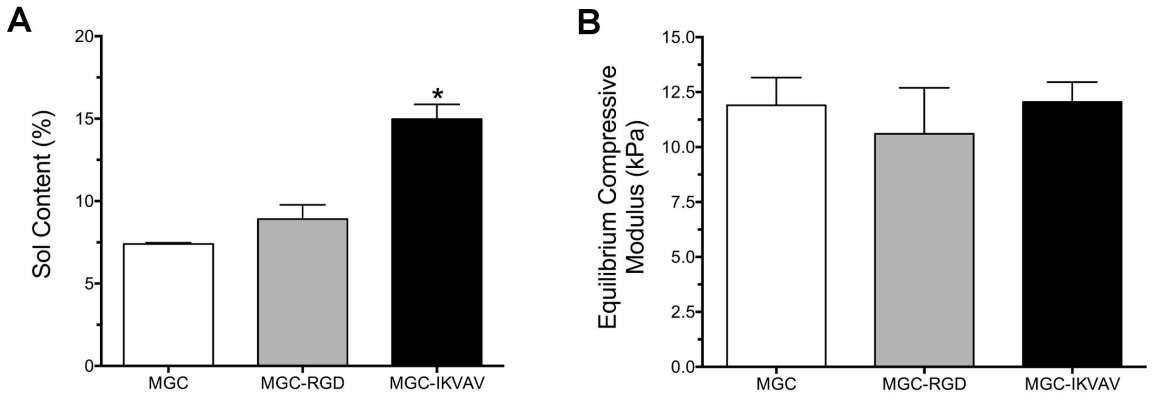

Figure 3.1. Sol content and equilibrium compressive moduli of MGC, MGC-RGD and MGC-IKVAV hydrogels. (A) The cross-linking efficiency of each type of hydrogel was assessed by measurement of the sol content following thermally-induced cross-linking and extraction in deionized water (n=2). The MGC-IKVAV hydrogel group had a significantly higher sol content than the other hydrogel groups, suggesting that modification with the IKVAV peptide may have interfered with cross-linking process. (B) The equilibrium compressive modulus of the three hydrogel groups as measured through micromechanical compression testing, confirming that all hydrogels had similar mechanical properties (n=6). Data represents mean ± SD (*$p<0.05$).

3.1.2 Equilibrium Compressive Modulus Analysis

The cross-linking efficiency can influence the mechanical properties of the resultant hydrogels. Since the response of encapsulated cells can be impacted by both biochemical and biomechanical effects,[210–212] the equilibrium compressive moduli of the MGC, MGC-RGD and MGC-IKVAV hydrogels were quantified to assess whether there were any differences in gel stiffness between the groups. Despite the variation in the sol content for the MGC-IKVAV group, there were no statistically significant differences in the equilibrium compressive moduli of the hydrogels, with calculated values of 11.9 ± 1.3 kPa for the MGC group, 10.6 ± 2.1 kPa for the MGC-RGD group, and 12.0 ± 0.9 kPa for the MGC-IKVAV group (Figure 3.1B). Based on this analysis, it was decided that no further optimization of the hydrogel formulation was required, as the equivalent compressive moduli controlled for the possible confounding effects of the hydrogel biomechanical properties in assessing the impact of the peptide groups on cell function.

3.2 Adipose-derived Stromal/Stem Cell (ASC) Immunophenotype Analysis

The immunophenotype of passage 3 (P3) human adipose-derived stem/stromal cells (ASCs) expanded on tissue culture polystyrene (TCPS) was assessed by flow cytometry (Figure 3.2). Consistent with the expected expression of stromal cell markers, ASCs dependably expressed CD90 (99.8 ± 0.1%), CD44 (99.6 ± 0.2%), CD29 (95.8 ± 2.6%), CD73 (84.7 ± 8.1) and CD105 (97.2 ± 2.2%). Further, ASCs showed minimal expression of the endothelial cell marker CD31 (0.3 ± 0.2%) and the hematopoietic pan-leukocyte marker CD45 (1.3 ± 1.2%). The pericyte marker CD146 (4.6 ± 3.2%) and the progenitor cell marker CD34 (0.6 ± 0.1%) demonstrated low expression, consistent with previous studies reporting a steady decline in the expression of these markers during culture and successive passaging.[100,213,214] Overall, the immunophenotype of the ASCs used in this study was consistent with the guidelines established by the International Society of Cellular Therapy (ISCT) and the International Federation for Adipose Therapeutics and Science (IFATS) for human ASCs.[112]

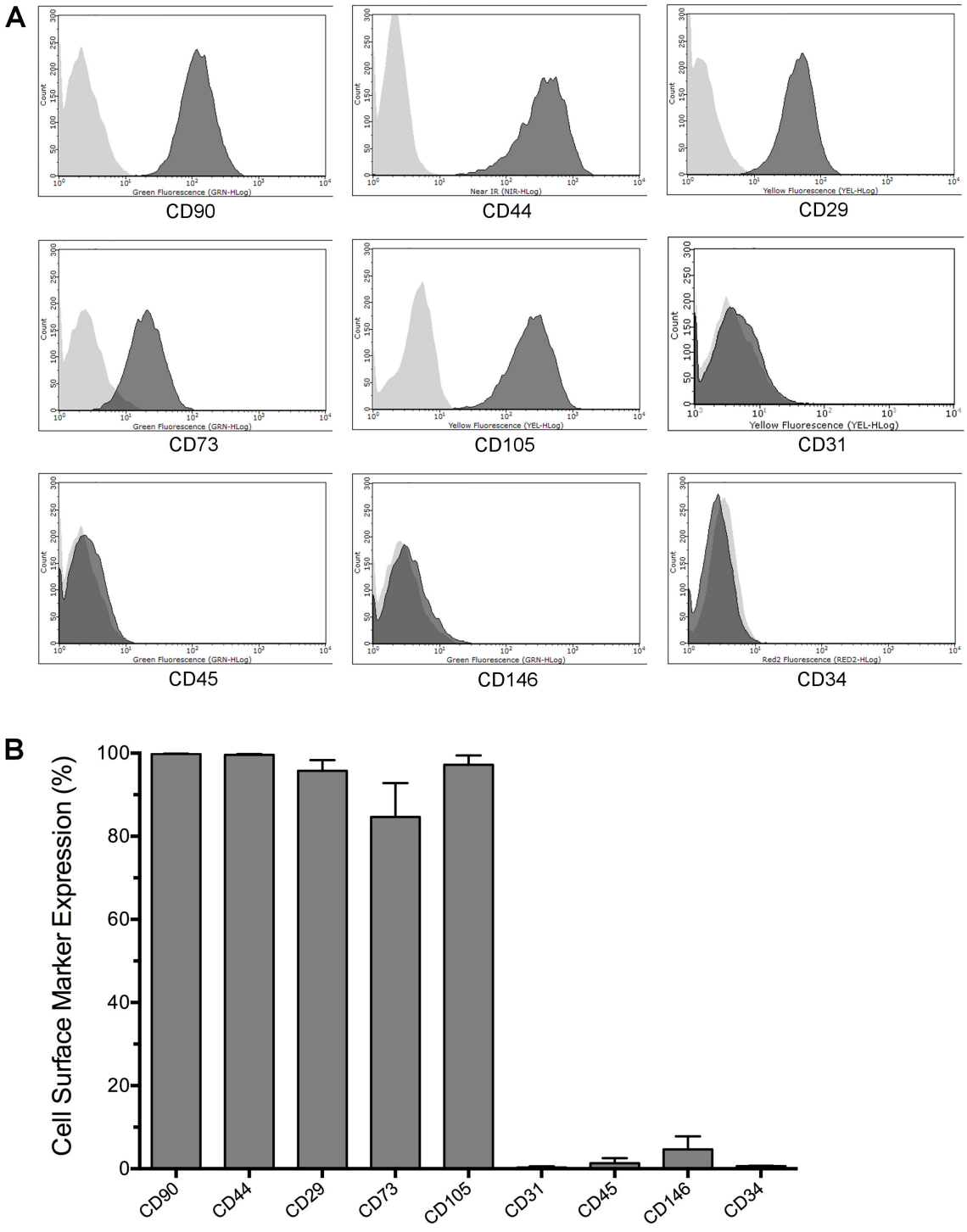

Figure 3.2. Immunophenotype of human ASCs at passage 3. (A) Representative flow cytometry histograms showing expression of analyzed cell surface markers. Unstained controls are shown in light grey. (B) Frequency of cells expressing each of the analyzed markers. The ASC immunophenotype was consistent with guidelines set forth by the International Federation for Adipose Therapeutics (IFATS) and the International Society for Cellular Therapy (ISCT), with high expression (>80%) of CD90, CD44, CD29, CD73 and CD105, and low expression (<2%) of CD31 (endothelial) and CD45 (hematopoietic). Data represents mean ± SD ($p<0.05$; n=3, N=3).

3.3 ASC Encapsulation within Hydrogels

Human ASCs at P3 were encapsulated within the MGC, MGC-RGD and MGC-IKVAV hydrogels at a concentration of 10×10^6 ASCs/mL through thermally-induced free radical polymerization with ammonium persulfate (APS) and *N*,*N*,*N'*,*N'*-tetramethylethylenediamine (TEMED) as the initiator system. Immediately after gelation, 50 µL hydrogel cylinders containing ~500,000 encapsulated ASCs were generated (Figure 3.3) and used for all subsequent *in vitro* and *in vivo* studies.

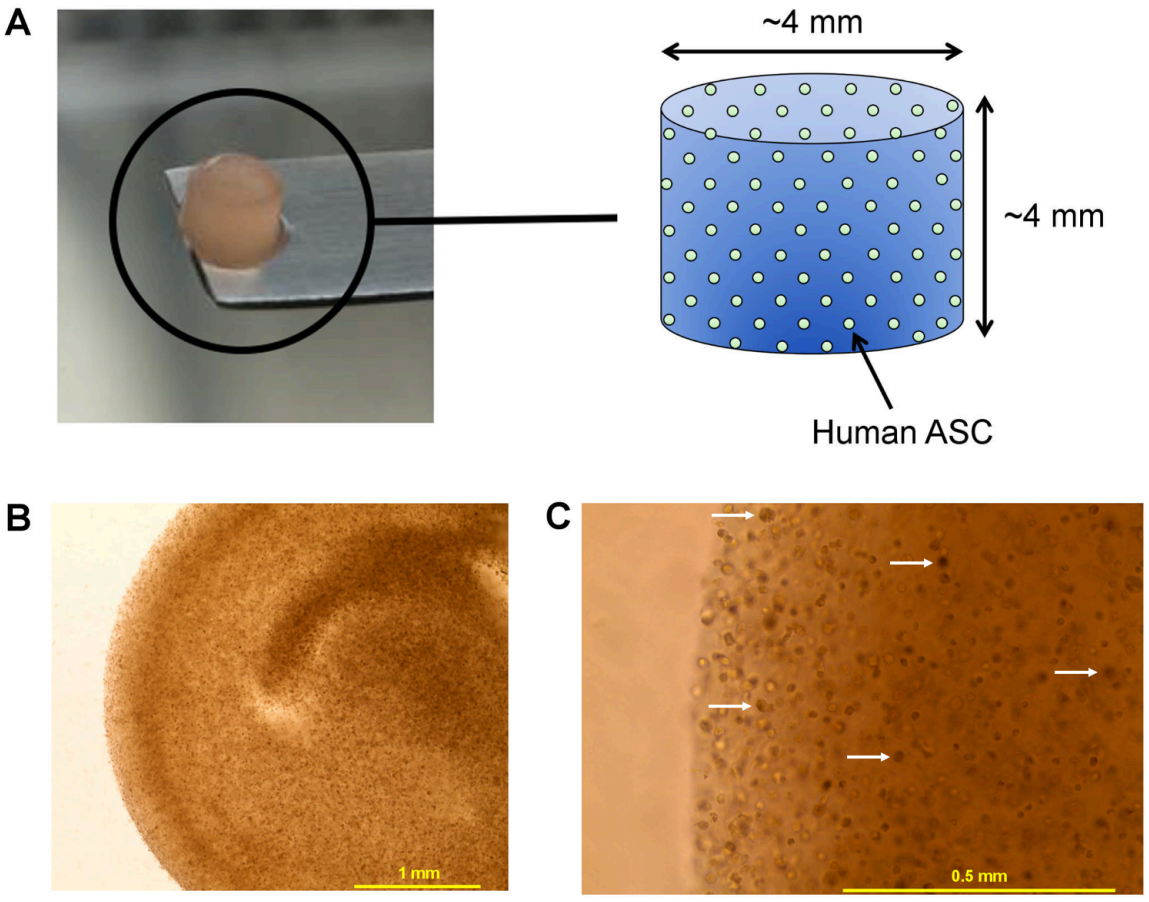

Figure 3.3. Representative images of an MGC hydrogel containing encapsulated ASCs. (A) Human ASCs were encapsulated within a 50 µL MGC hydrogel at a concentration of 10×10^6 ASCs/mL. Light photomicrographs taken at 24 h following encapsulation showing the ASCs (examples indicated with white arrows) distributed within the MGC hydrogel at (B) 4× and (C) 20× magnification.

3.4 *In Vitro* Analysis of ASCs following Encapsulation

3.4.1 ASC Viability

The LIVE/DEAD® assay with confocal imaging analysis was used to assess ASC viability following encapsulation within the MGC, MGC-RGD or MGC-IKVAV hydrogels over 14 days in culture under a simulated hypoxic environment (2% O_2) (Figure 3.4). Quantitative analysis revealed that ASC viability in the MGC (86.6 ± 4.5%) and MGC-RGD (87.4 ± 2.7%) hydrogels was significantly higher than the MGC-IKVAV (73.3 ± 12.3%) group at 24 h (Figure 3.4B). The high viability in the MGC and MGC-RGD groups validated that the radically-induced thermal cross-linking approach using APS and TEMED did not adversely impact cell viability.

Analysis of ASC viability over time revealed that cell viability was also significantly reduced in the MGC-IKVAV hydrogel group relative to the MGC and MGC-RGD groups at both 7 and 14 d. ASC viability significantly declined from 24 h to 14 d in both the MGC and MGC-IKVAV hydrogel groups, from 86.6 ± 4.5% to 75.0 ± 6.6% for the MGC group and 73.3 ± 12.3% to 54.4 ± 12.2% for the MGC-IKVAV group (Figure 3.4B). In contrast, there was no significant difference observed in ASC viability over time in the MGC-RGD group, with >80% viability observed over the course of the study.

To complement the viability analysis, the average number of live and dead ASCs within each hydrogel cross-section was plotted for the MGC, MGC-RGD and MGC-IKVAV hydrogel groups at each time point (Figure 3.4C). Notably, there was no significant difference in the total number of cells per plane (live + dead) for all hydrogel groups. However, at both 7 d and 14 d, there was significantly lower number of live cells in the MGC-IKVAV group relative to both the MGC and MGC-RGD groups, with a significant decline in the number of live cells observed over time from 24 h to 14 d.

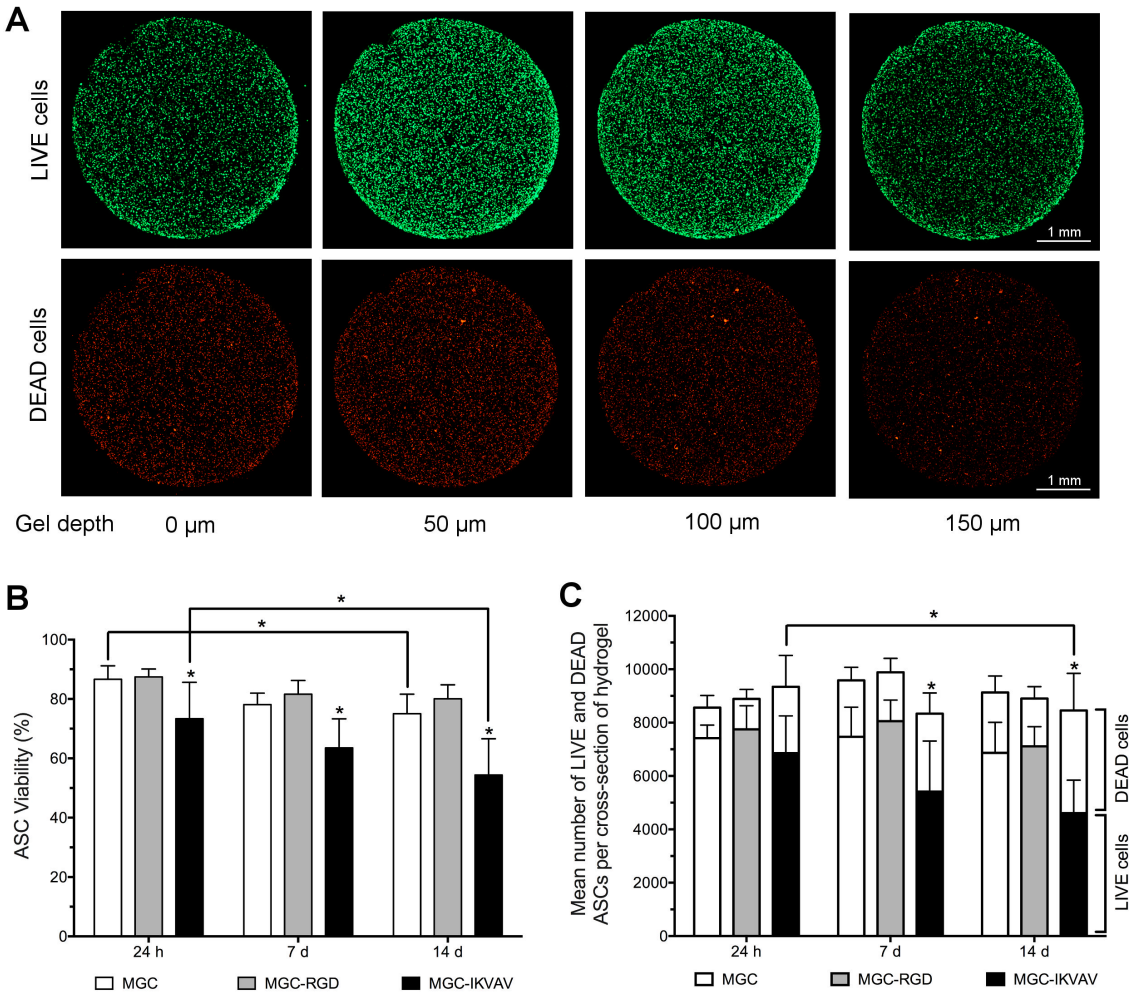

Figure 3.4. Viability analysis of ASCs encapsulated within MGC, MGC-RGD and MGC-IKVAV hydrogels cultured under simulated hypoxic conditions (2% O_2). (A) Representative confocal microscopy photomicrographs of LIVE/DEAD®-stained ASCs encapsulated within an MGC hydrogel at 24 h. Live cells (upper row; green) and dead cells (bottom row; red) were imaged across 4 planes within the hydrogel using a mosaic stitch technique to visualize the entire cross-section of the scaffold at varying depths. (B) The number of live and dead cells were quantified to assess the percent viability of the ASCs in each of the hydrogel groups at 24 h, 7 d and 14 d. The MGC-IKVAV hydrogel had significantly lower ASC viability than the other hydrogel groups across each time-point. ASC viability declined in the MGC and MGC-IKVAV groups from 24 h to 14 d, but no significant differences in viability were observed over time for the MGC-RGD group. (C) The average number of live (lower bar) and dead (upper bar) ASCs within each hydrogel group at 24 h, 7 d and 14 d based on the LIVE/DEAD® assay. The MGC-IKVAV hydrogel demonstrated a significantly reduced number of live ASCs at 7 d and 14 d compared to the other hydrogel groups, as well as a significant decline in live ASCs between 24 h and 14 d. Data represents mean ± SD (*$p<0.05$; n=3, N=3).

3.4.2 ASC Morphology

The confocal imaging analysis in the LIVE/DEAD® assay also enabled the assessment of qualitative changes in ASC morphology following encapsulation and culture (Figure 3.5). At 24 h, the ASCs in all three hydrogel groups had a rounded morphology. Following

culture, ASCs with a distinct elongated fibroblastic morphology were observed within the two most superficial planes (0-50 μm) of the MGC-RGD hydrogel group, with a qualitative increase noted in the frequency of spreading from 7 to 14 d (Figure 3.5E&F). In contrast, ASCs encapsulated in the MGC and MGC-IKVAV hydrogels maintained a rounded shape over the course of the study.

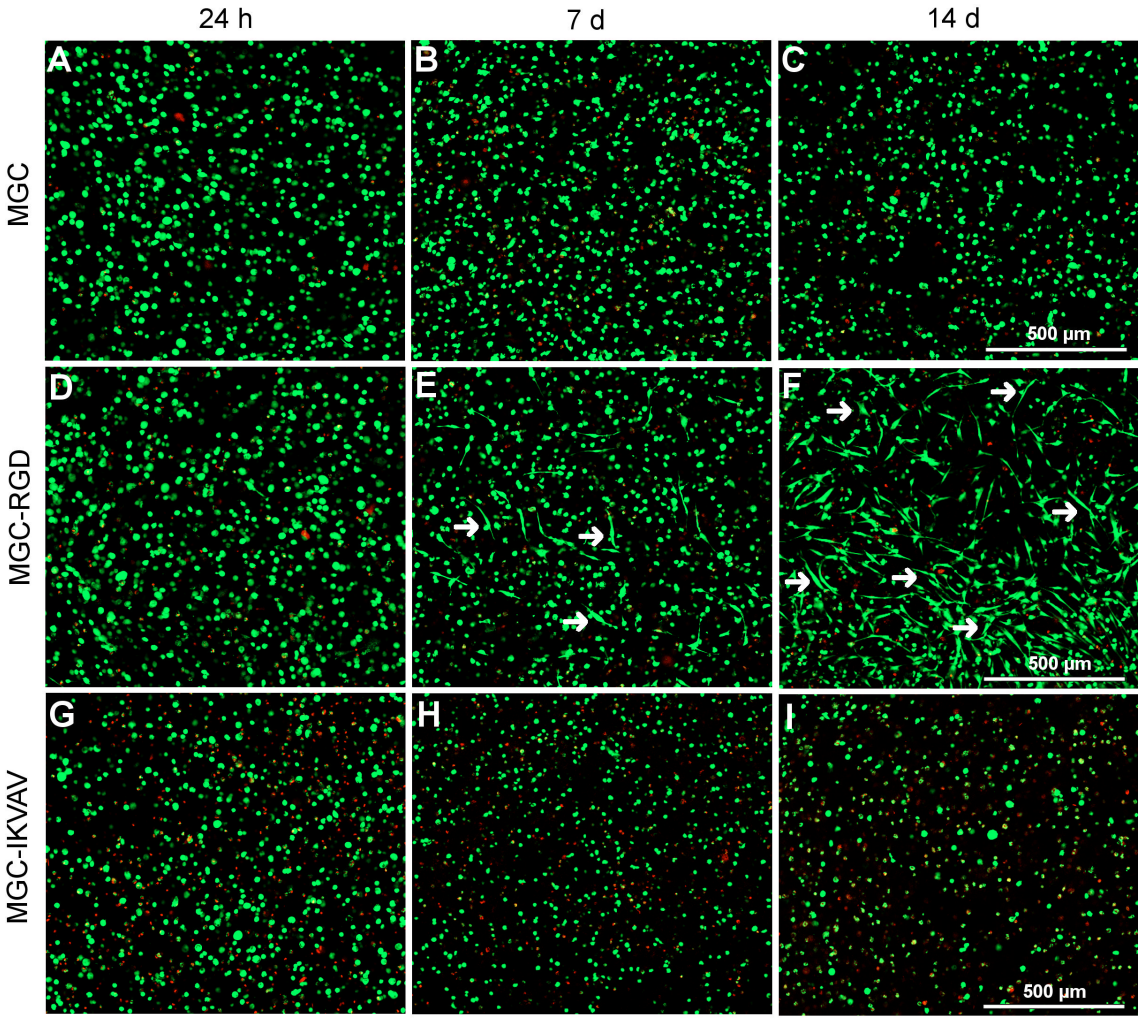

Figure 3.5. Representative photomicrographs of LIVE/DEAD®-stained ASCs encapsulated within MGC, MGC-RGD or MGC-IKVAV hydrogels cultured under simulated hypoxic conditions (2% O_2). Photomicrographs showing live cells (green) and dead cells (red) within each hydrogel group at 24 h, 7 d, and 14 d. White arrows indicate ASCs with an elongated morphology in the superficial plane of the MGC-RGD hydrogel group at 7 and 14 d.

3.4.3 ASC Metabolic Activity

In order to more fully examine ASC viability and function following encapsulation within the various hydrogels, the MTT assay was performed to assess the metabolic activity of ASCs encapsulated within the MGC, MGC-RGD or MGC-IKVAV hydrogels over 14 days in culture under simulated hypoxic conditions (2% O_2) (Figure 3.6). The metabolic activity of the encapsulated ASCs significantly decreased between 24 h and 7 d for all hydrogel groups, and was then maintained at similar levels at 14 d. In comparing the groups, the ASCs encapsulated within the MGC-IKVAV hydrogels had significantly lower metabolic activity than the MGC and MGC-RGD groups at 24 h and 7 d. At 14 d, the metabolic activity was significantly higher in the MGC-RGD hydrogels as compared to the other groups.

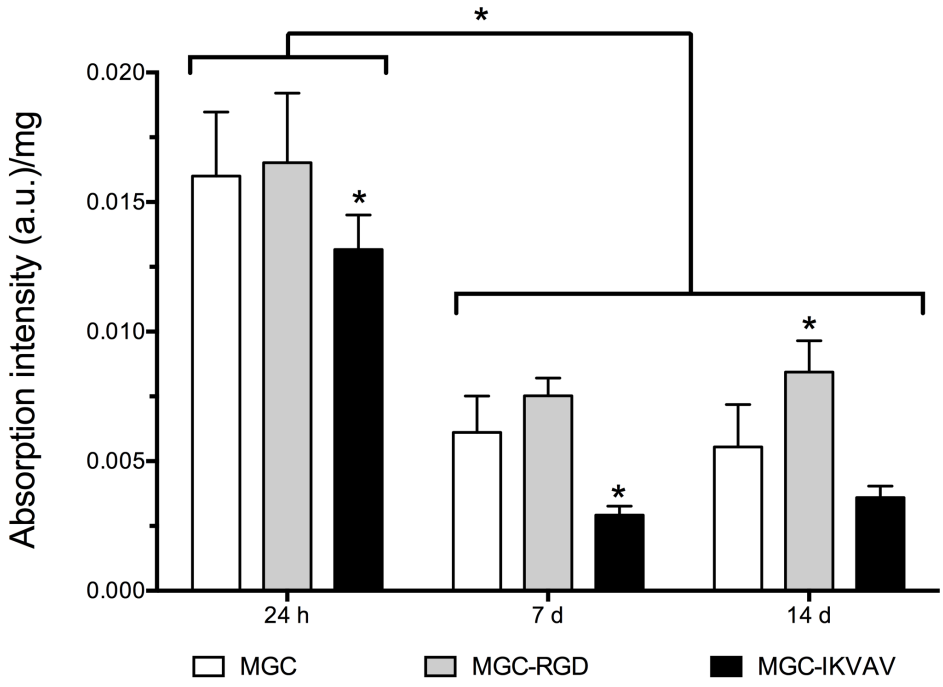

Figure 3.6. Metabolic activity of ASCs encapsulated within MGC, MGC-RGD and MGC-IKVAV hydrogels cultured under simulated hypoxic conditions (2% O_2). The MTT assay was performed at 24 h, 7 d and 14 d following ASC encapsulation. The absorption intensity was normalized to the gel weight (mg) to account for minor differences in the size of the individual hydrogels. All hydrogel groups demonstrated a significant decrease in ASC metabolic activity from 24 h to 7 d, and then levels were sustained at 14 d. The MGC-IKVAV hydrogel showed significantly lower ASC metabolic activity at 24 h and 7 d as compared to the MGC and MGC-RGD hydrogel groups. The MGC-RGD hydrogel group demonstrated a significantly higher ASC metabolic activity at 14 d as compared to both the MGC and MGC-IKVAV groups. Data represents mean ± SD (*$p<0.05$; n=3, N=3).

3.4.4 ASC Angiogenic Gene Expression

The human angiogenesis RT^2 Profiler™ PCR array was used as a high throughput screening approach to assess the potential effects of 3-D hydrogel encapsulation and MGC peptide modification on the mRNA expression of 84 genes associated with angiogenesis in ASCs encapsulated within the MGC, MGC-RGD or MGC-IKVAV hydrogels in comparison to 2-D TCPS controls after 7 days of culture under simulated hypoxic conditions (2% O_2). Genes that demonstrated >2-fold change relative to the TCPS controls across all cell donors (N=4) were selected for further statistical analysis.

3.4.4.1 Upregulated Angiogenesis-associated Genes

There was a >2-fold upregulation in gene expression of several secreted angiogenic factors including hepatocyte growth factor (*HGF*), vascular endothelial growth factor A (*VEGFA*), angiopoietin-like 4 (*ANGPTL4*) and angiopoietin-2 (*ANGPT2*) in the encapsulated ASCs as compared to the TCPS controls (Figure 3.7). In general, the most notable differences were associated with culturing the ASCs in the 3-D hydrogels versus the 2-D culture conditions, rather than due to the effects of modifying the MGC with the peptide ligands. For a number of the genes, there was significant variability in the magnitude of the expression between donors, so the data was plotted separately to show the response of the individual donors, as well as the averaged values used for statistical analysis.

When comparing the hydrogel groups, a trend for enhanced *HGF* gene expression was noted in the MGC group relative to both peptide-modified MGC groups across all four donors. Moreover, the pooled values indicated that there was a significant difference in *HGF* expression between the MGC and MGC-IKVAV groups (Figure 3.7A). For *VEGFA*, *ANGPTL4* and *ANGPT2*, the mRNA expression levels were significantly upregulated in the MGC, MGC-RGD, and MGC-IKVAV groups relative to the TCPS controls, but there were no notable differences between the various hydrogel groups in comparing the response of all cell donors (Figure 3.7B-D).

A >2-fold upregulation in gene expression was also noted in comparing the hydrogels to the TCPS controls for the extracellular matrix (ECM) protein collagen XVIII α1

(*COL18A1*), the matrix-remodeling factor matrix metalloproteinase 14 (*MMP14*), and the cell adhesion glycoprotein integrin β3 (*ITGB3*) (Figure 3.8). For *COL18A1*, there was a trend for enhanced mRNA expression in the MGC group relative to the MGC-RGD and MGC-IKVAV groups for 3 out of 4 of the cell donors, but the only significant difference noted in the pooled values was between the MGC group and the 2-D TCPS control (Figure 3.8A). Similarly, for *MMP14*, significantly higher expression levels were noted in the MGC hydrogel group as compared to the TCPS control, but there were no notable differences between the hydrogel groups (Figure 3.8B). Finally, while there was a trend for enhanced *ITGB3* expression in all three hydrogel groups relative to the 2-D controls, the difference in the pooled data was not statistically significant and the expression levels were relatively consistent across all 3 hydrogel groups (Figure 3.8C).

3.4.4.2 Downregulated Angiogenesis-associated Genes

A >2-fold downregulation was observed in the gene expression levels of the secreted factors thrombospondin-1 (*THBS1*), angiopoetin-1 (*ANGPT1*), connective tissue growth factor (*CTGF*) and fibroblast growth factor 1 (*FGF1*) in the ASCs encapsulated in the hydrogels as compared to the TCPS controls for all cell donors (Figure 3.9). For 3 out of 4 of the cell donors studied, there was a trend for reduced mRNA expression of the anti-angiogenic factor *THBS1* in the MGC-IKVAV group relative to both the MGC and MGC-RGD groups. Moreover, analysis of the pooled data indicated that there was a significant difference in the *THBS1* expression levels between the MGC-IKVAV group and the TCPS controls (Figure 3.9A). Similarly, for 2 of the 4 cells donors, the expression of the angiogenic factor *ANGPT1* was downregulated in the MGC-IKVAV group relative to all other groups, with a significant difference observed in the pooled data relative to the TCPS controls (Figure 3.9B). There were no obvious trends in comparing the expression levels of *CTGF* and *FGF1* between the hydrogel groups across all 4 cell donors (Figure 3.9C&D). However, in analyzing the pooled data, there was a significant reduction in *CTGF* gene expression in the MGC-IKVAV group relative to the TCPS controls, as well as significantly lower levels of *FGF1* mRNA expression in all three hydrogel groups relative to the 2-D controls.

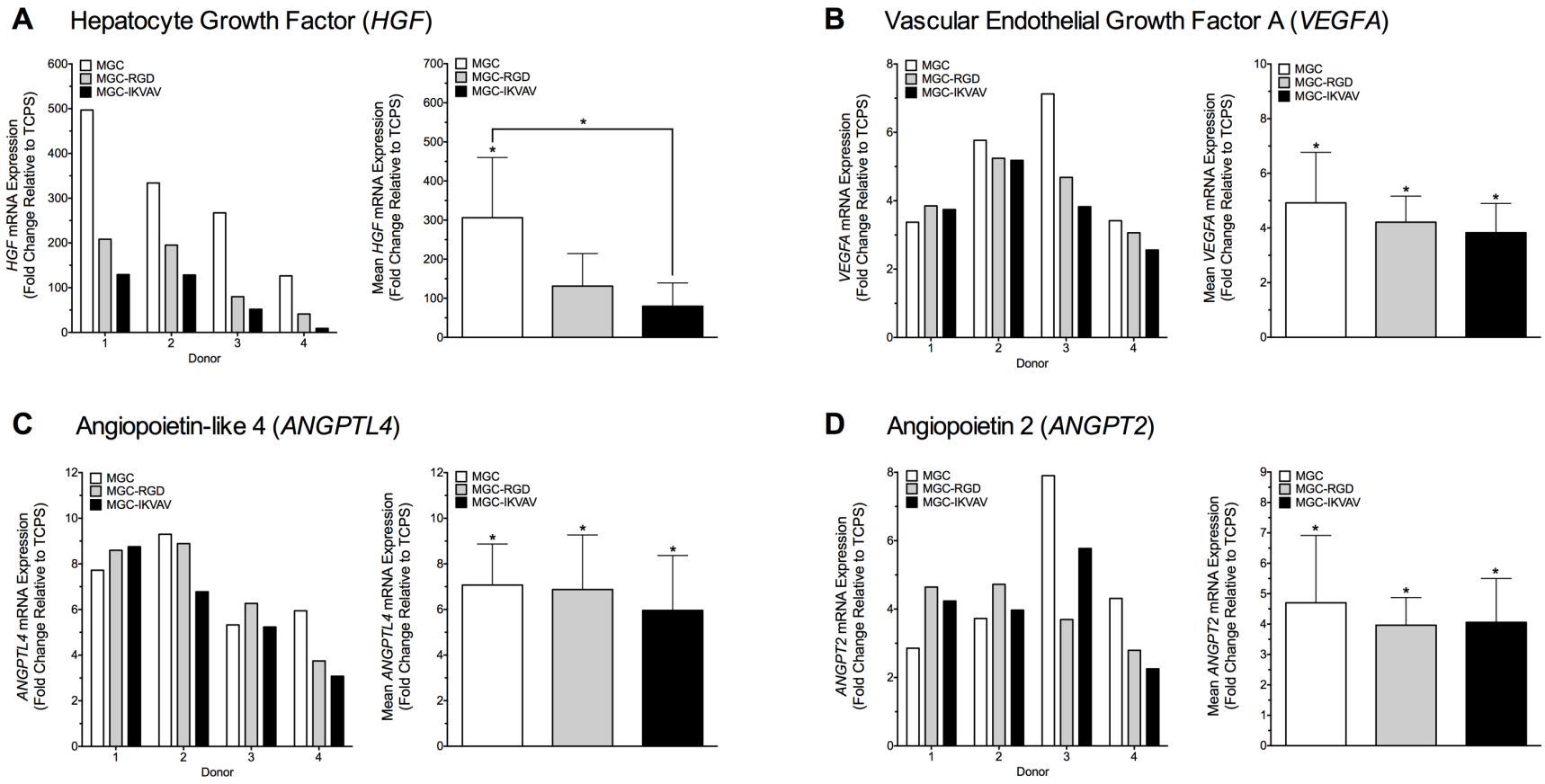

Figure 3.7. Gene expression of upregulated secreted angiogenic factors in ASCs encapsulated within MGC, MGC-RGD or MGC-IKVAV hydrogels and cultured under simulated hypoxic conditions (2% O_2). Results are expressed as fold change in the mRNA expression at 7 d relative to TCPS controls. Gene expression of (A) *HGF* was significantly enhanced in the MGC hydrogel group compared to the TCPS controls, and also compared to the MGC-IKVAV hydrogel. Transcript levels of (B) *VEGF*, (C) *ANGPTL4* and (D) *ANGPT2* were significantly upregulated for all hydrogel groups relative to the TCPS controls, suggesting enhanced transcription of these pro-angiogenic factors in the ASCs encapsulated in the hydrogels. Data shows transcript levels from the individual donors (left) and the pooled data from all 4 donors expressed as mean ± SD (right) (*$p<0.05$; n=6, N=4).

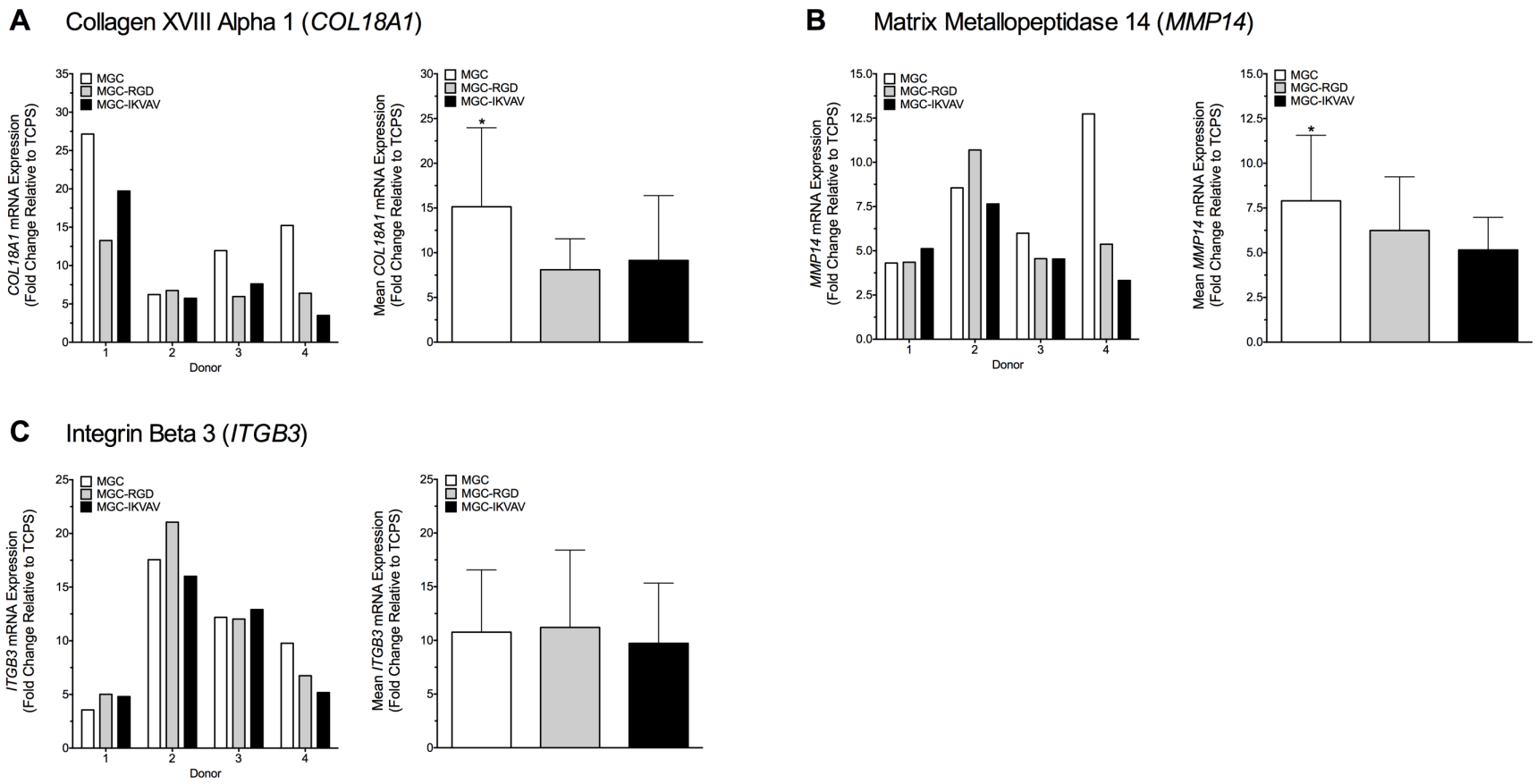

Figure 3.8. Gene expression of upregulated ECM-associated factors in ASCs encapsulated within MGC, MGC-RGD or MGC-IKVAV hydrogels and cultured under simulated hypoxic conditions (2% O_2). Results are expressed as fold change in the mRNA expression at 7 d relative to the TCPS controls. Gene expression of (A) the ECM protein *COL18A1* and (B) the matrix remodeling factor *MMP14* were significantly upregulated in the MGC hydrogel group relative to TCPS controls, suggesting enhanced transcription of regulatory and remodeling proteins involved in angiogenic processes in the encapsulated ASCs. (C) A trend for enhanced transcript levels of *ITGB3* was noted for all hydrogel groups relative to the TCPS controls for all 4 cell donors, but the difference was not significant. Data shows transcript levels from the individual donors (left) and the pooled data from all 4 donors expressed as mean ± SD (right) (*$p<0.05$; n=6, N=4).

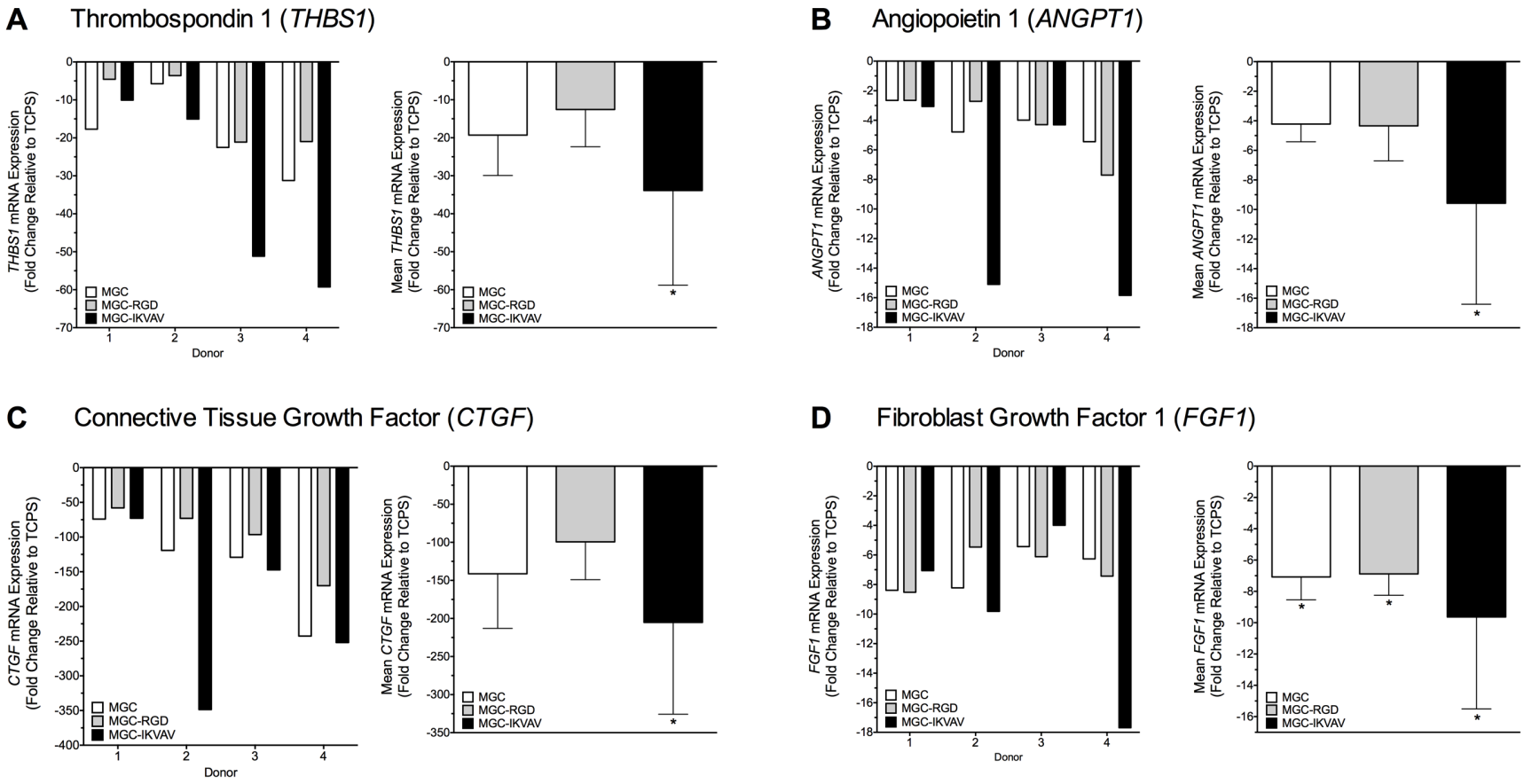

Figure 3.9. Gene expression of downregulated secreted factors in ASCs encapsulated within MGC, MGC-RGD or MGC-IKVAV hydrogels and cultured under simulated hypoxic conditions (2% O_2). Results are expressed as fold change in the mRNA expression at 7 d relative to the TCPS controls. The mRNA expression of (A) *THBS1*, (B) *ANGPT1* and (C) *CTGF* was significantly decreased in the MGC-IKVAV hydrogel group as compared to the TCPS controls. Transcript levels of (D) *FGF1* were significantly downregulated in all hydrogel groups relative to the TCPS controls. Data shows transcript levels from the individual donors (left) and the pooled data from all 4 donors expressed as mean ± SD (right) (*$p<0.05$; n=6, N=4).

3.5 *In Vivo* Analysis of ASCs following Encapsulation

3.5.1 ASC Retention within the Implanted Hydrogels

Human ASCs were encapsulated within the MGC, MGC-RGD or MGC-IKVAV hydrogels and subcutaneously implanted into NOD/SCID mice to assess whether peptide modification of the MGC influenced ASC retention within the hydrogels *in vivo*. At 14 d post-transplantation, the animals were euthanized to collect the hydrogels, which were easily visualized within the subcutaneous space (Figure 3.10A). Immunostaining for HLA-ABC was performed to detect human cells (Figure 3.10B), and quantitative analysis revealed that there were significantly more HLA-ABC$^+$ cells per unit area in the gel phase of the MGC-RGD hydrogel group at 144 ± 31 cells/mm^2 as compared to the MGC-IKVAV hydrogel group at 67 ± 16 cells/mm^2 (Figure 3.10C). While there was a trend for a higher density of HLA-ABC$^+$ cells in the MGC-RGD group as compared to the non-peptide modified MGC hydrogel group (103 ± 27 cells/mm^2), the difference was not statistically significant.

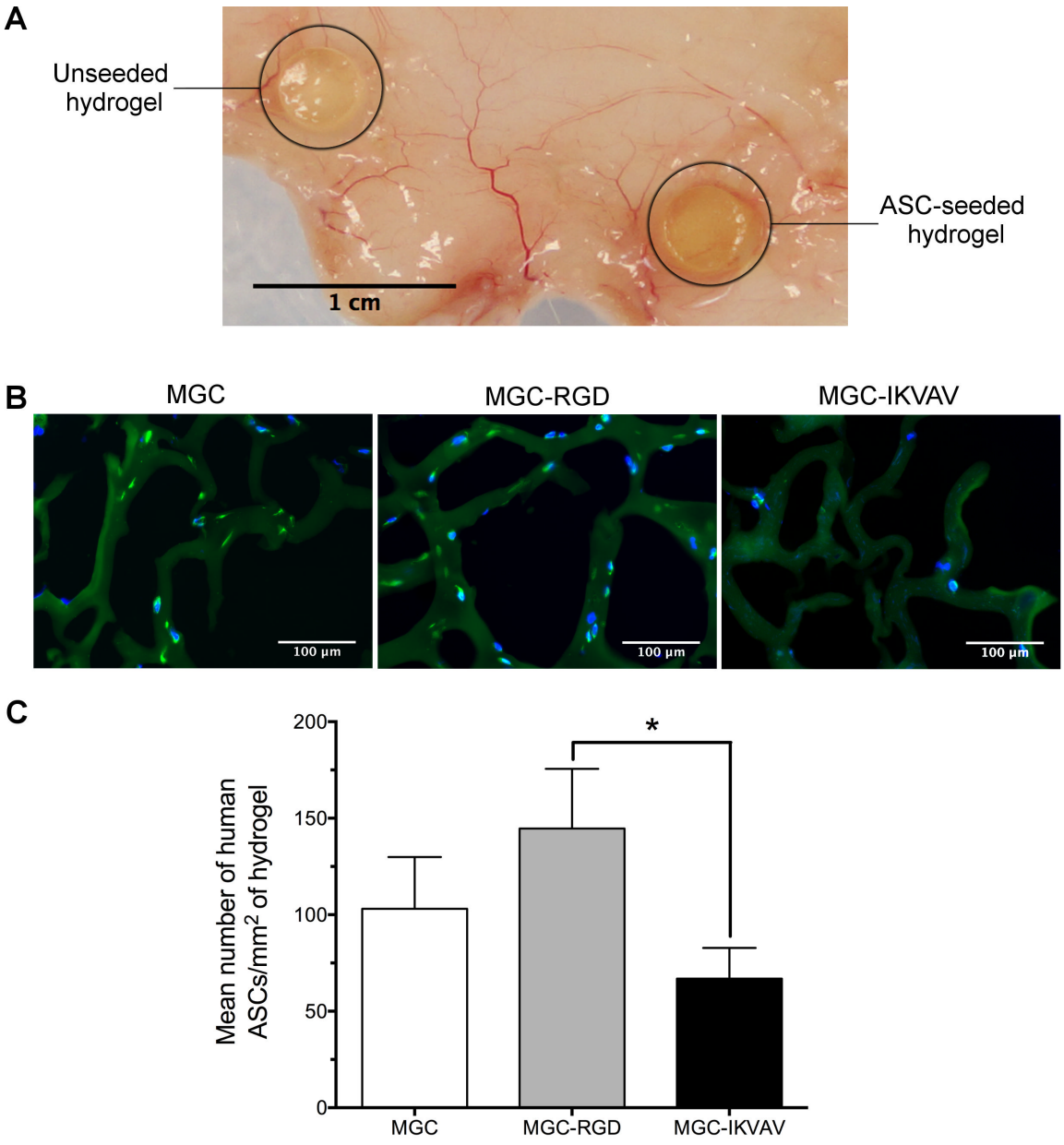

Figure 3.10. Analysis of human ASC retention within subcutaneously implanted MGC, MGC-RGD or MGC-IKVAV hydrogels. (A) Representative photograph of an unseeded (left) and ASC-seeded (right) MGC hydrogel subcutaneously implanted into NOD/SCID mice and excised at 14 d. (B) Representative immunohistochemical photomicrographs of HLA-ABC$^+$ (bright green) and DAPI (blue) stained human ASCs within the hydrogels (lighter green due to autofluorescence). (C) Mean number of HLA-ABC$^+$ DAPI$^+$ human ASCs/mm^2 visualized within each of the hydrogel groups. The MGC-RGD hydrogel showed significantly higher ASC retention within the scaffold at 14 d as compared to the MGC-IKVAV hydrogel group. Data represents mean ± SD analyzing 8-10 non-overlapping frames within the scaffold per section, from a total of 3 sections per hydrogel sample (*$p<0.05$; n=2, N=3).

3.5.2 CD31$^+$ Cell Recruitment and Proliferation in the Peri-implant Region

Murine endothelial cell (EC) and myeloid cell recruitment and proliferation were assessed within the host tissues in the peri-implant region (Figure 3.11) immediately adjacent to the MGC, MGC-RGD and MGC-IKVAV implants at 14 d through immunostaining for CD31, combined with EdU incorporation to detect proliferating CD31$^+$ cells (Figure 3.12A). CD31, named platelet-derived endothelial cell adhesion molecule, is a well-accepted endothelial cell marker, but is also expressed on early myeloid cells and macrophages.[215] Unseeded control hydrogels were also included in the analysis to more fully characterize the influence of the encapsulated ASCs versus the hydrogel alone on CD31$^+$ cell recruitment *in vivo*.

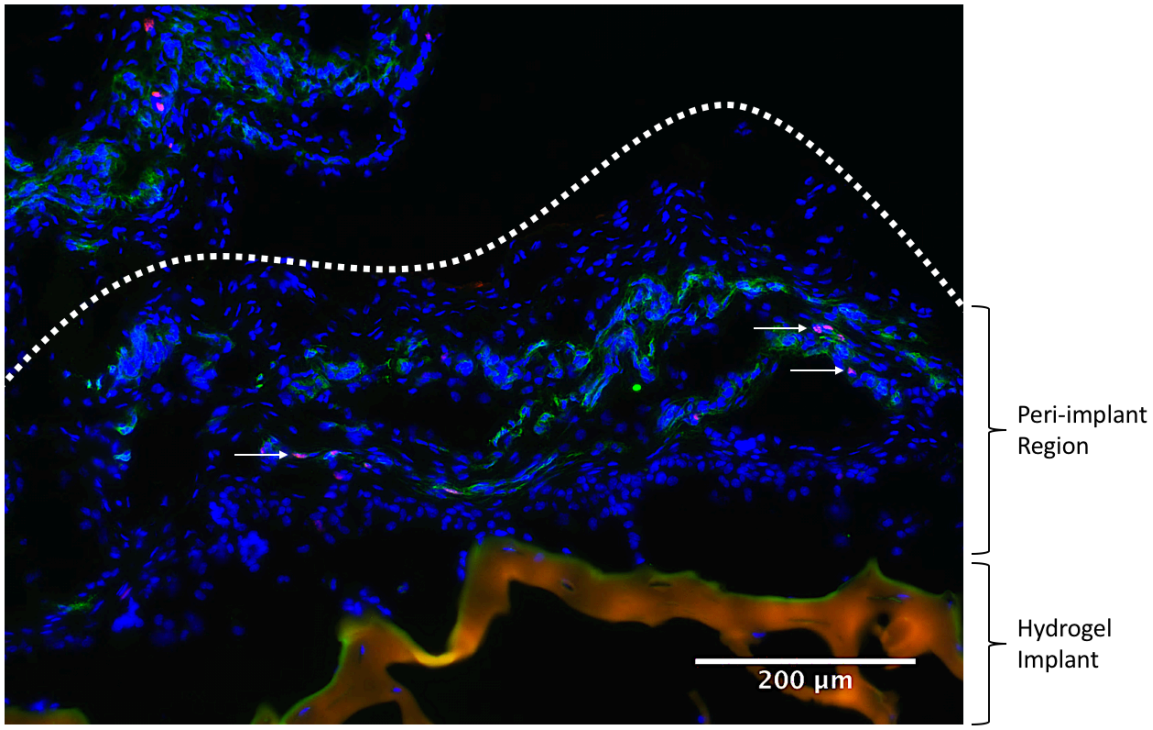

Figure 3.11. Representative immunohistochemical photomicrograph showing the peri-implant region in the subcutaneous hydrogel implants. The peri-implant region was identified by DAPI nuclear staining as the dense cell layer immediately adjacent to the implanted hydrogel. Photomicrograph shows CD31$^+$ cells (green) and proliferating cells (EdU$^+$, pink nuclei; examples indicated with white arrows) within the peri-implant region at 14 d post-transplantation.

A significantly higher number of murine $CD31^+$ cells were detected in the surrounding tissues of the ASC-seeded MGC (168 ± 5 cells/mm^2) and MGC-RGD (161 ± 12 cells/mm^2) hydrogels as compared to their corresponding unseeded controls (89 ± 14 cells/mm^2 and 94 ± 7 cells/mm^2, respectively) (Figure 3.12B). In contrast, there was no difference noted in $CD31^+$ cell recruitment between the seeded (113 ± 31 cells/mm^2) and unseeded (97 ± 4 cells/mm^2) hydrogels for the MGC-IKVAV group. Analysis of EdU incorporation indicated that there were proliferating $CD31^+$ cells in the peri-implant regions. However, there was significant variability in the number of proliferating cells, with no statistically significant differences observed between any of the groups (Figure 3.12C).

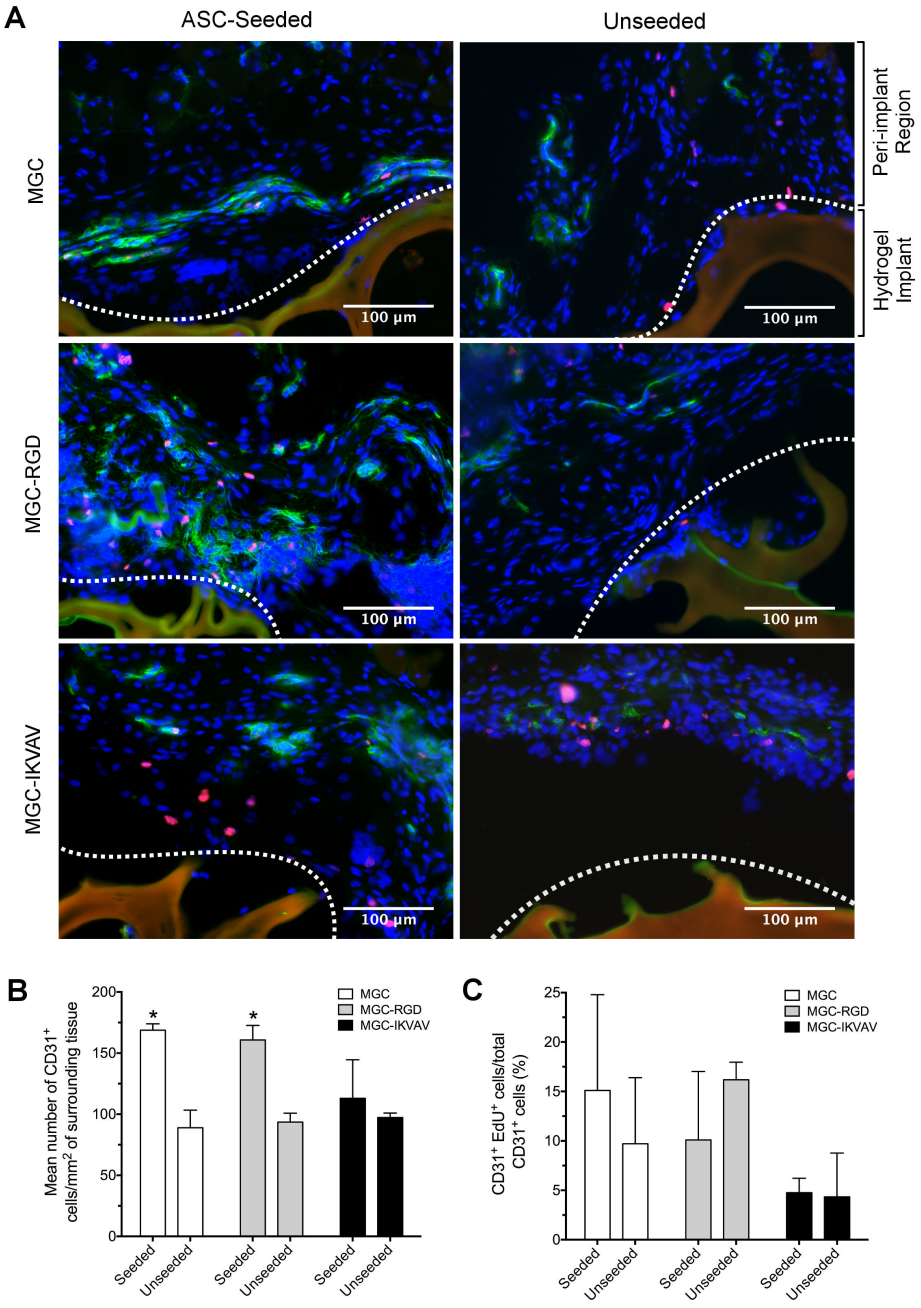

Figure 3.12. Analysis of CD31⁺ cell recruitment and proliferation in the peri-implant region of subcutaneously-implanted MGC, MGC-RGD or MGC-IKVAV hydrogels. (A) Representative photomicrographs of CD31⁺ (green) and proliferating cells (EdU⁺, pink nuclei) within the host tissues surrounding the ASC-seeded or unseeded hydrogels at 14 d post-transplantation. (B) Mean number of CD31⁺ cells recruited to the peri-implant region for each type of hydrogel with or without ASCs. ASC-seeded MGC and MGC-RGD hydrogels had a significantly higher number of CD31⁺ cells within the peri-implant region as compared to their corresponding unseeded controls, suggesting that ASCs may provide paracrine signals that promote CD31⁺ cell recruitment. (C) Frequency of CD31⁺ EdU⁺ cells within the peri-implant region of the ASC-seeded and unseeded hydrogel groups. No significant differences in CD31⁺ proliferation were observed between any of the groups. Data represents mean ± SD analyzed from 4-5 non-overlapping frames at the scaffold-tissue boundary per section, from a total of 3 sections per hydrogel sample (*$p<0.05$; n=2, N=2).

Chapter 4

4 DISCUSSION

There is growing interest in the design and application of biomaterials as cell delivery vehicles to improve the efficacy of cell-based treatments for peripheral artery disease (PAD). A range of synthetic, semi-synthetic and naturally-derived biomaterials have been explored to enhance the localization, retention and function of pro-regenerative cell populations.[85] Notably, hydrogels have shown promise as cell delivery scaffolds for therapeutic angiogenesis due to their capacity to cross-link *in situ* under mild conditions to enable minimally-invasive cell delivery via intramuscular injection.[216] Hydrogels also have high water content similar to that of the native extracellular matrix (ECM), which allows for efficient nutrient exchange and supports *in vivo* integration with minimal mechanical irritation to the surrounding tissues.[216] Therefore, a major focus of current research in the biomaterials field is on the design of novel hydrogel-based cell-delivery platforms. Overall, the goal in these strategies is to provide a cell-supportive and bioactive microenvironment for transplanted cells to support their sustained localization, viability and pro-regenerative secretory functions.[217]

Chitosan has emerged as a promising biomaterial due to its cytocompatible, biodegradable, antimicrobial, and pro-angiogenic properties.[170–172,218] The cationic nature of chitosan supports its interactions with negatively-charged glycosaminoglycans (GAGs) and proteoglycans, which naturally sequester growth factors and cytokines from within the ECM.[175] The innate wound healing properties of chitosan are well recognized. For example, in a canine wound model, chitosan scaffolds were shown to enhance the infiltration of polymorphonuclear cells, stimulate the production of collagen type III by fibroblasts, and promote granulation tissue formation at the wound site to accelerate wound closure.[219] The immunomodulatory properties of chitosan and its oligomeric degradation products have been postulated to be associated with its pro-regenerative characteristics.[174] More specifically, chitosan has been shown to promote macrophage recruitment,[220] as well as polarization of macrophages towards a more anti-inflammatory (M2) phenotype that is associated with enhanced tissue regeneration.[221]

Chitosan is generally insoluble in aqueous media under neutral and basic pH conditions.[177] Therefore, for cell delivery applications, chitosan is often modified to generate glycol chitosan (GC), which is soluble in aqueous solutions at physiological pH.[140,177] Chitosan contains reactive functional groups that can serve as targets for chemical modification, such as methacrylation, to generate *N*-methacrylate glycol chitosan (MGC) that can be cross-linked to form a stable hydrogel network via UV- or thermally-initiated cross-linking.[140,178] More specifically, in previous studies in the Amsden lab, photopolymerization of MGC has been explored using the photoinitiator Irgacure 2959 with low intensity UV light to produce hydrogel scaffolds for tissue engineering and growth factor delivery.[140,141] Amsden *et al*. initially showed that MGC with a 5% degree of substitution (DOS; methacrylate groups per 100 disaccharide units) cross-linked with high efficiency following UV irradiation (25 mW/cm^2) for 5 min.[140] The hydrogels supported the viability of C-28/I2 cells (human chondrocyte cell line) seeded on the scaffold surface over 7 days.[140] A later study demonstrated that human adipose-derived stem/stromal cells (ASCs) encapsulated in the MGC hydrogels via UV-initiated cross-linking (10.8 mW/cm^2; 3 min) maintained an average viability of 62.2% over 14 days.[141] Although UV cross-linking enables rapid and efficient gelation of MGC, the need for direct exposure to a UV light source at the site of administration limits the clinical applicability of this approach for patients with PAD.

In the present study, a chemical initiator system consisting of ammonium persulfate (APS) and *N,N,N′,N′*-tetramethylethylenediamine (TEMED) was used to cross-link the MGC-based pre-polymers at 37ºC, thereby encapsulating human ASCs within the hydrogel. This strategy allows for easy handling of the pre-polymer/cell suspension due to the slow rate of cross-linking at room temperature, while enabling the delivery of regenerative cells into ischemic tissues through minimally-invasive injections via a small gauge needle. The efficacy of these initiators has been previously shown *in vitro* to encapsulate rat bone marrow-derived mesenchymal stem/stromal cells (BM-MSCs) in oligo[poly(ethelene glycol) fumarate] hydrogels.[144] Similarly, Hong *et al*. used the thermally-sensitive cross-linking approach to encapsulate rabbit chondrocytes in chitosan-based gels and observed maintenance of cell number within the hydrogels over 6

days, further confirming the cytocompatibilty of the chemical initiators.[178] In addition, the efficacy of the APS/TEMED initiator system has been demonstrated *in vivo* with methacrylated hyaluronic acid (MeHA) hydrogels in an ovine myocardial infarction (MI) model.[129]

Modification of scaffolds with bioactive moieties has allowed researchers to further control the fate of transplanted cells, influencing their viability, proliferation, migration and differentiation.[222] In particular, short integrin-binding sequences derived from ECM molecules have been explored to promote cell adhesion, retention and survival within otherwise bio-inert scaffolds.[223–225] These small peptides offer several advantages as compared to the incorporation of complete proteins, including higher stability with temperature and pH variations, easier characterization, and cost-effective synthesis.[226,227] Building upon these concepts, one of the main objectives of the present study was to investigate the effects of incorporating the integrin-binding RGD and IKVAV peptide ligands on human ASC viability, retention and function following encapsulation in the MGC hydrogels.

Due to its widespread distribution in various ECM proteins, the arginine-glycine-aspartic acid (RGD) motif found in collagen and fibronectin is one of the most extensively studied sequences in the biomaterials field.[145] One study demonstrated that incorporating RGD motifs within poly(ethylene glycol) (PEG) hydrogels enhanced the survival of encapsulated human BM-MSCs, increasing the viability from 15 ± 7% to 73 ± 7% after 1 week in culture.[228] In addition, BM-MSCs seeded onto the surface of the PEG-RGD hydrogels showed improved cell attachment and spreading within 4 hours of seeding as compared to the unmodified controls.[228] Salinas *et al*. reported that human BM-MSCs encapsulated in PEG hydrogels with covalently tethered RGD ligands were able to maintain their viability at 84% over a 14-day culture period.[229] In a previous study with ASCs, rat preadipocytes were shown to bind preferentially to laminin-derived ECM substrata as compared to fibronectin- and collagen I or IV-derived ECM substrata,[166] providing a rationale for the exploration of the laminin-derived IKVAV peptide group in the current study. While laminin-derived peptides have been less extensively explored in the literature to date, Patel *et al*. demonstrated that incorporating YIGSR motifs in PEG

hydrogels improved cell adhesion and increased cell proliferation of rat preadipocytes seeded onto the scaffold surfaces, as evidenced by the 4.5-fold increase in DNA content over a 6-day culture period.[230]

With the recognition that cell response is mediated by the biochemical and biomechanical properties of the local cellular microenvironment,[210–212] the initial experiments focused on the physical characterization of the hydrogels. Analysis of the sol content revealed a lower cross-linking efficiency for the MGC-IKVAV hydrogel as compared to the MGC and MGC-RGD groups. One possible reason for this difference is that the larger IKVAV peptide, comprised of 19 amino acids (CSRARKQAAS**IKVAV**SADR), may have sterically hindered the cross-linking process to a greater extent than the shorter 8 amino acid sequence of the RGD peptide (GGGG**RGD**S). The 19-mer IKVAV sequence was selected for the current study based on previous work that indicated it had favorable bioactive effects on cells in culture.[231–233] A concern with using untested shorter sequences was that the peptides might not have an appropriate 3-D conformation to support integrin binding. However, the length and hydrophobic nature of the 19-mer IKVAV peptide, attributed to the relative abundance of hydrophobic alanine (A), isoleucine (I) and valine (V) amino acid residues, may have had inhibitory effects on cross-linking. This possibility is supported by the fact that challenges were encountered when attempting to dissolve the MGC-IKVAV material to obtain an aqueous pre-polymer solution, which necessitated blending of unmodified MGC with the peptide-modified MGC to be able to create stable gels with the MGC-IKVAV. While there were no issues dissolving the more hydrophilic MGC-RGD pre-polymer, it was also blended in a 40:60 ratio with unmodified MGC to ensure there were an equivalent number of peptide moieties between the two groups for comparative purposes. While the blended pre-polymers appeared macroscopically homogenous, it is possible that the more poorly soluble MGC-IKVAV may not have incorporated into the hydrogel network as efficiently.

The sol content is an important design consideration, as the presence of unreacted methacrylate may negatively impact cell viability.[234] However, the primary goal in fabricating the hydrogels in the current study was to ensure that the scaffolds had similar

equilibrium compressive moduli to assess the impact of the peptide modification of MGC on the response of the encapsulated cell populations without the potentially confounding biomechanical effects. Scaffold stiffness has been shown to influence cell adhesion, cytoskeletal organization, motility and differentiation capacity.[212,235,236] For example, a previous study showed that the rate of proliferation of human dermal fibroblasts cultured on collagen matrices was dependant on scaffold stiffness.[237] Specifically, fibroblasts seeded on stiffer matrices (143 kPa) showed an 87% increase in cell number, while there was only a 25% increase on softer the matrices (42 kPa) over a 2-day culture period.[237]

For the cell culture studies, human ASCs were selected as the regenerative cell type due to their accessibility, relative abundance, and documented capacity to secrete a broad array of pro-angiogenic paracrine factors.[93,102–104] These cells have been studied extensively in the Flynn lab, and previous work has validated that the ASCs isolated with the established culture protocols have multipotent differentiation capacity towards the adipogenic, osteogenic and chondrogenic lineages.[203,238] The immunophenotype analysis of the passage 3 (P3) human ASCs used in the current study confirmed that the cells had the expected stromal cell phenotype prior to encapsulation. The flow cytometry data was in agreement with the International Society of Cellular Therapy (ISCT) and the International Federation for Adipose Therapeutics and Science (IFATS) guidelines for ASCs as a stromal cell population,[112] with >80% positive stromal marker expression and <2% negative marker expression. The variable expression of CD34 and CD146 was also consistent with previous reports showing a steady decline in the expression of these markers with serial passaging.[100,213]

Following the initial characterization of the hydrogels and ASCs, subsequent *in vitro* studies focused on examining the effects of incorporating the peptide-modified MGC formulations containing the cell-adhesive RGD or IKVAV sequences within the hydrogels on ASC viability following encapsulation and culture under simulated hypoxic conditions (2% O_2). Notably, the unmodified MGC hydrogels supported high levels of ASC viability over the 14-day culture period, although there was a statistically significant decline in viability from 24 h to 14 days. In general, the viability results suggest that the MGC base material provides a cell-supportive microenvironment, and validates the use of

the thermally-induced cross-linking approach with APS and TEMED for ASC encapsulation.

The investigation of the RGD-modified MGC was motivated in part by the pro-survival effects noted in previous collaborative studies in the Amsden and Flynn labs with human ASCs.[141] More specifically, the team demonstrated that photocross-linked MGC hydrogels grafted with the RGD peptide maintained the viability of encapsulated ASCs above 85% over 14 days in culture under atmospheric conditions, relative to the average viability of ~62% in the unmodified controls.[141] In contrast, in the current study, the viability in the MGC and MGC-RGD groups were quite similar. However, the MGC-RGD group was the only one that demonstrated no statistically significant changes in viability over time, suggesting that the inclusion of the RGD peptides may be favorable for long-term ASC survival. In addition to the cross-linking approach, one key difference with the previous study was that all culturing in the current study was performed under simulated hypoxic conditions (2% O_2), which may have enhanced the survival of the encapsulated ASCs across all groups, including the unmodified MGC hydrogel. This possibility is supported by the work of Stubbs *et al*., who showed that preconditioning human ASCs under hypoxic conditions attenuated cell apoptosis.[120]

In contrast, ASC viability in the MGC-IKVAV hydrogel group was significantly reduced at all time points as compared to the MGC and MGC-RGD groups, with 54.4 ± 12.2% viability observed at 14 days. A possible reason for the poor initial survival of the ASCs in the MGC-IKVAV hydrogels at 24 h could be the higher proportion of uncross-linked methacrylate groups in this scaffold associated with the higher sol content, which may have had adverse effects on the cells.[239] More importantly, the decline in ASC viability over 14 days indicates that the inclusion of the IKVAV peptide limited the cytocompatibility of the MGC scaffolds. It is possible that the hydrophobic nature of the IKVAV-containing peptide may have promoted interactions with the plasma membrane that were detrimental to cell viability. For example, hydrophobic peptides have been applied as cell-penetrating peptides for peptide and protein delivery.[240] While past studies using the same 19-mer IKVAV peptide have not reported impaired viability, one key difference is that the cell response was previously explored in cells cultured on peptide-

modified 2-D surfaces.[232,233] Therefore, it is possible that the interaction between the cells and the peptide groups could vary substantially following encapsulation within a 3-D microenvironment. Future studies could probe whether the 3-D configuration was a factor by exploring ASC attachment and viability on the surface of pre-formed MGC-IKVAV hydrogels in comparison to unmodified MGC controls.

Further analysis of the confocal imaging results in the viability study revealed that the total number of ASCs within all of the hydrogel groups remained relatively constant over the course of 14 days. These findings suggest that the ASCs did not proliferate within the hydrogels during culture. Similar findings have been previously reported with human ASCs encapsulated within MGC hydrogels with varying degrees of RGD functionalization (0%, 2% and 5%), showing no differences in the number of ASCs over a 14-day culture period.[141] Likewise, Duggal *et al*. also demonstrated that the number of human ASCs remained constant over 21 days when encapsulated in alginate scaffolds covalently modified with the G**RGD**SP peptide sequence.[241] In the future, additional studies could be performed using complementary assays such as quantification of total dsDNA content to validate the LIVE/DEAD® imaging results, confirming that there were no changes in total cell number over time within the hydrogels.

The LIVE/DEAD® assay also allowed for the qualitative assessment of ASC morphology within the hydrogels. The findings suggest that the RGD peptide promoted ASC spreading within the superficial layers of the hydrogels, with a fraction of the encapsulated cells in the MGC-RGD group having an elongated fibroblastic morphology at 7 and 14 days. A previous study has reported similar findings with human BM-MSCs seeded onto the surface of MeHA scaffolds.[210] Specifically, MeHA scaffolds modified with varying RGD peptide densities demonstrated a concentration-dependent increase in cell adhesion and spreading area over 14 days. The study's findings also indicated that these morphological changes were attributed to vinculin-rich focal adhesions formed at the periphery of the well-spread MSCs in the higher density RGD-modified MeHA hydrogels.[210] Similarly, Burdick *et al*. reported that PEG hydrogels modified with RGD ligands increased osteoblast spreading within 24 h of seeding on the surface of the gels.[242] Several other authors have reported similar effects in terms of cell adhesion and

spreading when incorporating RGD ligands into various scaffolds including alginate gels, and *N*-isopropylacrylamide and acrylic acid-based hydrogels.[183,243]

In contrast to the results observed for the MGC-IKVAV group in the current study, a previous study showed that IKVAV peptide coatings on 2-D tissue culture polystyrene (TCPS) increased murine myoblast attachment and spreading as compared to uncoated controls within 3 h of seeding.[244] More recently, Li *et al*. reported that human neural stem/progenitor cells cultured on the surface of IKVAV-modified PEG hydrogels displayed a spread morphology, with migration into the scaffolds observed at 7 days.[245] However, a key difference is that these studies involved 2-D systems rather than 3-D cell encapsulation, and many cell types have a more rounded morphology within 3-D *in vivo* microenvironments than what is observed in 2-D culture systems.[246] Another notable difference is that Li *et al*. incorporated a shorter 12 amino acid sequence (CCRR**IKVAV**WLC) in their PEG hydrogels, which may have interacted with the cells differently than the peptide used in the current study. In addition, peptide conformation[247] and concentration[169] have also been shown to influence the interaction between cells and the IKVAV peptides, thereby impacting cell attachment and viability. Future studies could explore the effects of varying concentrations of the peptides, including more detailed analysis of the structure of the cytoskeleton using immunohistochemistry to assess differences in cell morphology. While cell spreading within the hydrogels is an indication of altered phenotype, the effects on cell function are not yet clear and may be an interesting area for future exploration.[248]

While the LIVE/DEAD® assay allowed for the direct assessment of the number of live and dead ASCs within the hydrogels, the MTT assay was performed to probe the metabolic activity of the encapsulated ASCs within the hydrogels. The attenuated metabolic activity in the MGC-IKVAV group at 7 and 14 days was likely attributed to the decline in the number of viable ASCs over the course of the study. However, while this assay is commonly used as a measure of cell proliferation, cellular metabolic activity can be altered for other reasons, with notable variations observed in cell responses between 2-D and 3-D culture systems.[249] For example, cells at different densities demonstrate different metabolic activities, which may not correlate in a linear fashion.[249]

The increased metabolic activity observed at 24 h for all hydrogel groups may have been associated with the cells responding to the redox-initiated cross-linking process used for encapsulation, with effects subsiding over time. Notably, the findings also indicated that the metabolic activity of the encapsulated ASCs was augmented in the MGC-RGD hydrogels at 14 days as compared to the other groups. Combined with the observed cell spreading, this data could support that there may be differences in ASC function after encapsulation in the MGC-RGD hydrogels at the later time points. In another study with human BM-MSCs encapsulated within RGD-grafted alginate scaffolds, metabolic activity initially declined over 14 days, but rebounded at 21 d to the same levels measured at 1 d.[160] Therefore, it may be interesting to explore the viability and metabolic activity of the ASCs encapsulated in the MGC-RGD and MGC hydrogels at later time points in future work.

With a view towards the future application of the platforms in pro-angiogenic cell therapies for the treatment of PAD, the final *in vitro* studies focused on assessing the expression of angiogenesis-associated genes in ASCs encapsulated within the hydrogels cultured under simulated hypoxic conditions (2% O_2) for 7 days relative to 2-D TCPS controls. Overall, the most notable differences were observed between the 3-D and 2-D culture conditions, indicating that encapsulation within the 3-D microenvironment altered cell function. These findings are consistent with a growing body of literature that supports that cell behavior, including proliferation, differentiation, and responses to various stimuli, differ substantially when cells are cultured on 2-D substrates as compared to 3-D culture systems or *in vivo*.[250,251] For example, variations in the surface chemistry and biomechanical properties of the 3-D hydrogels and rigid 2-D TCPS substrates[252] may have contributed to the differences in angiogenic gene expression in the ASCs cultured on these two platforms. It is also worth noting that the ASCs cultured on TCPS were not exposed to the free-radical initiator system with APS and TEMED, which may have impacted ASC function. Regardless of the differences, the 2-D TCPS controls were useful as a calibrator to normalize the gene expression levels and allow for comparisons between the different donors.

While this study is the first to apply a high throughput approach, these findings are supported by previous work investigating the effects of 3-D culture conditions on pro-angiogenic gene expression. For example, enhanced *VEGF* gene expression was observed in human ASCs seeded on polyglycolic acid/polylactic acid scaffolds relative to 2-D culture controls at 14 and 21 days.[253] Similarly, higher levels of *VEGFA*, *HGF*, *FGF-2* and *SDF-1* gene expression were reported in murine ASCs cultured within collagen-pullulan hydrogels over 48 h as compared to TCPS controls.[254]

In terms of the effects of the peptide modification, with the exception of hepatocyte growth factor (*HGF*), there were no statistically significant differences in the gene expression levels of the 84 analyzed angiogenic markers between the MGC, MGC-RGD and MGC-IKVAV hydrogel groups under the hypoxic culture conditions (2% O_2) in the current study. It is worth noting that the gene expression levels for HGF and connective tissue growth factor (CTGF) demonstrated a >80-fold change in the hydrogel groups as compared to the TCPS controls. However, it is also important to recognize that the response may vary over time, and that gene expression levels do not always directly correlate with protein expression levels. Therefore, it would be worthwhile to explore additional time points in future work, such as the 14-day time point, where there were notable differences in cell spreading and metabolic activity in the MGC-RGD group. Further, it would be interesting to perform additional follow-up studies using ELISAs or cytokine arrays to quantify secreted factors in media conditioned by encapsulated ASCs at the protein level.

In terms of the secreted pro-angiogenic factors, there was enhanced gene expression of *HGF*, vascular endothelial growth factor A (*VEGFA*), angiopoietin-like 4 (*ANGPTL4*) and angiopoietin-2 (*ANGPT2*) in ASCs encapsulated in the hydrogels relative to the 2-D controls. These factors have been shown to play key roles during vascular regeneration, including promoting endothelial cell migration and proliferation,[255] regulating vessel permeability,[256,257] and modulating wound healing.[258] For example, both HGF and VEGF can induce pro-survival effects on the endothelium under hypoxic conditions,[259,260] and angiopoietin-like 4 has been shown to promote MSC survival under hypoxic conditions.[261] The ECM-associated genes collagen XVIII α1 (*COL18A1*), matrix

metalloproteinase 14 (*MMP14*) and integrin β3 (*ITGB3*) were also upregulated in the hydrogel groups as compared to the TCPS controls, consistent with previous reports of enhanced MMP and integrin expression in 3-D culture systems.[262] Therefore, culturing the ASCs within the hydrogels enhanced the expression of genes associated with ECM remodeling,[263,264] cell adhesion,[147] and cell survival.[155] For example, MMP14 has been shown to activate other proteases including MMP2 and MMP13 to facilitate degradation of ECM components and support vascular remodeling.[263,264]

While more factors were upregulated, there were several angiogenesis-associated genes that were consistently downregulated in the ASCs encapsulated in the hydrogels relative to the TCPS controls, including the secreted factors angiopoietin-1 (*ANGPT1*), *CTGF* and fibroblast growth factor 1 (*FGF1*), which play a role in promoting endothelial cell (EC) proliferation, migration and survival,[265–268] as well as vascular stabilization.[269] While the upregulated angiopoietin-2 is associated with pro-angiogenic sprouting, angiopoietin-1 reduces endothelial cell permeability and enhances vessel stabilization through mural cell recruitment.[270] As such, expression of this paracrine factor may be more critical during the later stages of regeneration. Interestingly, gene expression of the anti-angiogenic factor thrombospondin-1 (*THBS1*) was also downregulated in the hydrogel groups as compared to the TCPS controls. THBS1 is a potent inhibitor of angiogenesis that exerts its effects on EC proliferation, migration and apoptosis by antagonizing VEGF and FGF activity.[271,272] While these studies provide some preliminary insight into the pro-angiogenic capacity of the ASCs encapsulated within the hydrogels, further investigation is required to probe the response over time and more fully assess the biological relevance of these findings, including analysis of protein expression levels.

Following the *in vitro* studies, the hydrogels were subcutaneously implanted into NOD/SCID mice to compare ASC retention and the induction of angiogenesis between the MGC, MGC-RGD and MGC-IKVAV groups at 14 days. The highest cell density was observed in the MGC-RGD implants, which was significantly different than the MGC-IKVAV group. These results are consistent with the *in vitro* findings that indicated that long-term viability was impaired in the MGC-IKVAV group and improved in the MGC-RGD. In comparing the MGC and MGC-RGD groups, a relatively high density of

encapsulated ASCs could be visualized in both groups, suggesting that the hydrogels also supported local cell retention. Based on the observed trends, it is possible that increasing the peptide concentration beyond 2.5% in the MGC-RGD group could further augment cell adhesion and retention, as concentration-dependent effects on cell viability and attachment have been previously reported with human BM-MSCs encapsulated in RGD-modified HA hydrogels.[210]

As a surrogate measure of tissue revascularization, subsequent analyses focused on assessing murine $CD31^+$ cell recruitment and proliferation in the peri-implant regions. In comparing the unseeded hydrogel groups, the findings suggest that all of the hydrogels promoted similar levels of $CD31^+$ cell recruitment, which may be attributed to the pro-regenerative nature of the MGC base material, as discussed previously.[170–172,218] For example, the pro-angiogenic qualities of chitosan were shown in a previous study where EC recruitment and vascularization were enhanced in the periphery of collagen-chitosan composites implanted subcutaneously in mice as compared to collagen-only controls.[273]

In assessing the ASC-seeded groups, $CD31^+$ cell recruitment was significantly enhanced in the peri-implant region of the ASC-seeded MGC and MGC-RGD groups as compared to the unseeded controls. These findings suggest that ASCs encapsulated within these hydrogels secreted paracrine factors that promote $CD31^+$ cell migration to the implant interface. Similar pro-angiogenic paracrine effects have been previously reported with autologous BM-MSCs delivered in HA scaffolds in a subcutaneous rat model,[274] as well as with human ASCs delivered on collagen scaffolds in a nude rat model.[275] The consistency in the $CD31^+$ cell recruitment frequencies in the MGC and MGC-RGD groups is concordant with the similar viability and angiogenic gene expression profiles observed for these two groups in the *in vitro* studies. In contrast, the lack of ASC-mediated cell recruitment observed in the MGC-IKVAV implants is consistent with the *in vitro* findings that cell viability was lower in this group. Analysis of cell proliferation within the peri-implant region through semi-quantitative measurement of $CD31^+$ EdU^+ cells was suggestive of pro-angiogenic processes being induced in all of the groups. Overall, these *in vivo* findings support that the MGC and MGC-RGD hydrogels are

promising platforms for ASC delivery to promote local cell retention, viability, and beneficial paracrine factor production for applications in therapeutic angiogenesis.

Chapter 5

5 CONCLUSIONS

As the prevalence of peripheral artery disease (PAD) in North America rises, current treatments and surgical interventions remain limited in their efficacy to stimulate new blood vessel growth, restore long-term perfusion and promote functional recovery in the affected limb(s).[1,4,14] As such, there is a critical need for new clinically-translatable therapies that enhance perfusion in the affected tissues, minimize the risk of disease progression and improve the quality of life for patients with PAD. First generation cell-based therapies involving the injection of mesenchymal stem/stromal cell (MSC) suspensions into ischemic tissues have shown potential for stimulating new blood vessel formation.[58–60] However, the poor survival and retention of transplanted cells limits the pro-regenerative and pro-angiogenic functions of MSCs at the target ischemic sites.[85–87] To address these issues, the current project investigated an integrative approach combining cell-based therapy with a scaffold-based cell delivery strategy. Specifically, the survival and function of human adipose-derived stem/stromal cells (ASCs) was examined following encapsulation in *N*-methacrylate glycol chitosan (MGC) hydrogels. To further tune the approach, the MGC polymer was modified with integrin-binding RGD or IKVAV peptide ligands to assess the effects of these bioactive moieties in promoting ASC viability, retention and function within the hydrogels.

5.1 Summary of Findings

Prior to the cell-encapsulation studies, the initial experiments focused on characterizing the hydrogel scaffolds and the passage 3 (P3) human ASCs. While the sol content revealed that the MGC and MGC-RGD groups had a higher cross-linking efficiency than the MGC-IKVAV group, the equilibrium compressive moduli across all groups were similar, thus confirming consistent biomechanical properties which could potentially impact cell function. The immunophenotype analysis confirmed that the P3 ASCs aligned with the guidelines set forth by the International Society of Cellular Therapy (ISCT) and

the International Federation for Adipose Therapeutics and Science (IFATS) for stromal cell population.[112]

For aim 1, *in vitro* analyses were conducted to assess ASC viability, cell morphology and metabolic activity following cell encapsulation within the MGC, MGC-RGD or MGC-IKVAV hydrogels over 14 days in culture under hypoxic culture conditions (2% O_2) simulating the ischemic limb. The results demonstrated that ASCs encapsulated in the MGC and MGC-RGD hydrogels were able to maintain high viability (>75% and >80%, respectively) over the 14-day culture period. Notably, the MGC-RGD group was the only group that did not show a significant decline in ASC viability over the course of the study, suggesting that the incorporation of the RGD peptide supported long-term cell viability. In contrast, poor viability was noted in the MGC-IKVAV group, suggesting that the selected peptide was not conducive for promoting ASC viability or retention following encapsulation in the 3-D MGC-based hydrogel system. The assessment of cell morphology showed that ASCs encapsulated in the MGC and MGC-IKVAV hydrogels maintained a rounded shape over the course of the study. In contrast, ASCs encapsulated in the MGC-RGD hydrogels presented a more elongated fibroblastic morphology within the superficial layers at 7 and 14 days in culture, providing evidence for cell-scaffold interactions between the ASCs and RGD motifs. The metabolic activity of the encapsulated ASCs declined between 24 h and 7 days for all hydrogel groups, and was then maintained throughout the course of the study. In addition, the metabolic activity was enhanced in the MGC-RGD group as compared to the MGC and MGC-IKVAV groups at 14 days, suggesting that the RGD peptide ligand may influence the metabolic functions of encapsulated ASCs over time.

For aim 2, ASC function was probed *in vitro* by comparing the expression of angiogenesis-associated genes between ASCs encapsulated in the hydrogels versus 2-D tissue culture polystyrene (TCPS) controls cultured under simulated hypoxic conditions (2% O_2) for 7 days. In general, the most notable differences were associated with culturing the ASCs in the 3-D hydrogels versus the 2-D culture conditions across all 4 cell donors. More specifically, ASCs encapsulated in the hydrogels demonstrated a >2-fold upregulation in gene expression for the secreted angiogenic factors hepatocyte

growth factor (*HGF*), vascular endothelial growth factor A (*VEGFA*), angiopoietin-like 4 (*ANGPTL4*) and angiopoietin-2 (*ANGPT2*) relative to the TCPS controls. Furthermore, the extracellular matrix (ECM) protein collagen XVIII α1 (*COL18A1*), the matrix-remodeling factor matrix metalloproteinase 14 (*MMP14*), and the cell adhesion glycoprotein integrin β3 (*ITGB3*) also demonstrated a >2-fold enhancement in gene expression in the hydrogel groups relative to the TCPS controls. In contrast, a >2-fold downregulation in gene expression was consistently noted across all 4 cell donors for the secreted factors thrombospondin-1 (*THBS1*), angiopoetin-1 (*ANGPT1*), connective tissue growth factor (*CTGF*) and fibroblast growth factor 1 (*FGF1*) in the ASCs encapsulated in the hydrogels as compared to the TCPS controls. While transcription for the majority of the analyzed angiogenic factors was not considerably influenced by the presence of the RGD or IKVAV peptides under the conditions in the study, these preliminary findings suggest that the 3-D microenvironment of the MGC hydrogel induced transcriptional changes in the ASCs under hypoxic conditions that may be favorable for a pro-angiogenic response.

For aim 3, cell retention and angiogenic-induction potential of ASCs encapsulated within the hydrogels was assessed *in vivo* after subcutaneous implantation into NOD/SCID mice for 14 days. A significantly higher number of ASCs were retained in the MGC-RGD hydrogels relative to the MGC-IKVAV hydrogels, consistent with the *in vitro* viability studies. While there was a trend for enhanced retention in the MGC-RGD group as compared to the MGC group, the difference was not statistically significant. These findings suggest that the base MGC scaffold alone provided a supportive microenvironment for ASC retention *in vivo* over the course of the study. With respect to the pro-angiogenic potential, ASC-seeded MGC and MGC-RGD groups enhanced murine $CD31^+$ cell recruitment within the peri-implant region as compared to their corresponding unseeded controls, suggesting that the hydrogels were able to support the paracrine functions of ASCs to help establish accessory cell recruitment, a characteristic of a more pro-angiogenic microenvironment. In contrast, there was no difference in $CD31^+$ cell recruitment between the ASC-seeded and unseeded MGC-IKVAV group, potentially due to the low cell viability and retention within these hydrogels. Assessment

of $CD31^+$ EdU^+ cells in the peri-implant region indicated that $CD31^+$ cell proliferation was ongoing in all of the groups. Altogether, these findings suggest that the MGC and MGC-RGD hydrogels provide a cytocompatible microenvironment, supportive of ASC retention and accessory cell recruitment *in vivo*.

The collective findings highlight the potential of the MGC and MGC-RGD hydrogels as cell-delivery platforms, capable of supporting the viability, retention and sustained function of encapsulated ASCs. In addition, evidence of the pro-angiogenic capacity of encapsulated human ASCs was provided through the *in vitro* and *in vivo* studies, lending support for their use in therapeutic applications to promote vascular regeneration. Ultimately, the work presented in this thesis contributes to the fields of stem/stromal cell biology, biomaterials and therapeutic angiogenesis.

5.2 Future Recommendations

Although the current project offers insight into the development of an injectable cell-delivery platform for therapeutic angiogenesis, future studies should focus on optimizing the ASC viability, retention and function following encapsulation in the hydrogels. Continued refinement of the functionalization of the MGC hydrogels with peptides incorporating the RGD or IKVAV bioactive motifs, complemented with *in vitro* and *in vivo* studies to further assess ASC behaviour within the hydrogels, could help to establish a more effective cell-delivery vehicle.

Previous studies have provided support for the IKVAV peptide in promoting cell attachment and proliferation.[165,169,244] However, the current findings suggest that the inclusion of the 19-mer IKVAV peptide in the MGC hydrogels adversely impacted hydrogel cross-linking and the viability of encapsulated ASCs. Therefore, it would be beneficial to examine whether adjusting the length and/or hydrophobicity of the IKVAV peptide could provide a 3-D conformation that improves the ASC survival and better supports integrin-mediated cell attachment within the hydrogels. In addition, future studies could investigate the degree of RGD or IKVAV functionalization of the MGC hydrogels over a boarder range (e.g. 2.5%, 5%, and 10%), in order to delineate any concentration-dependent trends on ASC attachment, viability and metabolic function, as

observed in previous reports.[141] Collectively, these studies will help to establish the appropriate peptide sequence and concentration required to improve ASC adhesion and retention within the hydrogels.

The confocal imaging of ASCs encapsulated in the hydrogels in the current study allowed for the macroscopic assessment of ASC morphology following culture. Future studies should include more detailed immunohistochemial analysis to examine the changes in the cytoskeleton structure of the encapsulated ASCs. For example, ASCs could be stained for actin and vinculin at various time points (e.g. 7, 14 and 28 days), and analyzed through confocal imaging to validate the trends by more fully assessing cell spreading and focal adhesion formation. In order to better understand the regulation of integrins in ASCs during cell attachment, it would be of interest to examine the expression of various integrin subunits (e.g. $\alpha 1$, αV, $\beta 3$, etc.) through immunohistochemical staining. This study may help define the predominant α/β subunits involved in the cell-scaffold interactions due to the presence of integrin-binding RGD or IKVAV motifs.

While the metabolic activity of ASCs encapsulated in the hydrogels showed an initial decline across all groups, a rebounding trend was observed in the MGC-RGD group by day 14. Future studies should more fully probe this response by assessing the ASC metabolic activity at later time points (e.g. 28 days) to determine whether the bioactive peptide ligands in the hydrogels significantly enhance metabolic functions following long-term culture. In addition, the total dsDNA content in the ASC-encapsulated hydrogels should be assessed using the Quant-iT PicoGreen® dsDNA assay in order to validate the current semi-quantitative imaging data regarding the total cell number, and more fully assess whether the ASCs may be proliferating within the scaffolds, potentially in combination with Ki67 immunohistochemical staining.

The high-throughput screening of the angiogenesis-associated genes in the ASCs encapsulated within the hydrogels showed that the expression levels of several key pro-angiogenic genes were altered as compared to TCPS controls. Future studies could further probe the relevant genes through real-time RT-PCR and Western blotting of protein lysates to determine their regulation over the course of 14 or 28 days. The

conditioned medium from culturing the ASC-encapsulated hydrogels could also be examined through MultiPlex ELISA or proteomics analyses to assess whether detectable levels of factors are being secreted from the hydrogels over time. Furthermore, for a more controlled comparison between 3-D and 2-D culture conditions, future studies could probe the angiogenic response of ASCs seeded onto the surface of MGC, MGC-RGD or MGC-IKVAV hydrogels. Collectively, these studies would provide an in-depth analysis of the angiogenesis-associated secretory factors at the transcriptional and protein level.

MSCs have been previously shown to maintain the expression of typical stromal cell markers following prolonged 2-D culture conditions.[276] It would be of interest to investigate the MSC phenotype of ASCs following 3-D culture within the hydrogels. More specifically, the mRNA could be extracted from donor-matched ASCs prior to the encapsulation process, as well as after culture in the hydrogels for 14 or 28 days. The MSC marker expression could then be analyzed using a Human Mesenchymal Stem Cell RT^2 Profiler™ PCR array to compare the stem-cell state of ASCs prior to and following 3-D culture within the hydrogels.

In terms of future *in vivo* work, the efficacy of the injectable ASC delivery strategy should be investigated in a murine femoral artery ligation (FAL)-induced hindlimb ischemia model.[208] More specifically, ASC-loaded hydrogels could be injected intramuscularly into the hindlimb of NOD/SCID mice following FAL-induced hindlimb ischemia. Thereafter, the mice could be assessed in terms of limb reperfusion via Laser Doppler Perfusion Imaging (LDPI), functional limb improvement using a CatWalk™ system, and revascularization through more detailed immunohistochemical (CD31 and von willebrand factor) analysis. In addition, NOD/SCID/mucopolysaccharidosis type VII (MSPVII) mice could be used in a similar hindlimb ischemic model to allow for the more sensitive detection of transplanted viable ASCs in the ischemic tissue, as these mice lack beta-glucoronidase (GUSB) activity that is ubiquitously expressed in human cells.[208] This approach would enable the assessment of ASCs using a calorimetric substrate for GUSB in order to localize viable transplanted cells, at single cell resolution, within or around the new blood vessel growth. Together, these investigations would aid in understanding the potential of the MGC-based ASC-delivery strategy to retain the transplanted cells,

promote angiogenesis, and facilitate functional recovery of ischemic tissues, as a next-step towards clinical translation.

References

1. Lovell, M., Harris, K., Forbes, T., Twillman, G., Abramson, B., *et al.* Peripheral arterial disease: lack of awareness in Canada. *The Canadian Journal of Cardiology* **25,** 39–45 (2009).
2. Ko, S. H. & Bandyk, D. F. Therapeutic angiogenesis for critical limb ischemia. *Nature Reviews Cardiology* **27,** 23–31 (2014).
3. Lusis, A. J. Atherosclerosis. *Nature* **407,** 233–241 (2000).
4. Heuser, R. R. Treatment of lower extremity vascular disease: the Diamondback 360 degrees Orbital Atherectomy System. *Expert Review of Medical Devices* **5,** 279–286 (2008).
5. Varu, V. N., Hogg, M. E. & Kibbe, M. R. Critical limb ischemia. *Journal of Vascular Surgery* **51,** 230–241 (2010).
6. Golomb, B. A., Dang, T. T. & Criqui, M. H. Peripheral arterial disease: Morbidity and mortality implications. *Circulation* **114,** 688–699 (2006).
7. Annex, B. H. Therapeutic angiogenesis for critical limb ischaemia. *Nature Reviews Cardiology* **10,** 387–396 (2013).
8. Norgren, L., Hiatt, W. R., Dormandy, J. A., Nehler, M. R., Harris, K. A., *et al.* Inter-Society Consensus for the management of peripheral arterial disease (TASC II). *International Angiology* **26,** 82–157 (2007).
9. Ouriel, K. Peripheral arterial disease. *Lancet* **358,** 1257–1264 (2001).
10. Hirsch, A. T., Haskal, Z. J., Hertzer, N. R., Bakal, C. W., Creager, M. A., *et al.* Practice Guidelines for the Management of Patients With Peripheral Arterial Disease (Lower Extremity, Renal, Mesenteric, and Abdominal Aortic). *Circulation* **113,** 410–528 (2006).
11. Coats, P. & Wadsworth, R. Marriage of resistance and conduit arteries breeds critical limb ischemia. *American Journal of Physiology - Heart and Circulatory Physiology* **288,** H1044-1050 (2005).
12. Bradbury, A. W., Adam, D. J., Beard, J. D., Cleveland, T., Forbes, J. F., *et al.* Bypass versus angioplasty in severe ischaemia of the leg (BASIL): Multicentre, randomised controlled trial. *Lancet* **366,** 1925–1934 (2005).
13. Meininger, G. A. & Davis, M. J. Cellular mechanisms involved in the vascular myogenic response. *American Journal of Physiology* **263,** H647-659 (1992).
14. Davies, M. G. Criticial limb ischemia: epidemiology. *Methodist DeBakey Cardiovascular Journal* **8,** 10–14 (2012).
15. Attanasio, S. & Snell, J. Therapeutic angiogenesis in the management of critical limb ischemia: Current concepts and review. *Cardiology in Review* **17,** 115–120 (2009).
16. Amsden, B. G. Delivery approaches for angiogenic growth factors in the treatment

of ischemic conditions. *Expert Opinion on Drug Delivery* **8,** 873–890 (2011).

17. Brahmanandam, S. M., Messina, L. M., Belkin, M., Conte, M. S. & Nguyen, L. L. Determinants of Hospital Disposition after Lower Extremity Bypass Surgery. *Journal of Vascular Surgery* **49,** S27 (2009).

18. Carmeliet, P. & Jain, R. K. Angiogenesis in cancer and other diseases. *Nature* **407,** 249–257 (2000).

19. Cao, Y. & Langer, R. A review of Judah Folkman's remarkable achievements in biomedicine. *Proceedings of the National Academy of Sciences of the United States of America* **105,** 13203–13205 (2008).

20. Krock, B. L., Skuli, N. & Simon, M. C. Hypoxia-Induced Angiogenesis: Good and Evil. *Genes & Cancer* **2,** 1117–1133 (2011).

21. Kaelin, W. G. & Ratcliffe, P. J. Oxygen Sensing by Metazoans: The Central Role of the HIF Hydroxylase Pathway. *Molecular Cell* **30,** 393–402 (2008).

22. Wahlberg, E. Angiogenesis and arteriogenesis in limb ischemia. *Journal of Vascular Surgery* **38,** 198–203 (2003).

23. Clapp, C., Thebault, S., Jeziorski, M. C. & Martínez De La Escalera, G. Peptide hormone regulation of angiogenesis. *Physiological Reviews* **89,** 1177–1215 (2009).

24. Gerhardt, H. VEGF and endothelial guidance in angiogenic sprouting. *Organogenesis* **4,** 241–246 (2008).

25. Gerhardt, H., Golding, M., Fruttiger, M., Ruhrberg, C., Lundkvist, A., *et al.* VEGF guides angiogenic sprouting utilizing endothelial tip cell filopodia. *Journal of Cell Biology* **161,** 1163–1177 (2003).

26. Sneider, E. B., Nowicki, P. T. & Messina, L. M. Regenerative medicine in the treatment of peripheral arterial disease. *Journal of Cellular Biochemistry* **108,** 753–761 (2009).

27. Papetti, M. & Herman, I. M. Mechanisms of normal and tumor-derived angiogenesis. *American Journal of Physiology - Cell Physiology* **282,** C947-970 (2002).

28. Maragoudakis, M. E. Angiogenesis in health and disease. *General Pharmacology: Vascular System* **35,** 225–226 (2000).

29. Schmidt, A., Brixius, K. & Bloch, W. Endothelial precursor cell migration during vasculogenesis. *Circulation Research* **101,** 125–136 (2007).

30. Isner, J. M. & Asahara, T. Angiogenesis and vasculogenesis as therapeutic strategies for postnatal neovascularization. *Journal of Clinical Investigation* **103,** 1231–1236 (1999).

31. Risau, W. & Flamme, I. Vasculogenesis. *Annual Review of Cell and Developmental Biology* **11,** 73–91 (1995).

32. Cooke, J. P. & Losordo, D. W. Modulating the Vascular Response to Limb Ischemia: Angiogenic and Cell Therapies. *Circulation Research* **116,** 1561–1578 (2015).

33. Takayuki Asahara, Toyoaki Murohara, A. S. Isolation of Putative Progenitor Endothelial Cells for Angiogenesis. *Science* **275,** 964–967 (1997).

34. Murayama, T., Tepper, O. M., Silver, M., Ma, H., Losordo, D. W., *et al.* Determination of bone marrow-derived endothelial progenitor cell significance in angiogenic growth factor-induced neovascularization in vivo. *Experimental Hematology* **30,** 967–972 (2002).

35. Lawall, H., Bramlage, P. & Amann, B. Treatment of peripheral arterial disease using stem and progenitor cell therapy. *Journal of Vascular Surgery* **53,** 445–453 (2011).

36. Gnecchi, M., Zhang, Z., Ni, A. & Dzau, V. J. Paracrine mechanisms in adult stem cell signaling and therapy. *Circulation Research* **103,** 1204–1219 (2008).

37. Buschmann, I. & Schaper, W. The pathophysiology of the collateral circulation (arteriogenesis). *Journal of Pathology* **190,** 338–342 (2000).

38. Heil, M., Eitenmüller, I., Schmitz-Rixen, T. & Schaper, W. Arteriogenesis versus angiogenesis: Similarities and differences. *Journal of Cellular and Molecular Medicine* **10,** 45–55 (2006).

39. Takeda, Y., Costa, S., Delamarre, E., Roncal, C., Leite de Oliveira, R., *et al.* Macrophage skewing by Phd2 haplodeficiency prevents ischaemia by inducing arteriogenesis. *Nature* **479,** 122–126 (2011).

40. Van Royen, N., Piek, J. J., Buschmann, I., Hoefer, I., Voskuil, M., *et al.* Stimulation of arteriogenesis; a new concept for the treatment of arterial occlusive disease. *Cardiovascular Research* **49,** 543–553 (2001).

41. Jung, C., Rafnsson, A., Shemyakin, A., Böhm, F. & Pernow, J. Different subpopulations of endothelial progenitor cells and circulating apoptotic progenitor cells in patients with vascular disease and diabetes. *International Journal of Cardiology* **143,** 368–372 (2010).

42. Niiyama, H., Huang, N. F., Rollins, M. D. & Cooke, J. P. Murine model of hindlimb ischemia. *Journal of Visualized Experiments* 12–14 (2009). doi:10.3791/1035

43. Masaki, I., Yonemitsu, Y., Yamashita, A., Sata, S., Tanii, M., *et al.* Angiogenic gene therapy for experimental critical limb ischemia: Acceleration of limb loss by overexpression of vascular endothelial growth factor 165 but not of fibroblast growth factor-2. *Circulation Research* **90,** 966–973 (2002).

44. Chang, D. S., Su, H., Tang, G. L., Brevetti, L. S., Sarkar, R., *et al.* Adeno-associated viral vector-mediated gene transfer of VEGF normalizes skeletal muscle oxygen tension and induces arteriogenesis in ischemic rat hindlimb. *Molecular Therapy* **7,** 44–51 (2003).

45. Olea, F. D., Vera Janavel, G., Cuniberti, L., Yannarelli, G., Cabeza Meckert, P., *et al.* Repeated, but not single, VEGF gene transfer affords protection against ischemic muscle lesions in rabbits with hindlimb ischemia. *Gene Therapy* **16,** 716–723 (2009).

46. de Paula, E. V, Flores-Nascimento, M. C., Arruda, V. R., Garcia, R. A., Ramos, C. D., *et al.* Dual gene transfer of fibroblast growth factor-2 and platelet derived growth factor-BB using plasmid deoxyribonucleic acid promotes effective angiogenesis and arteriogenesis in a rodent model of hindlimb ischemia. *Translational Research* **153,** 232–239 (2009).

47. Bhang, S. H., Kim, J. H., Yang, H. S., La, W.-G., Lee, T.-J., *et al.* Combined gene therapy with hypoxia-inducible factor-1α and heme oxygenase-1 for therapeutic angiogenesis. *Tissue Engineering Part A* **17,** 915–926 (2011).

48. Smith, R. S., Lin, K. F., Agata, J., Chao, L. & Chao, J. Human endothelial nitric oxide synthase gene delivery promotes angiogenesis in a rat model of hindlimb ischemia. *Arteriosclerosis, Thrombosis, and Vascular Biology* **22,** 1279–1285 (2002).

49. Brevetti, L. S., Chang, D. S., Tang, G. L., Sarkar, R. & Messina, L. M. Overexpression of endothelial nitric oxide synthase increases skeletal muscle blood flow and oxygenation in severe rat hind limb ischemia. *Journal of Vascular Surgery* **38,** 820–826 (2003).

50. Shyu, K. G., Chang, H., Wang, B. W. & Kuan, P. Intramuscular vascular endothelial growth factor gene therapy in patients with chronic critical leg ischemia. *American Journal of Medicine* **114,** 85–92 (2003).

51. Baumgartner, I., Pieczek, A., Manor, O., Blair, R., Kearney, M., *et al.* Clinical Investigation and Reports Constitutive Expression of phVEGF 165 After Intramuscular Gene Transfer Promotes Collateral Vessel Development in Patients With Critical Limb Ischemia. *Circulation* **97,** 1114–1123 (1998).

52. Morishita, R., Makino, H., Aoki, M., Hashiya, N., Yamasaki, K., *et al.* Phase I/IIa clinical trial of therapeutic angiogenesis using hepatocyte growth factor gene transfer to treat critical limb ischemia. *Arteriosclerosis, Thrombosis, and Vascular Biology* **31,** 713–720 (2011).

53. Rajagopalan, S., Mohler, E. R., Lederman, R. J., Mendelsohn, F. O., Saucedo, J. F., *et al.* Regional Angiogenesis With Vascular Endothelial Growth Factor in Peripheral Arterial Disease A Phase II Randomized, Double-Blind, Controlled Study of Adenoviral Delivery of Vascular Endothelial Growth Factor 121 in Patients With Disabling Intermittent Cla. *Circulation* **108,** 1933–1938 (2003).

54. Rajagopalan, S., Olin, J. W., Young, S., Erikson, M., Grossman, P. M., *et al.* Design of the Del-1 for therapeutic angiogenesis trial (DELTA-1), a phase II multicenter, double-blind, placebo-controlled trial of VLTS-589 in subjects with intermittent claudication secondary to peripheral arterial disease. *Human Gene Therapy* **15,** 619–624 (2004).

55. Creager, M. A., Olin, J. W., Belch, J. J. F., Moneta, G. L., Henry, T. D., *et al.* Effect of hypoxia-inducible factor-1α gene therapy on walking performance in patients with intermittent claudication. *Circulation* **124,** 1765–1773 (2011).

56. Nikol, S., Baumgartner, I., Van Belle, E., Diehm, C., Visoná, A., *et al.* Therapeutic angiogenesis with intramuscular NV1FGF improves amputation-free survival in

patients with critical limb ischemia. *Molecular Therapy* **16,** 972–978 (2008).

57. Gore, M. E. Adverse effects of gene therapy: Gene therapy can cause leukaemia: no shock, mild horror but a probe. *Gene Therapy* **10,** 4 (2003).

58. Schweizer, R., Kamat, P., Schweizer, D., Dennler, C., Zhang, S., *et al.* Bone marrow-derived mesenchymal stromal cells improve vascular regeneration and reduce leukocyte-endothelium activation in critical ischemic murine skin in a dose-dependent manner. *Cytotherapy* **16,** 1345–1360 (2014).

59. Kim, Y. J., Kim, H. K., Cho, H. K., Bae, Y. C., Suh, K. T., *et al.* Direct comparison of human mesenchymal stem cells derived from adipose tissues and bone marrow in mediating neovascularization in response to vascular ischemia. *Cellular Physiology and Biochemistry* **20,** 867–876 (2007).

60. Rafii, S. & Lyden, D. Therapeutic stem and progenitor cell transplantation for organ vascularization and regeneration. *Nature Medicine* **9,** 702–712 (2003).

61. Iba, O., Matsubara, H., Nozawa, Y., Fujiyama, S., Amano, K., *et al.* Angiogenesis by implantation of peripheral blood mononuclear cells and platelets into ischemic limbs. *Circulation* **106,** 2019–2025 (2002).

62. Wang, J. S., Shum-Tim, D., Chedrawy, E. & Chiu, R. C. J. The coronary delivery of marrow stromal cells for myocardial regeneration: Pathophysiologic and therapeutic implications. *Journal of Thoracic and Cardiovascular Surgery* **122,** 699–705 (2001).

63. Tomita, S., Li, R. K., Weisel, R. D., Mickle, D. A., Kim, E. J., *et al.* Autologous transplantation of bone marrow cells improves damaged heart function. *Circulation* **100,** 247–256 (1999).

64. Ziegelhoeffer, T., Fernandez, B., Kostin, S., Heil, M., Voswinckel, R., *et al.* Bone Marrow-Derived Cells Do Not Incorporate into the Adult Growing Vasculature. *Circulation Research* **94,** 230–238 (2004).

65. Heil, M., Ziegelhoeffer, T., Mees, B. & Schaper, W. A Different Outlook on the Role of Bone Marrow Stem Cells in Vascular Growth: Bone Marrow Delivers Software not Hardware. *Circulation Research* **94,** 573–574 (2004).

66. Fadini, G. P., Losordo, D. & Dimmeler, S. Critical reevaluation of endothelial progenitor cell phenotypes for therapeutic and diagnostic use. *Circulation Research* **110,** 624–637 (2012).

67. Asahara, T., Masuda, H., Takahashi, T., Kalka, C., Pastore, C., *et al.* Bone marrow origin of endothelial progenitor cells responsible for postnatal vasculogenesis in physiological and pathological neovascularization. *Circulation research* **85,** 221–228 (1999).

68. Shintani, S., Murohara, T., Ikeda, H., Ueno, T., Sasaki, K. i, *et al.* Augmentation of Postnatal Neovascularization With Autologous Bone Marrow Transplantation. *Circulation* **103,** 897–903 (2001).

69. Tateishi-Yuyama, E., Matsubara, H., Murohara, T., Ikeda, U., Shintani, S., *et al.* Therapeutic angiogenesis for patients with limb ischaemia by autologous

transplantation of bone-marrow cells: A pilot study and a randomised controlled trial. *Lancet* **360,** 427–435 (2002).

70. Matoba, S., Tatsumi, T., Murohara, T., Imaizumi, T., Katsuda, Y., *et al.* Long-term clinical outcome after intramuscular implantation of bone marrow mononuclear cells (Therapeutic Angiogenesis by Cell Transplantation [TACT] trial) in patients with chronic limb ischemia. *American Heart Journal* **156,** 1010–1018 (2008).

71. Ozturk, A., Kucukardali, Y., Tangi, F., Erikci, A., Uzun, G., *et al.* Therapeutical potential of autologous peripheral blood mononuclear cell transplantation in patients with type 2 diabetic critical limb ischemia. *Journal of Diabetes and its Complications* **26,** 29–33 (2012).

72. Kalka, C., Masuda, H., Takahashi, T., Kalka-Moll, W. M., Silver, M., *et al.* Transplantation of ex vivo expanded endothelial progenitor cells for therapeutic neovascularization. *Proceedings of the National Academy of Sciences* **97,** 3422–3427 (2000).

73. Kawamoto, A., Katayama, M., Handa, N., Kinoshita, M., Takano, H., *et al.* Intramuscular transplantation of G-CSF-mobilized CD34+ cells in patients with critical limb ischemia: A phase I/IIa, multicenter, single-blinded, dose-escalation clinical trial. *Stem Cells* **27,** 2857–2864 (2009).

74. Losordo, D. W., Kibbe, M. R., Mendelsohn, F., Marston, W., Driver, V. R., *et al.* A randomized, controlled pilot study of autologous CD34+ cell therapy for critical limb ischemia. *Circulation: Cardiovascular Interventions* **5,** 821–830 (2012).

75. Balber, A. E. Concise review: Aldehyde dehydrogenase bright stem and progenitor cell populations from normal tissues: Characteristics, activities, and emerging uses in regenerative medicine. *Stem Cells* **29,** 570–575 (2011).

76. Moreb, J. S. Aldehyde dehydrogenase as a marker for stem cells. *Current Stem Cell Research and Therapy* **3,** 237–246 (2008).

77. Capoccia, B. J., Robson, D. L., Levac, K. D., Maxwell, D. J., Hohm, S. A., *et al.* Revascularization of ischemic limbs after transplantation of human bone marrow cells with high aldehyde dehydrogenase activity. *Blood* **113,** 5340–5351 (2009).

78. Perin, E. C., Silva, G., Gahremanpour, A., Canales, J., Zheng, Y., *et al.* A randomized, controlled study of autologous therapy with bone marrow-derived aldehyde dehydrogenase bright cells in patients with critical limb ischemia. *Catheterization & Cardiovascular Interventions* **78,** 1060–1067 (2011).

79. Madonna, R., Geng, Y.-J. & Caterina, R. De. Adipose Tissue-Derived Stem Cells Characterization and Potential for Cardiovascular Repair. *Arteriosclerosis, Thrombosis, and Vascular Biology* **29,** 1723–1729 (2009).

80. Alvarez-Viejo, M., Menendez-Menendez, Y., Blanco-Gelaz, M. A., Ferrero-Gutierrez, A., Fernandez-Rodriguez, M. A., *et al.* Quantifying mesenchymal stem cells in the mononuclear cell fraction of bone marrow samples obtained for cell therapy. *Transplantation Proceedings* **45,** 434–439 (2013).

81. Ingram, D. A., Mead, L. E., Tanaka, H., Meade, V., Fenoglio, A., *et al.*

Identification of a novel hierarchy of endothelial progenitor cells using human peripheral and umbilical cord blood. *Blood* **104,** 2752–2760 (2004).

82. Fehrer, C. & Lepperdinger, G. Mesenchymal stem cell aging. *Experimental Gerontology* **40,** 926–930 (2005).

83. Heeschen, C., Lehmann, R., Honold, J., Assmus, B., Aicher, A., *et al.* Profoundly Reduced Neovascularization Capacity of Bone Marrow Mononuclear Cells Derived from Patients with Chronic Ischemic Heart Disease. *Circulation* **109,** 1615–1622 (2004).

84. Teraa, M., Sprengers, R. W., Westerweel, P. E., Gremmels, H., Goumans, M. J. T. H., *et al.* Bone Marrow Alterations and Lower Endothelial Progenitor Cell Numbers in Critical Limb Ischemia Patients. *PLoS ONE* **8,** e55592 (2013).

85. Russo, V., Young, S., Hamilton, A., Amsden, B. G. & Flynn, L. E. Mesenchymal stem cell delivery strategies to promote cardiac regeneration following ischemic injury. *Biomaterials* **35,** 3956–3974 (2014).

86. Hong, S. J., Traktuev, D. O. & March, K. L. Therapeutic potential of adipose-derived stem cells in vascular growth and tissue repair. *Current Opinion in Organ Transplantation* **15,** 86–91 (2010).

87. Collins, M. C., Moore, J. L., Burrows, B. J., Kypson, A. P. & Muller-Borer, B. J. Early Cell Loss Associated with Mesenchymal Stem Cell Cardiomyoplasty. *Open Tissue* **3,** 17–24 (2012).

88. Ma, S., Xie, N., Li, W., Yuan, B., Shi, Y., *et al.* Immunobiology of mesenchymal stem cells. *Cell Death and Differentiation* **21,** 216–225 (2014).

89. Barry, F. P. & Murphy, J. M. M. Mesenchymal stem cells: clinical applications and biological characterization. *The International Journal of Biochemistry and Cell Biology* **36,** 568–584 (2004).

90. Crisan, M., Yap, S., Casteilla, L., Chen, C. W., Corselli, M., *et al.* A Perivascular Origin for Mesenchymal Stem Cells in Multiple Human Organs. *Cell Stem Cell* **3,** 301–313 (2008).

91. Caplan, A. I. & Dennis, J. E. Mesenchymal stem cells as trophic mediators. *Journal of Cellular Biochemistry* **98,** 1076–1084 (2006).

92. Iwase, T., Nagaya, N., Fujii, T., Itoh, T., Murakami, S., *et al.* Comparison of angiogenic potency between mesenchymal stem cells and mononuclear cells in a rat model of hindlimb ischemia. *Cardiovascular Research* **66,** 543–551 (2005).

93. Gimble, J. M., Katz, A. J. & Bunnell, B. A. Adipose-derived stem cells for regenerative medicine. *Circulation Research* **100,** 1249–1260 (2007).

94. Melief, S. M., Zwaginga, J. J., Fibbe, W. E. & Roelofs, H. Adipose Tissue-Derived Multipotent Stromal Cells Have a Higher Immunomodulatory Capacity Than Their Bone Marrow-Derived Counterparts. *Stem Cells Translational Medicine* **2,** 1–6 (2013).

95. Yan, J., Tie, G., Xu, T. Y., Cecchini, K. & Messina, L. M. Mesenchymal stem

cells as a treatment for peripheral arterial disease: current status and potential impact of type II diabetes on their therapeutic efficacy. *Stem Cell Reviews* **9,** 360–372 (2013).

96. Mikami, S., Nakashima, A., Nakagawa, K., Maruhashi, T., Iwamoto, Y., *et al.* Autologous Bone-Marrow Mesenchymal Stem Cell Implantation and Endothelial Function in a Rabbit Ischemic Limb Model. *PLoS ONE* **8,** e67739 (2013).

97. Xie, N., Li, Z., Adesanya, T. M., Guo, W., Liu, Y., *et al.* Transplantation of placenta-derived mesenchymal stem cells enhances angiogenesis after ischemic limb injury in mice. *Journal of Cellular and Molecular Medicine* **20,** 29–37 (2016).

98. Lu, D., Chen, B., Liang, Z., Deng, W., Jiang, Y., *et al.* Comparison of bone marrow mesenchymal stem cells with bone marrow-derived mononuclear cells for treatment of diabetic critical limb ischemia and foot ulcer: a double-blind, randomized, controlled trial. *Diabetes Research and Clinical Practice* **92,** 26–36 (2011).

99. Gupta, P. K., Chullikana, A., Parakh, R., Desai, S., Das, A., *et al.* A double blind randomized placebo controlled phase I/II study assessing the safety and efficacy of allogeneic bone marrow derived mesenchymal stem cell in critical limb ischemia. *Journal of translational medicine* **11,** 143 (2013).

100. Mitchell, J. B., McIntosh, K., Zvonic, S., Garrett, S., Floyd, Z. E., *et al.* Immunophenotype of human adipose-derived cells: temporal changes in stromal-associated and stem cell-associated markers. *Stem Cells* **24,** 376–385 (2006).

101. Kim, W.-S., Park, B.-S., Sung, J.-H., Yang, J.-M., Park, S.-B., *et al.* Wound healing effect of adipose-derived stem cells: a critical role of secretory factors on human dermal fibroblasts. *Journal of Dermatological Science* **48,** 15–24 (2007).

102. Kondo, K., Shintani, S., Shibata, R., Murakami, H., Murakami, R., *et al.* Implantation of adipose-derived regenerative cells enhances ischemia-induced angiogenesis. *Arteriosclerosis, Thrombosis, and Vascular Biology* **29,** 61–66 (2009).

103. Zvonic, S., Lefevre, M., Kilroy, G., Floyd, Z. E., DeLany, J. P., *et al.* Secretome of Primary Cultures of Human Adipose-derived Stem Cells: Modulation of Serpins by Adipogenesis. *Molecular & Cellular Proteomics* **6,** 18–28 (2006).

104. Fraser, J. K., Wulur, I., Alfonso, Z. & Hedrick, M. H. Fat tissue: an underappreciated source of stem cells for biotechnology. *Trends in Biotechnology* **24,** 150–154 (2006).

105. Fraser, J. K., Wulur, I., Alfonso, Z., Zhu, M. & Wheeler, E. S. Differences in stem and progenitor cell yield in different subcutaneous adipose tissue depots. *Cytotherapy* **9,** 459–467 (2007).

106. Jones, E. & McGonagle, D. Human bone marrow mesenchymal stem cells in vivo. *Rheumatology* **47,** 126–131 (2008).

107. Moon, M. H., Kim, S. Y., Kim, Y. J., Kim, S. J., Lee, J. B., *et al.* Human adipose

tissue-derived mesenchymal stem cells improve postnatal neovascularization in a mouse model of hindlimb ischemia. *Cellular Physiology and Biochemistry* **17,** 279–290 (2006).

108. Nakagami, H., Maeda, K., Morishita, R., Iguchi, S., Nishikawa, T., *et al.* Novel autologous cell therapy in ischemic limb disease through growth factor secretion by cultured adipose tissue-derived stromal cells. *Arteriosclerosis, Thrombosis, and Vascular Biology* **25,** 2542–2547 (2005).

109. Bura, A., Planat-Benard, V., Bourin, P., Silvestre, J. S., Gross, F., *et al.* Phase I trial: The use of autologous cultured adipose-derived stroma/stem cells to treat patients with non-revascularizable critical limb ischemia. *Cytotherapy* **16,** 245–257 (2014).

110. Marino, G., Moraci, M., Armenia, E., Orabona, C., Sergio, R., *et al.* Therapy with autologous adipose-derived regenerative cells for the care of chronic ulcer of lower limbs in patients with peripheral arterial disease. *Journal of Surgical Research* **185,** 36–44 (2013).

111. Lindroos, B., Suuronen, R. & Miettinen, S. The Potential of Adipose Stem Cells in Regenerative Medicine. *Stem Cell Reviews and Reports* **7,** 269–291 (2011).

112. Bourin, P., Bunnell, B. A., Casteilla, L., Dominici, M., Katz, A. J., *et al.* Stromal cells from the adipose tissue-derived stromal vascular fraction and culture expanded adipose tissue-derived stromal/stem cells: A joint statement of the International Federation for Adipose Therapeutics and Science (IFATS) and the International So. *Cytotherapy* **15,** 641–648 (2013).

113. McIntosh, K., Zvonic, S., Garrett, S., Mitchell, J. B., Floyd, Z. E., *et al.* The immunogenicity of human adipose-derived cells: temporal changes in vitro. *Stem Cells* **24,** 1246–1253 (2006).

114. Locke, M., Windsor, J. & Dunbar, P. R. Human adipose-derived stem cells: Isolation, characterization and applications in surgery. *ANZ Journal of Surgery* **79,** 235–244 (2009).

115. Benitez, E., Sumpio, B. J., Chin, J. & Sumpio, B. E. Contemporary assessment of foot perfusion in patients with critical limb ischemia. *Seminars in Vascular Surgery* **27,** 3–15 (2014).

116. Wang, X. Y., Liu, C. L., Li, S. D., Xu, Y., Chen, P., *et al.* Hypoxia precondition promotes adipose-derived mesenchymal stem cells based repair of diabetic erectile dysfunction via augmenting angiogenesis and neuroprotection. *PLoS ONE* **10,** e0118951 (2015).

117. Matsuda, K., Falkenberg, K. J., Woods, A. A., Choi, Y. S., Morrison, W. A., *et al.* Adipose-derived stem cells promote angiogenesis and tissue formation for in vivo tissue engineering. *Tissue Engineering Part A* **19,** 1327–1335 (2013).

118. Kilroy, G. E., Foster, S. J., Wu, X., Ruiz, J., Sherwood, S., *et al.* Cytokine profile of human adipose-derived stem cells: Expression of angiogenic, hematopoietic, and pro-inflammatory factors. *Journal of Cellular Physiology* **212,** 702–709 (2007).

119. Thangarajah, H., Vial, I. N., Chang, E. I. E., El-Ftesi, S., Januszyk, M., *et al.* IFATS collection: Adipose stromal cells adopt a proangiogenic phenotype under the influence of hypoxia. *Stem cells* **27,** 266–274 (2009).

120. Stubbs, S. L., Hsiao, S. T.-F., Peshavariya, H. M., Lim, S. Y., Dusting, G. J., *et al.* Hypoxic Preconditioning Enhances Survival of Human Adipose-Derived Stem Cells and Conditions Endothelial Cells In Vitro. *Stem Cells and Development* **21,** 1887–1896 (2012).

121. Lee, E. Y., Xia, Y., Kim, W. S., Kim, M. H., Kim, T. H., *et al.* Hypoxia-enhanced wound-healing function of adipose-derived stem cells: Increase in stem cell proliferation and up-regulation of VEGF and bFGF. *Wound Repair and Regeneration* **17,** 540–547 (2009).

122. Rehman, J., Traktuev, D., Li, J., Merfeld-Clauss, S., Temm-Grove, C. J., *et al.* Secretion of Angiogenic and Antiapoptotic Factors by Human Adipose Stromal Cells. *Circulation* **109,** 1292–1298 (2004).

123. Amos, P. J., Bailey, A. M., Shang, H., Katz, A. J., Lawrence, M. B., *et al.* Functional binding of human adipose-Derived stromal cells. *Annals of Plastic Surgery* **60,** 437–444 (2008).

124. Kakudo, N., Morimoto, N., Ogawa, T., Taketani, S. & Kusumoto, K. Hypoxia enhances proliferation of human adipose-derived stem cells via HIF-1α activation. *PLoS ONE* **10,** e0139890 (2015).

125. Hou, D., Youssef, E. A. S., Brinton, T. J., Zhang, P., Rogers, P., *et al.* Radiolabeled cell distribution after intramyocardial, intracoronary, and interstitial retrograde coronary venous delivery: Implications for current clinical trials. *Circulation* **112,** 150–156 (2005).

126. Laflamme, M. a & Murry, C. E. Heart regeneration. *Nature* **473,** 326–335 (2011).

127. Serbo, J. V & Gerecht, S. Vascular tissue engineering: biodegradable scaffold platforms to promote angiogenesis. *Stem Cell Research & Therapy* **4,** 8 (2013).

128. Lutolf, M. P. & Hubbell, J. a. Synthetic biomaterials as instructive extracellular microenvironments for morphogenesis in tissue engineering. *Nature Biotechnology* **23,** 47–55 (2005).

129. Ifkovits, J. L., Tous, E., Minakawa, M., Morita, M., Robb, J. D., *et al.* Injectable hydrogel properties influence infarct expansion and extent of postinfarction left ventricular remodeling in an ovine model. *Proceedings of the National Academy of Sciences* **107,** 11507–11512 (2010).

130. Shinohara, M., Sabra, K., Gennisson, J. L., Fink, M. & Tanter, M. L. Real-time visualization of muscle stiffness distribution with ultrasound shear wave imaging during muscle contraction. *Muscle and Nerve* **42,** 438–441 (2010).

131. Saul, J. M. & Williams, D. F. Hydrogels in Regenerative Medicine. *Handbook of Polymer Applications in Medicine and Medical Devices* 279–302 (2013). doi:10.1016/B978-0-323-22805-3.00012-8

132. Li, Z. & Guan, J. Hydrogels for cardiac tissue engineering. *Polymers* **3,** 740–761

(2011).

133. Böstman, O. M. & Pihlajamäki, H. K. Adverse tissue reactions to bioabsorbable fixation devices. *Clinical Orthopaedics and Related Research* 216–227 (2000).

134. Sittinger, M., Reitzel, D., Dauner, M., Hierlemann, H., Hammer, C., *et al.* Resorbable polyesters in cartilage engineering: Affinity and biocompatibility of polymer fiber structures to chondrocytes. *Journal of Biomedical Materials Research* **33,** 57–63 (1996).

135. Bertrand, N., Fleischer, J. G., Wasan, K. M. & Leroux, J. C. Pharmacokinetics and biodistribution of N-isopropylacrylamide copolymers for the design of pH-sensitive liposomes. *Biomaterials* **30,** 2598–2605 (2009).

136. Dai, W. S. & Barbari, T. A. Hydrogel membranes with mesh size asymmetry based on the gradient crosslinking of poly(vinyl alcohol). *Journal of Membrane Science* **156,** 67–79 (1999).

137. Peppas, N. A. & Berner, R. E. Proposed method of intracopdal injection and gelation of poly (vinyl alcohol) solution in vocal cords: polymer considerations. *Biomaterials* **1,** 158–162 (1980).

138. Gough, J. E., Scotchford, C. A. & Downes, S. Cytotoxicity of glutaraldehyde crosslinked collagen/poly(vinyl alcohol) films is by the mechanism of apoptosis. *Journal of Biomedical Materials Research* **61,** 121–130 (2002).

139. Tous, E., Ifkovits, J. L., Koomalsingh, K. J., Shuto, T., Soeda, T., *et al.* Influence of injectable hyaluronic acid hydrogel degradation behavior on infarction-induced ventricular remodeling. *Biomacromolecules* **12,** 4127–4135 (2011).

140. Amsden, B. G., Sukarto, A., Knight, D. K. & Shapka, S. N. Methacrylated glycol chitosan as a photopolymerizable biomaterial. *Biomacromolecules* **8,** 3758–3766 (2007).

141. Sukarto, A., Yu, C., Flynn, L. E. & Amsden, B. G. Co-delivery of adipose-derived stem cells and growth factor-loaded microspheres in RGD-grafted N-methacrylate glycol chitosan gels for focal chondral repair. *Biomacromolecules* **13,** 2490–2502 (2012).

142. Yu, H., Fang, Y., Chen, L. & Chen, S. Investigation of redox initiators for free radical frontal polymerization. *Polymer International* **58,** 851–857 (2009).

143. Mironi-Harpaz, I., Wang, D. Y., Venkatraman, S. & Seliktar, D. Photopolymerization of cell-encapsulating hydrogels: Crosslinking efficiency versus cytotoxicity. *Acta Biomaterialia* **8,** 1838–1848 (2012).

144. Temenoff, J. S., Park, H., Jabbari, E., Conway, D. E., Sheffield, T. L., *et al.* Thermally cross-linked oligo(poly(ethylene glycol) fumarate) hydrogels support osteogenic differentiation of encapsulated marrow stromal cells in vitro. *Biomacromolecules* **5,** 5–10 (2004).

145. Hersel, U., Dahmen, C. & Kessler, H. RGD modified polymers: Biomaterials for stimulated cell adhesion and beyond. *Biomaterials* **24,** 4385–4415 (2003).

146. Weber, L. M., Hayda, K. N., Haskins, K. & Anseth, K. S. The effects of cell-matrix interactions on encapsulated beta-cell function within hydrogels functionalized with matrix-derived adhesive peptides. *Biomaterials* **28,** 3004–3011 (2007).

147. Hynes, R. O. Integrins: Versatility, modulation, and signaling in cell adhesion. *Cell* **69,** 11–25 (1992).

148. Takada, Y., Ye, X. & Simon, S. The integrins. *Genome Biology* **8,** 215 (2007).

149. Caniggia, I., Liu, J., Han, R., Wang, J., Tanswell, a K., *et al.* Identification of receptors binding fibronectin and laminin on fetal rat lung cells. *The American journal of physiology* **270,** L459-468 (1996).

150. Comisar, W. A., Mooney, D. J. & Linderman, J. J. Integrin organization: Linking adhesion ligand nanopatterns with altered cell responses. *Journal of Theoretical Biology* **274,** 120–130 (2011).

151. Angers-Loustau, A., Côté, J. F., Charest, A., Dowbenko, D., Spencer, S., *et al.* Protein tyrosine phosphatase-PEST regulates focal adhesion disassembly, migration, and cytokinesis in fibroblasts. *Journal of Cell Biology* **144,** 1019–1031 (1999).

152. Koo, L. Y., Irvine, D. J., Mayes, A. M., Lauffenburger, D. a & Griffith, L. G. Co-regulation of cell adhesion by nanoscale RGD organization and mechanical stimulus. *Journal of Cell Science* **115,** 1423–1433 (2002).

153. Aplin, A. E., Howe, A. K. & Juliano, R. Cell adhesion molecules, signal transduction and cell growth. *Current Opinion in Cell Biology* **11,** 737–744 (1999).

154. Adams, J. C. & Watt, F. M. Regulation of development and differentiation by the extracellular matrix. *Development* **117,** 1183–1198 (1993).

155. Shahidi-Dadras, M., Saeedi, M., Shakoei, S. & Ayatollahi, A. Langerhans cell histiocytosis: an uncommon presentation, successfully treated by thalidomide. *Indian journal of Dermatology, Venereology and Leprology* **77,** 587–590 (2011).

156. Matter, M. L. & Ruoslahti, E. A Signaling Pathway from the α5β1 and αvβ3 Integrins that Elevates bcl-2 Transcription. *Journal of Biological Chemistry* **276,** 27757–27763 (2001).

157. Millard, M. Integrin Targeted Therapeutics. *Theranostics* **1,** 154 (2011).

158. Ruoslahti, E. Rgd and Other Recognition Sequences for Integrins. *Annual Review of Cell and Developmental Biology* **12,** 697–715 (1996).

159. Sayyar, B. & Dodd, M. Cell-matrix Interactions of Factor IX (FIX)-engineered human mesenchymal stromal cells encapsulated in RGD-alginate vs. Fibrinogen-alginate microcapsules. *Artificial Cells, Nanomedicine, and Biotechnology* **42,** 102–9 (2014).

160. Bidarra, S. J., Barrias, C. C., Barbosa, M. A., Soares, R. & Granja, P. L. Immobilization of human mesenchymal stem cells within RGD-grafted alginate microspheres and assessment of their angiogenic potential. *Biomacromolecules* **11,**

1956–1964 (2010).

161. Bidarra, S. J., Barrias, C. C., Fonseca, K. B., Barbosa, M. A., Soares, R. A., *et al.* Injectable in situ crosslinkable RGD-modified alginate matrix for endothelial cells delivery. *Biomaterials* **32,** 7897–7904 (2011).

162. Shin, H., Jo, S. & Mikos, A. G. Modulation of marrow stromal osteoblast adhesion on biomimetic oligo[poly(ethylene glycol) fumarate] hydrogels modified with Arg-Gly-Asp peptides and a poly(ethylene glycol) spacer. in *Journal of Biomedical Materials Research* **61,** 169–179 (2002).

163. Lam, J. & Segura, T. The modulation of MSC integrin expression by RGD presentation. *Biomaterials* **34,** 3938–3947 (2013).

164. Jongpaiboonkit, L., King, W. J. & Murphy, W. L. Screening for 3D environments that support human mesenchymal stem cell viability using hydrogel arrays. *Tissue Engineering Part A* **15,** 343–353 (2009).

165. Tashiro, K., Sephel, G. C., Weeks, B., Sasaki, M., Martin, G. R., *et al.* A synthetic peptide containing the IKVAV sequence from the A chain of laminin mediates cell attachment, migration, and neurite outgrowth. *Journal of Biological Chemistry* **264,** 16174–16182 (1989).

166. Patrick, C. W. & Wu, X. Integrin-mediated preadipocyte adhesion and migration on Laminin-1. *Annals of Biomedical Engineering* **31,** 505–514 (2003).

167. Nakamura, M., Mie, M., Mihara, H., Nakamura, M. & Kobatake, E. Construction of multi-functional extracellular matrix proteins that promote tube formation of endothelial cells. *Biomaterials* **29,** 2977–2986 (2008).

168. Sun, W., Incitti, T., Migliaresi, C., Quattrone, A., Casarosa, S., *et al.* Viability and neuronal differentiation of neural stem cells encapsulated in silk fibroin hydrogel functionalized with an IKVAV peptide. *Journal of Tissue Engineering and Regenerative Medicine* (2015). doi:10.1002/term.2053

169. Li, B., Qiu, T., Zhang, P., Wang, X., Yin, Y., *et al.* IKVAV regulates ERK1/2 and Akt signalling pathways in BMMSC population growth and proliferation. *Cell Proliferation* **47,** 133–145 (2014).

170. Ishihara, M., Nakanishi, K., Ono, K., Sato, M., Kikuchi, M., *et al.* Photocrosslinkable chitosan as a dressing for wound occlusion and accelerator in healing process. *Biomaterials* **23,** 833–840 (2002).

171. Rao, S. B. & Sharma, C. P. Use of chitosan as a biomaterial: Studies on its safety and hemostatic potential. *Journal of Biomedical Materials Research* **34,** 21–28 (1997).

172. Bae, K., Jun, E. J., Lee, S. M., Paik, D. I. & Kim, J. B. Effect of water-soluble reduced chitosan on Streptococcus mutans, plaque regrowth and biofilm vitality. *Clinical Oral Investigations* **10,** 102–107 (2006).

173. Wang, H., Zhang, X., Li, Y., Ma, Y., Zhang, Y., *et al.* Improved myocardial performance in infarcted rat heart by co-injection of basic fibroblast growth factor with temperature-responsive Chitosan hydrogel. *Journal of Heart and Lung*

Transplantation **29,** 881–887 (2010).

174. Liu, Z., Wang, H., Wang, Y., Lin, Q., Yao, A., *et al.* The influence of chitosan hydrogel on stem cell engraftment, survival and homing in the ischemic myocardial microenvironment. *Biomaterials* **33,** 3093–3106 (2012).

175. Kim, I.-Y., Seo, S.-J., Moon, H.-S., Yoo, M.-K., Park, I.-Y., *et al.* Chitosan and its derivatives for tissue engineering applications. *Biotechnology Advances* **26,** 1–21 (2008).

176. Hirano, S., Tsuchida, H. & Nagao, N. N-acetylation in chitosan and the rate of its enzymic hydrolysis. *Biomaterials* **10,** 574–576 (1989).

177. Sugimoto, M., Morimoto, M., Sashiwa, H., Saimoto, H. & Shigemasa, Y. Preparation and characterization of water-soluble chitin and chitosan derivatives. *Carbohydrate Polymers* **36,** 49–59 (1998).

178. Hong, Y., Song, H., Gong, Y., Mao, Z., Gao, C., *et al.* Covalently crosslinked chitosan hydrogel: Properties of in vitro degradation and chondrocyte encapsulation. *Acta Biomaterialia* **3,** 23–31 (2007).

179. Silva, E. A., Kim, E.-S., Kong, H. J. & Mooney, D. J. Material-based deployment enhances efficacy of endothelial progenitor cells. *Proceedings of the National Academy of Sciences of the United States of America* **105,** 14347–14352 (2008).

180. Landa, N., Miller, L., Feinberg, M. S., Holbova, R., Shachar, M., *et al.* Effect of injectable alginate implant on cardiac remodeling and function after recent and old infarcts in rat. *Circulation* **117,** 1388–1396 (2008).

181. Leor, J., Tuvia, S., Guetta, V., Manczur, F., Castel, D., *et al.* Intracoronary Injection of In Situ Forming Alginate Hydrogel Reverses Left Ventricular Remodeling After Myocardial Infarction in Swine. *Journal of the American College of Cardiology* **54,** 1014–1023 (2009).

182. Alshamkhani, A. & Duncan, R. Radioiodination of alginate via covalently-bound tyrosinamide allows monitoring of its fate in-vivo. *Journal of Bioactive and Compatible Polymers* **10,** 4–13 (1995).

183. Rowley, J. A., Madlambayan, G. & Mooney, D. J. Alginate hydrogels as synthetic extracellular matrix materials. *Biomaterials* **20,** 45–53 (1999).

184. Rosenblatt, J., Devereux, B. & Wallace, D. G. Injectable collagen as a pH-sensitive hydrogel. *Biomaterials* **15,** 985–995 (1994).

185. Williams, B. R., Gelman, R. A., Poppke, D. C. & Piez, K. Collagen fibril formation. Optimal in vitro conditions and preliminary kinetic results. *Journal of Biological Chemistry* **253,** 6578–6585 (1978).

186. Achilli, M. & Mantovani, D. Tailoring mechanical properties of collagen-based scaffolds for vascular tissue engineering: The effects of pH, temperature and ionic strength on gelation. *Polymers* **2,** 664–680 (2010).

187. Dai, W., Hale, S. L., Kay, G. L., Jyrala, A. J. & Kloner, R. A. Delivering stem cells to the heart in a collagen matrix reduces relocation of cells to other organs as

assessed by nanoparticle technology. *Regenerative Medicine* **4,** 387–395 (2009).

188. Breen, A., O'Brien, T. & Pandit, A. Fibrin as a delivery system for therapeutic drugs and biomolecules. *Tissue Engineering Part B* **15,** 201–214 (2009).

189. Kubota, K., Kogure, H., Masuda, Y., Toyama, Y., Kita, R., *et al.* Gelation dynamics and gel structure of fibrinogen. in *Colloids and Surfaces B: Biointerfaces* **38,** 103–109 (2004).

190. Bootle-Wilbraham, C. A., Tazzyman, S., Thompson, W. D., Stirk, C. M. & Lewis, C. E. Fibrin fragment E stimulates the proliferation, migration and differentiation of human microvascular endothelial cells in vitro. *Angiogenesis* **4,** 269–275 (2001).

191. Zhang, X., Wang, H., Ma, X., Adila, A., Wang, B., *et al.* Preservation of the cardiac function in infarcted rat hearts by the transplantation of adipose-derived stem cells with injectable fibrin scaffolds. *Experimental Biology and Medicine* **235,** 1505–1515 (2010).

192. Frenkel, S. R. & Di Cesare, P. E. Scaffolds for articular cartilage repair. *Annals of Biomedical Engineering* **32,** 26–34 (2004).

193. Silverman, R. P., Passaretti, D., Huang, W., Randolph, M. A. & Yaremchuk, M. J. Injectable tissue-engineered cartilage using a fibrin glue polymer. *Plastic and Reconstructive Surgery* **103,** 1809–1818 (1999).

194. Christman, K. L., Fok, H. H., Sievers, R. E., Fang, Q. & Lee, R. J. Fibrin glue alone and skeletal myoblasts in a fibrin scaffold preserve cardiac function after myocardial infarction. *Tissue Engineering* **10,** 403–409 (2004).

195. Stern, R., Asari, A. A. & Sugahara, K. N. Hyaluronan fragments: An information-rich system. *European Journal of Cell Biology* **85,** 699–715 (2006).

196. Tang, Z. C. W., Liao, W. Y., Tang, A. C. L., Tsai, S. J. & Hsieh, P. C. H. The enhancement of endothelial cell therapy for angiogenesis in hindlimb ischemia using hyaluronan. *Biomaterials* **32,** 75–86 (2011).

197. Stern, R. Hyaluronan catabolism: a new metabolic pathway. *European Journal of Cell Biology* **83,** 317–325 (2004).

198. Laflamme, M. a, Chen, K. Y., Naumova, A. V, Muskheli, V., Fugate, J. a, *et al.* Cardiomyocytes derived from human embryonic stem cells in pro-survival factors enhance function of infarcted rat hearts. *Nature Biotechnology* **25,** 1015–1024 (2007).

199. Hughes, C. S., Postovit, L. M. & Lajoie, G. A. Matrigel: a complex protein mixture required for optimal growth of cell culture. *Proteomics* **10,** 1886–1890 (2010).

200. Li, G.-Z., Randev, R., Soeriyadi, A. H., Rees, G. J., Boyer, C., *et al.* Investigation into thiol-(meth)acrylate Michael addition reactions using amine and phosphine catalysts. *Polymer Chemistry* **1,** 1196–1204 (2010).

201. Hayami, J. W. S., Waldman, S. D. & Amsden, B. G. Chondrocyte Generation of

Cartilage-Like Tissue Following Photoencapsulation in Methacrylated Polysaccharide Solution Blends. *Macromolecular Bioscience* 1083–1095 (2016). doi:10.1002/mabi.201500465

202. Flynn, L., Semple, J. L. & Woodhouse, K. a. Decellularized placental matrices for adipose tissue engineering. *Journal of Biomedical Materials Research - Part A* **79,** 359–369 (2006).

203. Russo, V., Yu, C., Belliveau, P., Hamilton, A. & Flynn, L. E. Comparison of Human Adipose-Derived Stem Cells Isolated from Subcutaneous, Omental, and Intrathoracic Adipose Tissue Depots for Regenerative Applications. *Stem Cells Translational Medicine* **3,** 206–217 (2014).

204. Cina, C., Katsamouris, A., Megerman, J., Brewster, D. C., Strayhorn, E. C., *et al.* Utility of transcutaneous oxygen tension measurements in peripheral arterial occlusive disease. *Journal of Vascular Surgery* **1,** 362–371 (1984).

205. Ruangsetakit, C., Chinsakchai, K., Mahawongkajit, P., Wongwanit, C. & Mutirangura, P. Transcutaneous oxygen tension: a useful predictor of ulcer healing in critical limb ischaemia. *Journal of Wound Care* **19,** 202–206 (2010).

206. Hayami, J. W. S., Waldman, S. D. & Amsden, B. G. A photocurable hydrogel/elastomer composite scaffold with bi-continuous morphology for cell encapsulation. *Macromolecular Bioscience* **11,** 1672–1683 (2011).

207. Yu, C., Young, S., Russo, V., Amsden, B. G. & Flynn, L. E. Techniques for the Isolation of High-Quality RNA from Cells Encapsulated in Chitosan Hydrogels. *Tissue Engineering Part C: Methods* **19,** 829–838 (2013).

208. Putman, D. M., Liu, K. Y., Broughton, H. C., Bell, G. I. & Hess, D. A. Umbilical cord blood-derived aldehyde dehydrogenase-expressing progenitor cells promote recovery from acute ischemic injury. *Stem Cells* **30,** 2248–2260 (2012).

209. Bell, G. I., Broughton, H. C., Levac, K. D., Allan, D. A., Xenocostas, A., *et al.* Transplanted human bone marrow progenitor subtypes stimulate endogenous islet regeneration and revascularization. *Stem Cells and Development* **21,** 97–109 (2012).

210. Kim, I. L., Khetan, S., Baker, B. M., Chen, C. S. & Burdick, J. A. Fibrous hyaluronic acid hydrogels that direct MSC chondrogenesis through mechanical and adhesive cues. *Biomaterials* **34,** 5571–5580 (2013).

211. Dado, D. & Levenberg, S. Cell-scaffold mechanical interplay within engineered tissue. *Seminars in Cell and Developmental Biology* **20,** 656–664 (2009).

212. Breuls, R. G. M., Jiya, T. U. & Smit, T. H. Scaffold stiffness influences cell behavior: opportunities for skeletal tissue engineering. *The Open Orthopaedics Journal* **2,** 103–109 (2008).

213. Scherberich, A., Di Maggio, N. Di & McNagny, K. M. A familiar stranger: CD34 expression and putative functions in SVF cells of adipose tissue. *World Journal of Stem Cells* **5,** 1–8 (2013).

214. Sidney, L. E., Branch, M. J., Dunphy, S. E., Dua, H. S. & Hopkinson, A. Concise

review: Evidence for CD34 as a common marker for diverse progenitors. *Stem Cells* **32,** 1380–1389 (2014).

215. Stockinger, H., Gadd, S. J., Eher, R., Majdic, O., Schreiber, W., *et al.* Molecular characterization and functional analysis of the leukocyte surface protein CD31. *The Journal of Immunology* **145,** 3889–3897 (1990).

216. Tsou, Y.-H., Khoneisser, J., Huang, P.-C. & Xu, X. Hydrogel as a bioactive material to regulate stem cell fate. *Bioactive Materials* **1,** 39–55 (2016).

217. Zhu, J. & Marchant, R. E. Design properties of hydrogel tissue-engineering scaffolds. *Expert Review of Medical Devices* **8,** 607–626 (2011).

218. Kong, M., Chen, X. G., Xing, K. & Park, H. J. Antimicrobial properties of chitosan and mode of action: A state of the art review. *International Journal of Food Microbiology* **144,** 51–63 (2010).

219. Ueno, H., Yamada, H., Tanaka, I., Kaba, N., Matsuura, M., *et al.* Accelerating effects of chitosan for healing at early phase of experimental open wound in dogs. *Biomaterials* **20,** 1407–1414 (1999).

220. Peluso, G., Petillo, O., Ranieri, M., Santin, M., Ambrosic, L., *et al.* Chitosan-mediated stimulation of macrophage function. in *Biomaterials* **15,** 1215–1220 (1994).

221. Oliveira, M. I., Santos, S. G., Oliveira, M. J., Torres, A. L. & Barbosa, M. A. Chitosan drives anti-inflammatory macrophage polarisation and pro-inflammatory dendritic cell stimulation. *European Cells and Materials* **24,** 136–153 (2012).

222. Collier, J. H. & Segura, T. Evolving the use of peptides as components of biomaterials. *Biomaterials* **32,** 4198–4204 (2011).

223. Bačáková, L., Filová, E., Rypáček, F., Švorčík, V. & Starý, V. Cell Adhesion on Artificial Materials for Tissue Engineering. *Physiological Research* **53,** S35-45 (2004).

224. Hosseinkhani, H., Hiraoka, Y., Li, C. H., Chen, Y. R., Yu, D. S., *et al.* Engineering three-dimensional collagen-IKVAV matrix to mimic neural microenvironment. *ACS Chemical Neuroscience* **4,** 1229–1235 (2013).

225. Bellis, S. L. Advantages of RGD peptides for directing cell association with biomaterials. *Biomaterials* **32,** 4205–4210 (2011).

226. Ito, Y., Kajihara, M. & Imanishi, Y. Materials for enhancing cell adhesion by immobilization of cell-adhesive peptide. *Journal of Biomedical Materials Research* **25,** 1325–1337 (1991).

227. Neff, J. A., Caldwell, K. D. & Tresco, P. A. A novel method for surface modification to promote cell attachment to hydrophobic substrates. *Journal of Biomedical Materials Research* **40,** 511–519 (1998).

228. Nuttelman, C. R., Tripodi, M. C. & Anseth, K. S. Synthetic hydrogel niches that promote hMSC viability. *Matrix Biology* **24,** 208–218 (2005).

229. Salinas, C. N. & Anseth, K. S. The influence of the RGD peptide motif and its

contextual presentation in PEG gels on human mesenchymal stem cell viability. *Journal of Tissue Engineering and Regenerative Medicine* **2,** 296–304 (2008).

230. Patel, P. N., Gobin, A. S., West, J. L. & Patrick, C. W. Poly(ethylene glycol) hydrogel system supports preadipocyte viability, adhesion, and proliferation. *Tissue Engineering* **11,** 1498–1505 (2005).

231. Kuo, Y. C. & Lin, C. C. Accelerated nerve regeneration using induced pluripotent stem cells in chitin-chitosan-gelatin scaffolds with inverted colloidal crystal geometry. *Colloids and Surfaces B: Biointerfaces* **103,** 595–600 (2013).

232. Sephel, G. C., Tashiro, K. I., Sasaki, M., Greatorex, D., Martin, G. R., *et al.* Laminin a chain synthetic peptide which supports neurite outgrowth. *Biochemical and Biophysical Research Communications* **162,** 821–829 (1989).

233. Ranieri, J. P., Bellamkonda, R., Bekos, E. J., Gardella, J. A., Mathieu, H. J., *et al.* Spatial control of neuronal cell attachment and differentiation on covalently patterned laminin oligopeptide substrates. *International Journal of Developmental Neuroscience* **12,** 725–735 (1994).

234. Pradeep, N. & Sreekumar, A. V. An in vitro investigation into the cytotoxicity of methyl methacrylate monomer. *Journal of Contemporary Dental Practice* **13,** 838–841 (2012).

235. Engler, A. J., Griffin, M. A., Sen, S., Bönnemann, C. G., Sweeney, H. L., *et al.* Myotubes differentiate optimally on substrates with tissue-like stiffness: Pathological implications for soft or stiff microenvironments. *Journal of Cell Biology* **166,** 877–887 (2004).

236. Yeung, T., Georges, P. C., Flanagan, L. A., Marg, B., Ortiz, M., *et al.* Effects of substrate stiffness on cell morphology, cytoskeletal structure, and adhesion. *Cell Motility and the Cytoskeleton* **60,** 24–34 (2005).

237. Hadjipanayi, E., Mudera, V. & Brown, R. A. Close dependence of fibroblast proliferation on collagen scaffold matrix stiffness. *Journal of Tissue Engineering and Regenerative Medicine* **3,** 77–84 (2009).

238. Zuk, P. A., Zhu, M., Mizuno, H., Huang, J. I., Futrell, W. J., *et al.* Multilineage cells from human adipose tissue: implications for cell-based therapies. *Tissue Engineering* **7,** 211–228 (2001).

239. Fujisawa, S., Atsumi, T. & Kadoma, Y. Cytotoxicity of methyl methacrylate (MMA) and related compounds and their interaction with dipalmitoylphosphatidylcholine (DPPC) liposomes as a model for biomembranes. *Oral diseases* **6,** 215–221 (2000).

240. Kristensen, M., Birch, D. & Nielsen, H. M. Applications and challenges for use of cell-penetrating peptides as delivery vectors for peptide and protein cargos. *International Journal of Molecular Sciences* **17,** e185 (2016).

241. Duggal, S., Frønsdal, K. B., Szöke, K., Shahdadfar, A., Melvik, J. E., *et al.* Phenotype and gene expression of human mesenchymal stem cells in alginate scaffolds. *Tissue Engineering Part A* **15,** 1763–1773 (2009).

242. Burdick, J. A. & Anseth, K. S. Photoencapsulation of osteoblasts in injectable RGD-modified PEG hydrogels for bone tissue engineering. *Biomaterials* **23,** 4315–4323 (2002).

243. Stile, R. A. & Healy, K. E. Thermo-responsive peptide-modified hydrogels for tissue regeneration. *Biomacromolecules* **2,** 185–194 (2001).

244. Lin, X., Takahashi, K., Liu, Y. & Zamora, P. O. Enhancement of cell attachment and tissue integration by a IKVAV containing multi-domain peptide. *Biochimica et Biophysica Acta* **1760,** 1403–1410 (2006).

245. Li, X., Liu, X., Josey, B., Chou, C. J., Tan, Y., *et al.* Short Laminin Peptide for Improved Neural Stem Cell Growth. *Stem Cells Translational Medicine* **3,** 1–10 (2014).

246. Modulevsky, D. J., Lefebvre, C., Haase, K., Al-Rekabi, Z. & Pelling, A. E. Apple derived cellulose scaffolds for 3D mammalian cell culture. *PLoS ONE* **9,** e97835 (2014).

247. Nomizu, M., Weeks, B. S., Weston, C. A., Kim, W. H., Kleinman, H. K., *et al.* Structure-activity study of a laminin alpha-1 chain active peptide segment Ile-Lys-Val-Ala-Val (IKVAV). *FEBS Letters* **365,** 227–231 (1995).

248. Masaeli, E., Wieringa, P. A., Morshed, M., Nasr-Esfahani, M. H., Sadri, S., *et al.* Peptide functionalized polyhydroxyalkanoate nanofibrous scaffolds enhance Schwann cells activity. *Nanomedicine: Nanotechnology, Biology, and Medicine* **10,** 1559–1569 (2014).

249. Ng, K. W., Leong, D. T. W. & Hutmacher, D. W. The challenge to measure cell proliferation in two and three dimensions. *Tissue Engineering* **11,** 182–191 (2005).

250. Rubashkin, M. G., Ou, G. & Weaver, V. M. Deconstructing signaling in three dimensions. *Biochemistry* **53,** 2078–2090 (2014).

251. Anton, D., Burckel, H., Josset, E. & Noel, G. Three-dimensional cell culture: A breakthrough in vivo. *International Journal of Molecular Sciences* **16,** 5517–5527 (2015).

252. Tibbitt, M. W. & Anseth, K. S. Hydrogels as extracellular matrix mimics for 3D cell culture. *Biotechnology and Bioengineering* **103,** 655–663 (2009).

253. Deng, M., Gu, Y., Liu, Z., Qi, Y., Ma, G. E., *et al.* Endothelial Differentiation of Human Adipose-Derived Stem Cells on Polyglycolic Acid/Polylactic Acid Mesh. *Stem Cells International* **28,** (2015).

254. Garg, R. K., Rennert, R. C., Duscher, D., Sorkin, M., Kosaraju, R., *et al.* Capillary force seeding of hydrogels for adipose-derived stem cell delivery in wounds. *Stem Cells Translational Medicine* **3,** 1079–1089 (2014).

255. Kaga, T., Kawano, H., Sakaguchi, M., Nakazawa, T., Taniyama, Y., *et al.* Hepatocyte growth factor stimulated angiogenesis without inflammation: Differential actions between hepatocyte growth factor, vascular endothelial growth factor and basic fibroblast growth factor. *Vascular Pharmacology* **57,** 3–9 (2012).

256. Huang, R. L., Teo, Z., Chong, H. C., Zhu, P., Tan, M. J., *et al.* ANGPTL4 modulates vascular junction integrity by integrin signaling and disruption of intercellular VE-cadherin and claudin-5 clusters. *Blood* **118,** 3990–4002 (2011).

257. Felcht, M., Luck, R., Schering, A., Seidel, P., Srivastava, K., *et al.* Angiopoietin-2 differentially regulates angiogenesis through TIE2 and integrin signaling. *Journal of Clinical Investigation* **122,** 1991–2005 (2012).

258. Goh, Y. Y., Pal, M., Chong, H. C., Zhu, P., Tan, M. J., *et al.* Angiopoietin-like 4 interacts with matrix proteins to modulate wound healing. *Journal of Biological Chemistry* **285,** 32999–33009 (2010).

259. Yamamoto, K., Morishita, R., Hayashi, S., Matsushita, H., Nakagami, H., *et al.* Contribution of Bcl-2, but not Bcl-xL and Bax, to antiapoptotic actions of hepatocyte growth factor in hypoxia-conditioned human endothelial cells. *Hypertension* **37,** 1341–1348 (2001).

260. Xin, X., Yang, S., Ingle, G., Zlot, C., Rangell, L., *et al.* Hepatocyte growth factor enhances vascular endothelial growth factor-induced angiogenesis in vitro and in vivo. *American Journal of Pathology* **158,** 1111–1120 (2001).

261. Hou, M., Cui, J., Liu, J., Liu, F., Jiang, R., *et al.* Angiopoietin-like 4 confers resistance to hypoxia/serum deprivation-induced apoptosis through PI3K/Akt and ERK1/2 signaling pathways in mesenchymal stem cells. *PLoS ONE* **9,** e85808 (2014).

262. Edmondson, R., Broglie, J. J., Adcock, A. F. & Yang, L. Three-dimensional cell culture systems and their applications in drug discovery and cell-based biosensors. *Assay and Drug Development Technologies* **12,** 207–218 (2014).

263. Zigrino, P., Ayachi, O., Schild, A., Kaltenberg, J., Zamek, J., *et al.* Loss of epidermal MMP-14 expression interferes with angiogenesis but not with re-epithelialization. *European Journal of Cell Biology* **91,** 748–756 (2012).

264. Holmbeck, K., Bianco, P., Yamada, S. & Birkedal-Hansen, H. MT1-MMP: A tethered collagenase. *Journal of Cellular Physiology* **200,** 11–19 (2004).

265. Fagiani, E. & Christofori, G. Angiopoietins in angiogenesis. *Cancer Letters* **328,** 18–26 (2013).

266. Brigstock, D. R. Regulation of angiogenesis and endothelial cell function by connective tissue growth factor (CTGF) and cysteine-rich 61 (CYR61). *Angiogenesis* **5,** 153–165 (2002).

267. Mühlhauser, J., Pili, R., Merrill, M. J., Maeda, H., Passaniti, A., *et al.* In vivo angiogenesis induced by recombinant adenovirus vectors coding either for secreted or nonsecreted forms of acidic fibroblast growth factor. *Human Gene Therapy* **6,** 1457–1465 (1995).

268. Xue, L. & Greisler, H. P. Angiogenic effect of fibroblast growth factor-1 and vascular endothelial growth factor and their synergism in a novel in vitro quantitative fibrin-based 3-dimensional angiogenesis system. *Surgery* **132,** 259–267 (2002).

269. Fukuhara, S., Sako, K., Noda, K., Zhang, J., Minami, M., *et al.* Angiopoietin-1/Tie2 receptor signaling in vascular quiescence and angiogenesis. *Histology and Histopathology* **25,** 387–396 (2010).

270. Fagiani, E., Lorentz, P., Kopfstein, L. & Christofori, G. Angiopoietin-1 and -2 exert antagonistic functions in tumor angiogenesis, yet both induce lymphangiogenesis. *Cancer Research* **71,** 5717–5727 (2011).

271. Gupta, K., Gupta, P., Wild, R., Ramakrishnan, S. & Hebbel, R. P. Binding and displacement of vascular endothelial growth factor (VEGF) by thrombospondin: effect on human microvascular endothelial cell proliferation and angiogenesis. *Angiogenesis* **3,** 147–158 (1999).

272. Margosio, B., Marchetti, D., Vergani, V., Giavazzi, R., Rusnati, M., *et al.* Thrombospondin 1 as a scavenger for matrix-associated fibroblast growth factor 2. *Blood* **102,** 4399–4406 (2003).

273. Deng, C., Zhang, P., Vulesevic, B., Kuraitis, D., Li, F., *et al.* A collagen–chitosan hydrogel for endothelial differentiation and angiogenesis. *Tissue engineering. Part A* **16,** 3099–3109 (2010).

274. Jin, K., Li, B., Lou, L., Xu, Y., Ye, X., *et al.* In vivo vascularization of MSC-loaded porous hydroxyapatite constructs coated with VEGF-functionalized collagen/heparin multilayers. *Scientific Reports* **6,** 19871 (2016).

275. Chan, E. C., Kuo, S. M., Kong, A. M., Morrison, W. A., Dusting, G. J., *et al.* Three dimensional collagen scaffold promotes intrinsic vascularisation for tissue engineering applications. *PLoS ONE* **11,** e0149799 (2016).

276. Otte, A., Bucan, V., Reimers, K. & Hass, R. Mesenchymal stem cells maintain long-term in vitro stemness during explant culture. *Tissue Engineering Part C: Methods* **19,** 1–42 (2013).

Curriculum Vitae

Name:	Jobanpreet Singh Dhillon
Post-secondary Education and Degrees:	The University of Western Ontario London, Ontario, Canada 2010-2014 B.MSc. (Honors Specialization in Medical Science) The University of Western Ontario London, Ontario, Canada 2014-present M.Sc. candidate
Honours and Awards:	Dean's Honor Roll The University of Western Ontario 2010-2014 Western Graduate Scholarship Department of Anatomy and Cell Biology 2014-2016 Interdisciplinary Health Research Award Health Research Foundation (HRF) 2015-2016 Malcom Arnold Presentation Award in Cardiovascular Science Department of Physiology and Pharmacology 2015
Related Work Experience	Teaching Assistant The University of Western Ontario 2014-2016